

Carbohydrate Synthesis and Study of Carbohydrate-Lectin Interactions Using QCM Biosensors and Microarray Technologies

Zhichao Pei

裴志超



**KTH Chemical Science
and Engineering**

Doctoral Thesis

Stockholm 2006

Akademisk avhandling som med tillstånd av Kungliga Tekniska Högskolan i Stockholm framlägges till offentlig granskning för avläggande av filosofie doktorsexamen i kemi med inriktning mot organisk kemi, fredagen den 1 Dec., kl 10.00 i sal D3, KTH, Lindstedtsvägen 5, Stockholm. Avhandlingen försvaras på engelska. Opponent är Professor Roland J. Pieters, Utrecht University, the Netherlands.

ISBN 91-7178-503-5
ISRN KTH/IOK/FR--06/106--SE
ISSN 1100-7974
TRITA-IOK
Forskningsrapport 2006:106

© Zhichao Pei
Universitetsservice US AB, Stockholm

Carbohydrate Synthesis and Study of Carbohydrate-Lectin Interactions Using QCM Biosensors and Microarray Technologies

Zhichao Pei, Organic Chemistry, KTH Chemical Science and Engineering, SE-10044 Stockholm, Sweden

Dissertation for the degree of Doctor of Philosophy in Chemistry, 2006.

Abstract

Interactions between carbohydrates and proteins are increasingly being recognized as crucial in many biological processes, such as cellular adhesion and communication. In order to investigate the interactions of carbohydrates and proteins, the development of efficient analytic technologies, as well as novel strategies for the synthesis of carbohydrates, have to be explored. To date, several methods have been exploited to analyze interactions of carbohydrates and proteins, for example, biosensors, nuclear magnetic resonance (NMR); enzyme-linked immunosorbent assays (ELISA), X-ray crystallography and array technologies. This thesis describes the development of novel strategies for the synthesis of carbohydrates, as well as new efficient strategies to Quartz Crystal Microbalance- (QCM-) biosensors and carbohydrate microarrays technologies. These methodologies have been used to probe carbohydrate-lectin-interactions for a range of plant and animal lectins.

Keywords: Lectins; Carbohydrates; Molecular recognition; Biosensors; Quartz crystal microbalance; Carbohydrate microarrays.

This thesis is dedicated to my parents, my wife and my son,

-especially in memory of my father, whose spirits will inspire me forever.



裴志超

荣获二〇〇五年度国家优秀自费留学生
奖学金，特颁证嘉奖，以资鼓励。

CHINA SCHOLARSHIP COUNCIL

Presents the

**2005 Chinese Government Award
for Outstanding Self-financed
Students Abroad**

to

Pei Zhichao

Zhang Xiuqin, Secretary-General
China Scholarship Council

List of Publications

A. This thesis is based on the following papers, referred to in the text by their Roman numerals:

- I. **Quartz Crystal Microbalance Bioaffinity Sensor for Rapid Identification of Lectin Inhibitors From A Dynamic Combinatorial Library**
Zhichao Pei, Rikard Larsson, Teodor Aastrup, Henrik Anderson, Jean-Marie Lehn, and Olof Ramström
Biosens. Bioelectron. **2006**, *22*, 42-48
- II. **Glycosyldisulfides from Dynamic Combinatorial Libraries as O-Glycoside Mimetics for Plant and Endogenous Lectins: Their Reactivities in Solid-Phase and Cell Assays and Conformational Analysis by Molecular Dynamics Simulations**
Sabine André, Zhichao Pei, Hans-Christian Siebert, Olof Ramström, Hans-Joachim Gabius
Bioorg. Med. Chem. **2006**, *18*, 6314-6326
- III. **Stereospecific Ester Activation in Nitrite-Mediated Carbohydrate Epimerization**
Hai Dong, Zhichao Pei, and Olof Ramström
J. Org. Chem. **2006**, *71*, 3306-3309
- IV. **Study of Real-time Lectin–Carbohydrate Interactions on the Surface of a Quartz Crystal Microbalance**
Zhichao Pei, Henrik Anderson, Teodor Aastrup, and Olof Ramström.
Biosens. Bioelectron. **2005**, *21*, 60-66
- V. **Solvent-Dependent, Kinetically Controlled, Stereoselective Synthesis of 3- and 4-Thioglycosides**
Zhichao Pei, Hai Dong, and Olof Ramström.
J. Org. Chem. **2005**, *70*, 6952-6955
- VI. **Redox-Responsive and Calcium-Dependent Switching of Glycosyldisulfide Interactions with Concanavalin A**
Zhichao Pei, Teodor Aastrup, Henrik Anderson, and Olof Ramström.
Bioorg. Med. Chem. Lett. **2005**, *15*, 2693-2696

VII. Photogenerated Carbohydrate Microarrays

Zhichao Pei, Hui Yu, Matthias Theurer, Mingdi Yan, Annelie Waldén, Peter Nilsson, and Olof Ramström

ChemBioChem. **2006**, in press

VIII. Photoderivatized QCM Surfaces for the Study of Real-Time Lectin-Carbohydrate Interactions

Yuxin Pei, Hui Yu, Zhichao Pei, Matthias Theurer, Sabine André, Hans-Joachim Gabius, Mingdi Yan, and Olof Ramström.

To be submitted

IX. Synthesis of Thiogalactose derivatives for S-linked Oligosaccharides

Zhichao Pei, Hai Dong, and Olof Ramström.

To be submitted

B. Papers not included in this thesis:

X. Catalytic Self-Screening of Cholinesterase Substrates from a Dynamic Combinatorial Thioester Library

Rikard Larsson, Zhichao Pei, and Olof Ramström

Angew. Chem. Int. Ed. **2004**, *43*, 3716-3718

XI. UV-Crossinked Poly(vinylpyridine) Thin Films as Reversibly Responsive Surfaces

Bernadette Harnish, Joshua T Robinson, Zhichao Pei, Olof Ramström, Mingdi Yan

Chem. Mater. **2005**, *17*, 4092-4096

XII. Reagent-Dependent Regioselective Control in Multiple Carbohydrate Esterification

Hai Dong, Zhichao Pei, Styrbjörn Byström, and Olof Ramström

Submitted for publication

XIII. Efficient Synthesis of β -D-Mannosides and β -D-Talosides by Double Parallel or Double Serial Inversion

Hai Dong, Zhichao Pei, Marcus Angelin, Styrbjörn Byström, and Olof Ramström

Submitted for publication

- XIV. **Constitutional Dynamic Chemistry – A New Paradigm in Chemical Biology, Biomedical and Materials Sciences:** (1) Concept and General Principles.
Zhichao Pei, Hai Dong, Yuxin Pei, and Olof Ramström
In manuscript
- XV. **Constitutional Dynamic Chemistry – A New Paradigm in Chemical Biology, Biomedical and Materials Sciences:** (2) Applications in Chemical Biology and Biomedical Sciences
Hai Dong, Zhichao Pei, Yuxin Pei, and Olof Ramström
In manuscript
- XVI. **Constitutional Dynamic Chemistry – A New Paradigm in Chemical Biology, Biomedical and Materials Sciences:** (3) Dynamers: Dynamic Molecular and Supramolecular Polymers
Yuxin Pei, Hai Dong, Zhichao Pei, and Olof Ramström
In manuscript
- XVII. **Supramolecular Induction in Nitrite-Mediated Carbohydrate Epimerization**
Hai Dong, Zhichao Pei, Styrbjörn Byström, and Olof Ramström
In Manuscript
- XVIII. **Profiling of Secondary Hydroxyl Groups in Nitrite-mediated Carbohydrate Epimerization**
Zhichao Pei, Hai Dong, and Olof Ramström
In Manuscript

Appendix

My contributions to the papers in this thesis:

Paper I: I performed a majority of the experimental work and wrote parts of the article.

Paper II: I performed all synthetic work and wrote parts of the article.

Paper III: I performed some of the experimental work.

Paper IV: I performed a majority of the experimental work and wrote parts of the article.

Paper V: I performed a majority of the experimental work and wrote the article.

Paper VI: I performed a majority of the experimental work and wrote parts of the article.

Paper VII: I performed a majority of the experimental work and wrote parts of the article.

Paper VIII: I performed some of the experimental work and wrote the article.

Paper IX: I performed a majority of the experimental work and wrote the article.

Table of Contents

Abstract

List of publications

Appendix

Abbreviations

1. INTRODUCTION.....	1
1.1 Lectins	1
1.2 Carbohydrate-Lectin interactions.....	3
1.3 Quartz crystal microbalance	5
1.4 Carbohydrate microarrays.....	6
1.5 Aim of the study.....	8
2. CARBOHYDRATE SYNTHESIS	9
2.1 Synthesis of thioglycosides	9
2.1.1 Synthesis of thiogalactose derivatives	9
2.1.1.1 1-Thiol- β -D-galactopyranoside (1).....	10
2.1.1.2 Methyl 2-thiol- β -D-galactopyranoside (2)	11
2.1.1.3 Methyl 3-thiol- β -D-galactopyranoside (3)	15
2.1.1.4 Methyl 4-thiol- β -D-galactopyranoside (4)	22
2.1.1.5 Methyl 6-thiol- β -D-galactopyranoside (5)	24
2.1.2 Synthesis of other thiol-carbohydrates.....	25
2.1.2.1 1-Thiol- α -D-mannopyranoside sodium salt.....	25
2.1.2.2 Methyl 6-thiol- α -D-mannopyranoside.....	25
2.1.2.3 2-(acetylamino)-2-deoxy-1-thiol- β -D-glucopyranoside and 2- (acetylamino)-2-deoxy-1-thiol- β -D-galactopyranoside.....	26
2.1.2.4 1-Thiol- β -L-fucoside and 1-thiol- β -D-lactoside	27
2.2 Carbohydrate epimerization	28
2.3 Synthesis of PFPA derivatives	34
2.3.1 Synthetic routes for compounds 82, 83, 84, 85, 86.....	36
2.3.2 Synthetic routes for compounds 87, 88, 89, 90.....	37
2.3.3 Synthetic route for PFPA-linker (91).....	38
2.3.4 Synthetic route for PFPA-disulfide (94).....	38
3. ANALYSIS AND RECOGNITION	39
3.1 Target lectins.....	39
3.1.1 Concanavalin A (Con A)	39
3.1.2 <i>Viscum album</i> agglutinin (VAA).....	39
3.1.3 <i>Ulex europaeus</i> agglutinin I (UEA-I)	40
3.1.4 Soybean agglutinin (SBA).....	40
3.1.5 Peanut agglutinin (PNA).....	41
3.1.6 <i>Griffonia simplicifolia</i> lectin II (GS-II)	41

3.1.7 <i>Pisum sativum</i> agglutinin (PSA).....	42
3.1.8 Galectin-3.....	42
3.2 Quartz crystal microbalance (QCM).....	45
3.2.1 Mannan coated QCM system.....	45
3.2.1.1 Development of mannan-expressing surfaces for study of real-time lectin-carbohydrate interactions using QCM	45
3.2.1.1.1 Preparation of mannan surfaces	45
3.2.1.1.2 QCM conditions and surface regeneration	46
3.2.1.1.3 Evaluation of binding selectivity on the surface	47
3.2.1.1.4 Saturation binding of Con A to immobilised mannan surface	48
3.2.1.1.5 Competition binding study	49
3.2.1.2 Study of calcium-dependent binding effects in glycosyldisulfide interactions with Con A	53
3.2.1.3 Rapid identification of glycosyldisulfide lectin inhibitors from a dynamic combinatorial library.....	58
3.2.2 PEG coated QCM System	63
3.2.2.1 Development of a range of carbohydrate surfaces	63
3.2.2.2 Recognition by a range of lectins.....	64
3.2.2.3 Evaluation of VAA binding affinity to a range of carbohydrate-coated surfaces	65
3.3 Carbohydrate arrays.....	67
3.3.1 Microarray preparation	68
3.3.2 Screening by a range of lectins.....	68
3.4 Analysis of the carbohydrate-lectins interactions by other methods	71
3.4.1 Solid-phase assays	72
3.4.2 Cell-binding assays.....	74
4. CONCLUDING REMARKS.....	79

Acknowledgements

References

Abbreviations:

Ac ₂ O	Acetic anhydride
AgOTf	Silver triflate
BnBr	Benzyl bromide
BSA	Bovine serum albumin
Bu ₂ OSn	Dibutyltin oxide
BzCl	Benzoyl chloride
Con A	Concanavalin A
DCC	Dynamic combinatorial chemistry
DCL	Dynamic combinatorial library
DMAP	Dimethyl aminopyridine
DMF	Dimethylformamide
DTT	Dithiothreitol
EDCI	1-(3-Dimethylaminopropyl)-3-ethylcarbodiimide hydrochloride
ELISA	Enzyme-linked immunosorbent assay
GS-II	<i>Griffonia simplicifolia</i> II
HOAc	Acetic acid
NHS	<i>N</i> -Hydroxysuccinimide
NMR	Nuclear magnetic resonance
PEG	Poly(ethylene glycol)
PEO	Poly(ethylene oxide)
PFPAs	Perfluorophenylazides
PNA	Peanut agglutinin
PSA	<i>Pisum sativum</i>
QCM	Quartz crystal microbalance
SBR	Soybean agglutinin
SPR	Surface plasmon resonance
TBAI	Tetrabutylammonium iodide
TBANO ₂	Tetrabutylammonium nitrite
TBASAc	Tetrabutylammonium thioacetate
TBASH	Tetrabutylammonium hydrogen sulfate
Tf ₂ O	Trifluoroacetic anhydride
TIPSCl	Triisopropylsilyl chloride
TsCl	Toluenesulfonyl chloride
VAA	<i>Viscum album</i> agglutinin
UEA	<i>Ulex europaeus</i> agglutinin
XPS	X-ray photoelectron spectroscopy

Impact factors of some chemical journals (2005)

Journal Title	ISO Abbrev. Title	Impact factor
SCIENCE	Science	30.927
NATURE	Nature	29.273
CHEMICAL REVIEWS	Chem. Rev.	20.869
ANGEWANDTE CHEMIE- INTERNATIONAL EDITION	Angew. Chem.-Int. Edit.	9.596
JOURNAL OF THE AMERICAN CHEMICAL SOCIETY	J. Am. Chem. Soc.	7.419
ANALYTICAL CHEMISTRY	Anal. Chem.	5.635
CHEMISTRY-A EUROPEAN JOURNAL	Chem.-Eur. J.	4.907
CHEMISTRY OF MATERIALS	Chem. Mat.	4.818
ADVANCED SYNTHESIS & CATALYSIS	Adv. Synth. Catal.	4.632
CHEMICAL COMMUNICATIONS	Chem. Commun.	4.426
ORGANIC LETTERS	Org. Lett.	4.368
CHEMBIOCHEM	ChemBioChem	3.940
JOURNAL OF ORGANIC CHEMISTRY	J. Org. Chem.	3.675
ORGANOMETALLICS	Organometallics	3.473
BIOSENSORS & BIOELECTRONICS	Biosens. Bioelectron.	3.463
JOURNAL OF COMBINATORIAL CHEMISTRY	J. Comb. Chem.	3.459
GREEN CHEMISTRY	Green Chem.	3.255
CURRENT ORGANIC CHEMISTRY	Curr. Org. Chem.	3.102
ANALYTICA CHIMICA ACTA	Anal. Chim. Acta	2.760
SYNLETT	Synlett	2.693
SENSORS AND ACTUATORS B-CHEMICAL	Sens. Actuator B-Chem.	2.646
TETRAHEDRON	Tetrahedron	2.610
NEW JOURNAL OF CHEMISTRY	New J. Chem.	2.574
EUROPEAN JOURNAL OF ORGANIC CHEMISTRY	Eur. J. Org. Chem.	2.548
ORGANIC & BIOMOLECULAR CHEMISTRY	Org. Biomol. Chem.	2.547
BIOORGANIC & MEDICINAL CHEMISTRY LETTERS	Bioorg. Med. Chem. Lett.	2.478
TETRAHEDRON LETTERS	Tetrahedron Lett.	2.477
BIOORGANIC & MEDICINAL CHEMISTRY	Bioorg. Med. Chem.	2.286
JOURNAL OF ORGANOMETALLIC CHEMISTRY	J. Organomet. Chem.	2.025
CARBOHYDRATE RESEARCH	Carbohydr. Res.	1.669
ANALYTICAL LETTERS	Anal. Lett.	1.036
SYNTHETIC COMMUNICATIONS	Synth. Commun.	0.860

1. Introduction

1.1 Lectins

Proteins that interact with carbohydrates non-covalently occur widely in nature. These include for example carbohydrate-specific enzymes, and antibodies formed as a response to the carbohydrate antigens encountered by the immune system. The lectins (from *lectus*, the past participle of *legere*; to select or choose),¹⁻⁵ are defined as the third class of carbohydrate-specific proteins,⁶ which bind mono- and oligosaccharide reversibly with high specificity, but are devoid of catalytic activity compared with enzymes, and not products of an immune response such as antibodies. Lectins exist in most organisms ranging from viruses and bacteria to plants and animals. The first pure lectin, concanavalin A (Con A, from jack beans, see crystal structure in Figure 1) was isolated in 1919 by Sumner,⁷ who also demonstrated its carbohydrate specificity. Later, Watkins and Morgan found that lectins play a crucial role in elucidating the molecular base for blood group specificity.⁸ At present, the investigations of lectin-carbohydrate interactions focus on their roles in cell-cell recognition, as well as the application of these proteins for the study of carbohydrates in solution and on cell surfaces.

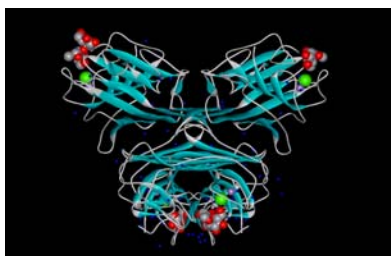


Figure 1. α -Man-1,2- α -Man-OME-concanavalin A complex (crystal structure) reveals a balance of forces involved in carbohydrate recognition.⁹

Each lectin molecule contains typically two or more carbohydrate-binding sites. Thus, their interactions on the surface of cells having multiple carbohydrate expressions (such as erythrocytes) result in the cross-linking of the cells and their subsequent precipitation. This phenomenon referred to as cell agglutination, is a major attribute of the activity of lectins and is used routinely for their detection and characterization. Both the agglutination and precipitation processes are inhibited by the sugar ligands for which the lectins are specific. Based on the specificity of lectins, they are classified into five groups according to the monosaccharide for which they exhibit the highest affinity: mannose, galactose/*N*-acetylgalactosamine, *N*-acetylglucosamine, fucose, and *N*-acetylneuraminic acid.¹⁰ Usually, the affinity of the lectins for monosaccharides is weak (association constants in the millimolar range), however highly selective (Table 1). Therefore, lectins specific for galactose do not react with glucose or mannose, nor do those specific for mannose bind galactose. However, the selectivity of lectins for monosaccharides is not always so high. For example, certain variations at the C-2 position of the pyranose ring may be tolerated,

resulting in that certain lectins that bind mannose can also interact with glucose, and certain lectins that bind galactose also interact with N-acetylgalactosamine (Table 1).

Table 1. Examples of lectins used and their ligand specificities

Lectins	Source	Family	Specificity
Plant lectins			
Concanavalin A (Con A)	Jack bean	Leguminosae	Man/Glc
Peanut agglutinin (PNA)	Peanut	Leguminosae	Gal β GalNAc
<i>Ulex europeus</i> (UEA I)	<i>Ulex europeus</i>	Leguminosae	L-Fucose
<i>Pisum Sativum</i> agglutinin (PSA)	Pea	Leguminosae	Man/Glc
<i>Griffonia simplicifolia</i> lectin II (GS II)	<i>Griffonia simplicifolia</i>	Leguminosae	GlcNAc
Soybean agglutinin (SBA)	Soybean	Leguminosae	Gal/GalNAc
<i>Viscum album</i> agglutinins (VAA)	Mistletoe	Viscaceae	Gal/GalNAc
Animal lectins			
Galectin-3		Galectin-3	Gal/GalNAc

Moreover, certain lectins can combine preferentially with either the α - or the β -anomer, whereas others lack anomeric specificity. Interestingly, the properties of the aglycon may markedly influence the interaction of a glycoside with the lectin. For example, aromatic glycosides bind to Con A much more strongly than aliphatic ones, attesting to the presence of a hydrophobic region in the proximity of the carbohydrate-binding site.¹¹

Lectins occurring in animals consist of 4 subgroups: 1) the S-type lectins; 2) the C-type lectins; 3) the P-type lectins; and 4) I-type lectins.¹⁰ The S-type lectins are also called galectins, which are found inside the cytoplasm, in the nucleus, at cell surfaces, and outside the cell. The galectins are a family of lectins defined by their affinity for β -galactosides and by conserved sequence elements. More than ten galectins from mammals are known, as well as many from other phylae including birds, amphibians, fish, nematodes, sponges and fungi. The galectins have been proposed to mediate cell adhesion, to regulate cell growth, and to trigger or inhibit apoptosis. There is strong evidence to suggest a role for galectins in immunity regulation, inflammation, and cancer, although their precise mechanisms of action remain unclear.¹²⁻¹⁴

1.2 Carbohydrate-Lectin interactions

Carbohydrate-protein interactions play crucial roles in many biological processes. The major function of lectins appears to be in cell-cell recognition (Table 2), where the carbohydrate-protein interactions have been found to be essential.

Table 2 Carbohydrate-protein interactions in cell-cell communication

Biological event	Carbohydrates on	Lectins on
Microbial infection	Host cells	Microorganisms
Immune response	Phagocytes, Microorganisms	Microorganisms, phagocytes
Fertilization	Eggs	Sperm
Leucocytes traffic	Phagocytes endothelial cells	Endothelial cells, phagocytes
Metastasis	Target organs, malignant	Malignant, target organs

Normally, the lectins possess shallow carbohydrate-binding sites. This is in contrast to enzymes and transport proteins, which often have buried binding sites. In lectins, the combining sites also appear to be preformed,¹⁵ since few conformational changes occur upon binding. Lectins bind carbohydrates through a network of hydrogen bonds, hydrophobic interactions, van der Waals' interactions, and metal ion coordinations.^{16,17} Hydrogen bonds are primarily formed between OH- and NH-groups (less to ring oxygen) of the carbohydrates, and corresponding groups on the proteins. Although carbohydrates are generally polar molecules, the steric disposition of hydroxyl groups creates hydrophobic patches on sugar surfaces that can interact with hydrophobic regions of the protein. Metal ions such as Ca^{2+} and Mg^{2+} can be found in close proximity to the carbohydrate combining pocket, but are not always directly involved in the carbohydrate binding. However, they assist in the positioning of the amino acid residues to interact with the carbohydrates. In addition, contacts between the ligand and the protein are sometimes mediated by water bridges. Water acts as a molecular "mortar" its small size and ability to act as both hydrogen donor and hydrogen receptor conferring ideal properties for this function. Therefore, water sometimes plays a very important role in carbohydrate recognition.

Most plant lectins belong to the legume family, also were used in the present research. Legume lectins can bind ligands through four invariant amino acid residues: an aspartic acid, an asparagine, a glycine, and an aromatic amino acid or leucine. In spite of this conservation of key amino acids involved in the binding of the carbohydrate, different lectins show different specificity. For example, PNA and SBA bind to galactose whereas Con A binds to mannose and glucose. The reason is that the amino acids that form the sugar combining sites of lectins are derived from four loops: designated A, B, C and D.¹⁸ The invariant aspartic acid and glycine belong to A and B, respectively, whereas the asparagine and the hydrophobic residue are in loop C. However, additional interactions are provided by amino acids in loop D, where loop D in length, sequence and conformation is highly variable to specify the monosaccharides for the lectins. For example, there is an

identical size in loop D in all mannose-specific lectins.¹⁹ In addition, normally the non-reducing residue of oligosaccharides/polysaccharides occupies the monosaccharide combining site when lectins bind to the such entities. The details for the interactions between PNA and the disaccharide Gal(β 1-3)GalNAc are displayed in Figure 2.^{10, 20}

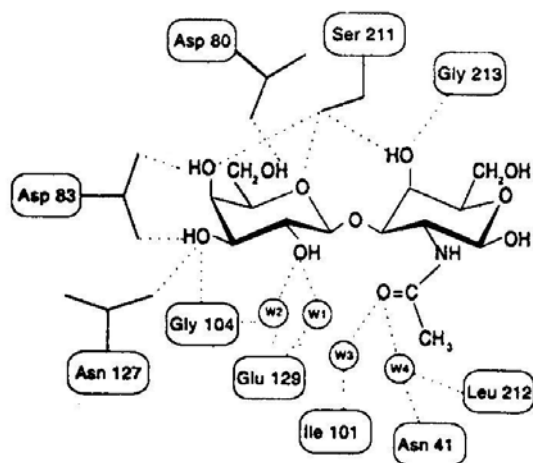


Figure 2. Schematic representation of carbohydrate-protein interactions in the peanut agglutinin (PNA) complex with Gal(β 1-3)GalNAc. The terminal galactose of the disaccharide form, in addition to the commonly occurring bonds with the side chains of asparagine (Asn127), aspartic acid (Asp83), and the main chain amide of glycine (Gly104), unique interactions between the 6-OH and the side chain of Asp80, and between the ring oxygen and Ser211. The 4-OH of the N-acetylgalactosamine is hydrogen-bonded to Ser211 and Gly213. Reprinted with permission from the American Chemical Society.¹⁰

1.2 Quartz crystal microbalance

Many important physical and chemical processes can be estimated from associated mass changes. The Quartz Crystal Microbalance (QCM), based upon the piezoelectric effect, is a simple, efficient and high resolution mass sensing technique.^{21,22} The signal transduction mechanism for the use of the piezoelectric effect in quartz crystals was first discovered by Curie in 1880.²³ Soon after, Raleigh reported that a change in inertia of a vibrating crystal was shown to change its resonant frequency, f .²⁴ The crucial breakthrough for the QCM technique was however when the AT-cut of a quartz crystal could be produced (Figure 3), since this geometry provide a stable oscillation with almost no temperature fluctuation in f at room temperature.^{25,26} Normally, the QCM technique depends upon circular quartz crystals operating in the thickness shear mode (TSM) where the lateral amplitude of a vibrating crystal is 1-2 nm (Figure 3). When a mass binds to the surface, it tends to oscillate with the identical lateral displacement and frequency as the crystal. The fundamental frequency relies upon the thickness of the wafer, its shape, mass. A QCM consists of a thin quartz disc with metal electrodes plated onto the surface. Gold is usually used as electrode materials, desposited on the upper and lower quartz surfaces. When an alternating electric field is applied across the quartz crystal, through the upper and lower metal electrode, a mechanical oscillation of characteristic frequency (f) is generated in the crystal.

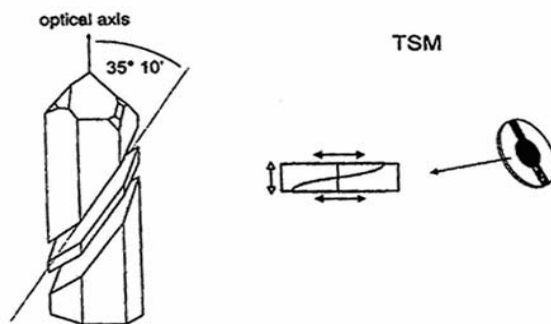


Figure 3. AT-cut of a quartz crystal from which the metal coated QCM quartz crystal are generated, and an end on crystal view of the thickness shear mode (TSM) of oscillation. Reprinted with permission from the American Chemical Society.²³

To date, the QCM methodology has been widely employed in biological studies, for example in immunoassays and DNA hybridization. The advantages of QCM biosensors in biological measurements are their ability to monitor the changes of small masses in real time, where such measurements can be performed by use of the native or synthetic molecules without any supplementary labeling.

1.4 Carbohydrate microarrays

Microarray technologies represent novel developments for studying biological processes in an efficient way. The advantage of these technologies is that only small amounts of compounds are needed for fabricating microarrays and many compounds can be screened in parallel in single operations. Over the last decade, DNA microarrays, which were the first to be developed, have been exploited for probing for example mutation of genes and alteration of patterns of gene expression in disease.^{27,28}

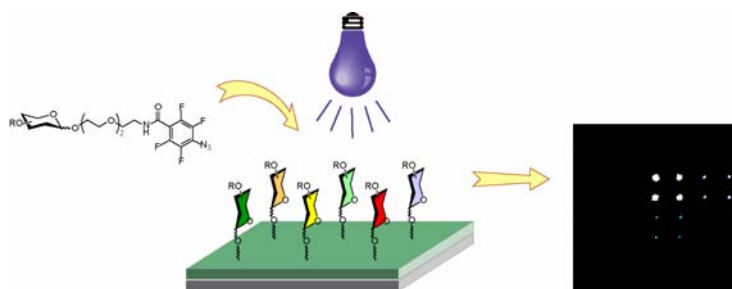


Figure 4. A strategy to carbohydrate microarrays based on photochemical ligation.

Protein microarrays, which were the second to be explored, have for example been applied to high-throughput investigations of protein-protein interactions and profiling of protein expression in normal and diseased conditions.^{29,30} Carbohydrate microarrays, which were only very recently developed, have so far been utilized primarily for investigations of carbohydrate-protein interactions and glycomics studies (Figure 4). Carbohydrate-protein interactions are known to be relative weak compared with DNA- and protein-protein interactions.^{31,32} Therefore, carbohydrates immobilized on solid surfaces can be advantageous for the detection of carbohydrate-protein interactions. The immobilized carbohydrates with proper spacing and orientation on the solid surface can result in multivalent interactions that produce stronger binding.³² Furthermore, the immobilized carbohydrates on the solid surface may act as glycans on cell surfaces for the functional studies of glycans, as well as for the high-throughput analysis of carbohydrate-protein interactions in novel carbohydrate-binding protein discovery campaigns.³³ However, new fabrication strategies for immobilization of carbohydrates on solid surfaces are being recognized as crucial in the development of carbohydrate microarrays technologies. In general, there are mainly three different methods for immobilizing carbohydrates to the solid surface (Figure 5): (1) site-nonspecific and noncovalent immobilization of chemically unconjugated carbohydrates on the unmodified surface,³⁴ (2) site-specific and covalent immobilization of chemically conjugated carbohydrates on the modified surface,³⁵⁻³⁹ (3) site-specific and covalent immobilization of chemically unmodified carbohydrates on the modified surface.⁴⁰ Among them, the site-specific and covalent immobilization of chemically conjugated carbohydrates on the modified surfaces

have been widely employed, where the experiments showed that carbohydrates attached with long tethers interacted more strongly with protein relative to those linked by short tethers. Therefore, immobilization of carbohydrates on the surface with a long linker is a crucial for carbohydrate microarrays technologies. To date, the carbohydrate microarrays technologies have been employed in investigating carbohydrate-lectin interactions,^{35-38,40} carbohydrate-antibody interactions, and detecting the substrate specificity or enzyme activity of carbohydrate-processing enzymes.³⁹

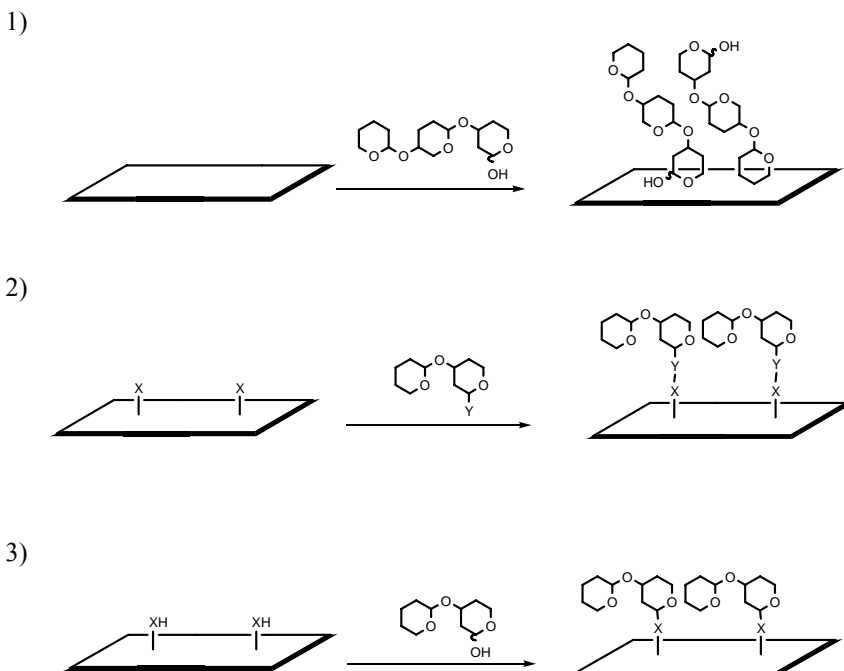


Figure 5. Methods for carbohydrates immobilized on the solid surfaces: 1) site-nonspecific and noncovalent immobilization of chemically unconjugated carbohydrates on the unmodified surface; 2) site-specific and covalent immobilization of chemically conjugated carbohydrates on the modified surface; 3) site-specific and covalent immobilization of chemically unmodified carbohydrates on the modified surface.

1.5 Aim of the study

Interactions between carbohydrates and proteins have been found to be of essential importance in many biological processes, such as cellular adhesion and communication.⁴¹⁻⁴³ To thoroughly understand these interactions, well-defined carbohydrate ligands must be synthesized. Such as thioglycosides, where the glycosidic oxygen atom is replaced with sulfur are quite often the glycosyl donors of choice for the synthesis of thio-oligosaccharides. Investigations of thio-oligosaccharide-binding proteins indicate that thiolinkages offer a higher degree of flexibility between glycols units and possess more conformers than their natural *O*-linked ligands.⁴⁴ Thiol-containing carbohydrates may also be subjected to mild oxidation in forming disulfide-bridged dimers, and glycosyldisulfides have more recently been identified as efficient glycosyl donors and potentially useful glycomimetics.⁴⁵⁻⁴⁷ In addition, thiosaccharides can be used to generate dynamic combinatorial libraries by mild oxidation in aqueous solution through reversible thio-disulfide interchange. Synthesis of thiosugars has been developed by several research groups for use as biological probes and potential enzyme inhibitors.^{48,49} However, systematic investigation for the synthesis of all positional thio-glycoside derivatives has not been fully explored. Therefore, in order to investigate carbohydrate-lectin interactions, the aim of this study was firstly to explore the novel strategies for the synthesis of thio-glycoside derivatives, as well as other glycoside derivatives.⁵⁰⁻⁵⁵ Secondly, to develop novel technologies and means to study the carbohydrate-lectin interactions.⁵⁶⁻⁵⁸ It is well known that QCM biosensor systems are able to measure small mass changes for the study of molecular interactions in real time, where such measurements can be performed by use of the native or synthetic molecules without any labeling. Furthermore, the advantage for carbohydrate microarray technologies is that only small amounts of compound are needed for fabricating microarrays and many compounds can be screened against a range of lectins in parallel in single operation. Thus, much effort was focused on the development of new QCM biosensor systems, as well as novel strategies of the carbohydrate microarrays to study carbohydrate-lectin interactions.

2. Carbohydrate Synthesis

In order to investigate carbohydrate-lectin interactions, various strategies for the synthesis of carbohydrate ligands have been developed. Regioselectivity is a well-known problem in carbohydrate chemistry because carbohydrates contain several hydroxyl groups with often small differences in reactivity. Therefore, strategies of protecting group introduction and selective deprotection are of crucial importance in carbohydrate synthesis. In addition, epimerization of carbohydrate structures to the corresponding epi-hydroxyl stereoisomer plays a very important role in carbohydrate synthesis. However, investigation of the epimerization of carbohydrate structures has not been systematically explored. In our study, stereospecific ester activation in nitrite-mediate carbohydrate epimerization was investigated.⁵¹

2.1 Synthesis of thioglycosides

Thioglycosides, where the glycosidic oxygen atom is replaced with sulfur constitute an interesting group of compounds in glycochemistry, possessing unique characteristics compared to their oxygen-containing counterparts. They are often employed as efficient glycoside donors and acceptors in oligosaccharide and neoglycoconjugate synthesis. Moreover, thiol-containing carbohydrates can be oxidized at mild conditions to form glycosyldisulfides, which have differences in different properties compared to natural glycosides. In addition, they can occupy a larger conformational space, as compared to natural glycosides, due to the increased flexibility and extended length of the disulfide bond.^{45,46} Thus, It is interesting to explore the function of glycosyldisulfide in biological interactions. However, for the synthesis of sulfur-containing carbohydrates, the benzyl ether group is very difficult to remove since organic sulfur compounds are poisonous to metal hydrogenation catalysts.⁵⁹ Therefore, ester as well as benzylidene protecting groups are more prevalently used for the synthesis of sulfur-containing carbohydrates.

2.1.1 Synthesis of thiogalactose derivatives (paper V and paper IX)

Thio- β -D-galactopyranosides are important compounds for the study of biological processes. In an early study, the binding of a series of alkyl or aryl 1-thio- β -D-galactopyranosides to β -D-galactosidase from *Escherichia coli* was investigated. The results indicated that the compounds are competitive inhibitors for the β -galactosidase from *Escherichia coli*.⁶⁰ Thio- β -D-galactosides react as glycosyl donors for the synthesis of thio-oligosaccharides. Thio- β -D-galactosides can also be used to generate the glycosyldisulfide libraries by mild oxidation to offer a useful way to study carbohydrate-lectin interaction, where glycosyldisulfides libraries can be screened against a range of lectins. Moreover, galectins constitute a family of structurally related β -galactoside-binding proteins. In order to elucidate biological functions of galectin as lead compounds for novel anti-inflammatory and anticancer agents since galectins may be involved in these pathological conditions, powerful inhibitors of galectins based on β -galactoside building

blocks are highly desirable. Synthesis of thiosugars has been developed by several research groups for the use as biological probes and potential enzyme inhibitors.^{48,49} However, systematic investigation for the synthesis of the all positional thio-galactose derivatives has not been fully explored. In our study, the synthesis of thio- β -D-galactose derivatives was performed (Figure 6).

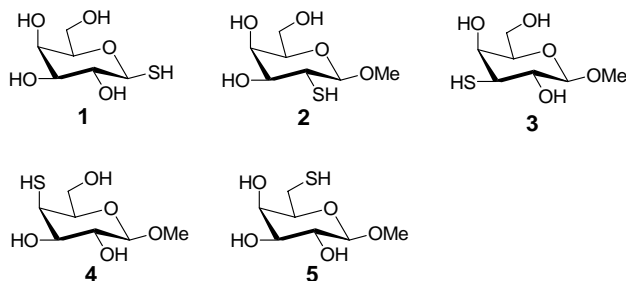
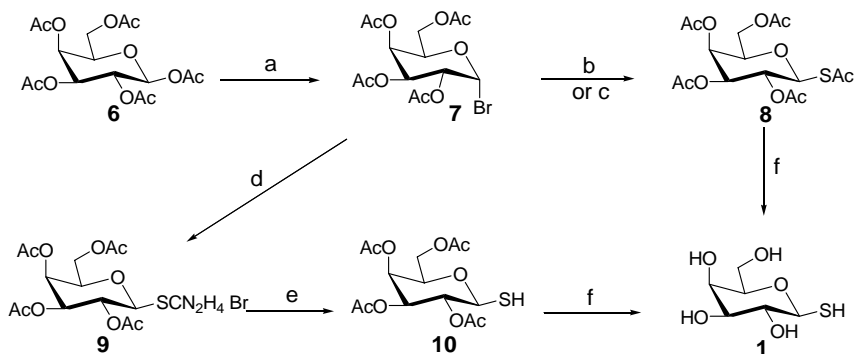


Figure 6. Thiogalactose derivatives

2.1.1.1 1-Thiol- β -D-galactopyranoside (**1**)

Compound **1** can be easily synthesized due to the high reactivity of the hydroxyl group at the anomeric center. Two different strategies for the synthesis of **1** have been developed from the corresponding glycosyl halide **7**, both in several steps.^{61,62} One way was to convert glycosyl halide **7** into thioglycoside **8** by treatment of **7** with HSAc in 1M aqueous Na_2CO_3 -solution ($\text{H}_2\text{O}/\text{CH}_2\text{Cl}_2$, 1:1) by use of the tetrabutylammonium hydrogen sulfate as phase transfer catalyst (pathway **b** in Scheme 1).⁶¹ The drawback of this method was that hydrolyzation of **7** generated a mixture of products for which it was difficult to isolate product **8**. In the alternative approach, **1** was obtained in 3 steps from the corresponding glycosyl halide **7**, with the key step involving treatment of **7** with thiourea (pathways **d-e-f** in Scheme 1).⁶² An improved method tested was to treat the glycosyl halide directly with tetrabutylammonium thioacetate in dry toluene or potassium thioacetate in dry acetone to afford thioglycoside in high yield (pathway **c** in Scheme 1).

SCHEME 1 ^a



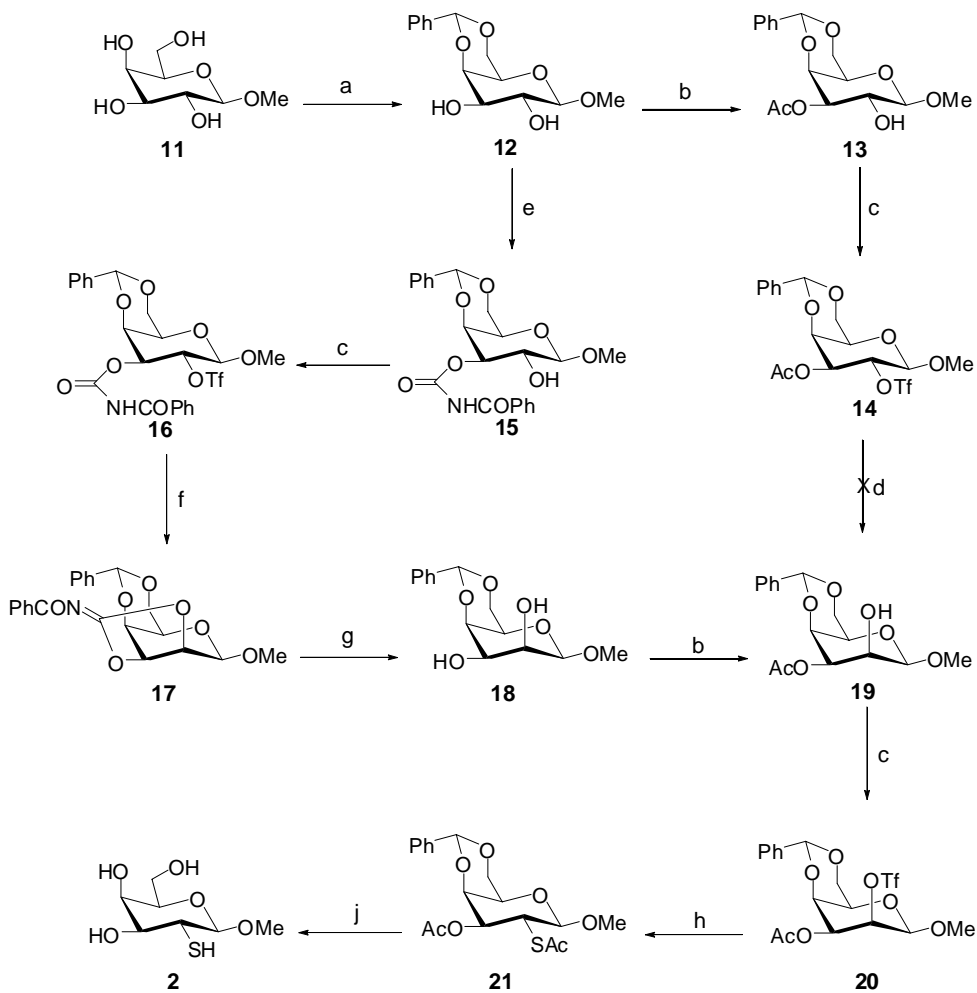
^a Reagents and conditions: (a) HOAc-HBr, CH₂Cl₂, rt, overnight, 70%; (b) HSAc, 1M Na₂CO₃, CH₂Cl₂, TBASH, rt, 2h, 55%; (c) i: TBASAc, toluene, rt, 2h; or ii: KSAC, acetone, rt, 2h, 88%; (d) thiourea, DMF or acetone, 60 °C, 4h, 69%; (e) ethanolamine, acetone, 60 °C, 2h, 81%; (f) NaOMe, MeOH, rt, 2h, 95%.

2.1.1.2 Methyl 2-thiol-β-D-galactopyranoside (2)

Efficient synthetic routes to **2** have not been fully described in the literature. When designing a viable synthesis, we opted for an inversion strategy. A suitable methyl taloside derivative, where the hydroxyl group in the 2-position was free and other positions were protected, was necessary for such a synthesis. Methyl β-D-galactoside was chosen as starting material due to the low cost. Therefore, the inversion of the equatorial OH at C-2 in the galactose derivative had to be performed. According to the literature, a common route to OH inversion in carbohydrate chemistry involves the triflation of a given hydroxyl group, followed by inversion with a nitrite anion at room temperature or heated up to 50 °C for 1-2 hours. An investigation of the literature revealed surprisingly few examples of the inversion of the equatorial OH at C-2. However, for the inversion of an equatorial OH at C-2 in methyl α-D-glucoside derivative, where the 2-OH was free and the other hydroxyl groups protected following a 4,6-*O*-benzylidene/3-OBz protecting strategy, has showed that the reaction can be performed at 80 °C for 6 hours.⁶³ We have previously found that the inversion of an equatorial OH at C-2 in methyl β-D-glucoside derivatives, where the same protecting group strategy was used as mentioned above, can be performed at 50 °C for 6 hours (entry **3** in Scheme 4).⁵¹ This suggested that the inversion of an equatorial OH at C-2 was much more difficult compared to the common inversion reactions. The 4,6-*O*-benzylidene was prevalently used because of the selective and simultaneous protection of two hydroxyl groups. The 4,6-*O*-benzylidene galactoside derivative treated with tin dioxide, followed by benzoyl chloride or acetic anhydride, selectively rendered the sub-key galactoside derivative, where the 2-OH was free and all other hydroxyl groups protected using a 4,6-*O*-benzylidene/3-OBz or 3-OAc protecting strategy. The key talose

derivative could then be obtained from the sub-key compound via the nitrite-mediate inversion reaction, where the 2-OH was free and all other hydroxyl groups protected using a 4,6-*O*-benzylidene/3-OBz or 3-OAc protecting strategy.

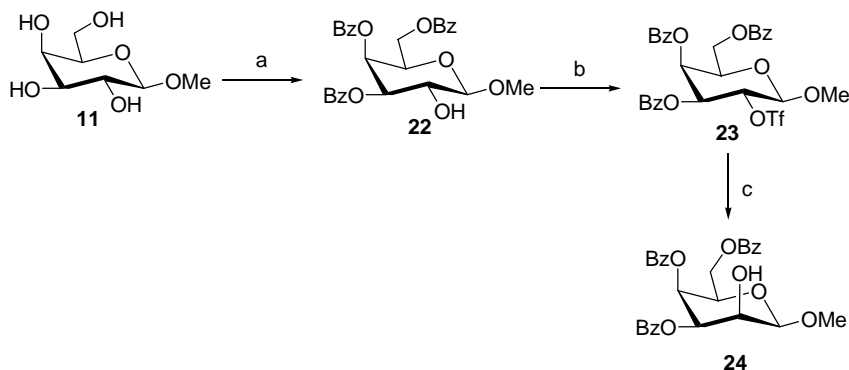
SCHEME 2 ^a



^a Reagents and conditions: (a) PhCH(OMe)_2 , TsOH, DMF, rt, 16h, 70%; (b) i: Bu_2OSn , dry MeOH, reflux, 2h; ii: Ac_2O , DMF, rt, 2h, 72%; (c) TiF_2O , pyridine, CH_2Cl_2 , $-30 - 0^\circ\text{C}$, 2h; (d) TBANO_2 , toluene, 50°C , 2h; (e) PhCONCO , CH_2Cl_2 , $-30 - 0^\circ\text{C}$, 3h, 60%; (f) NaH, THF, $0^\circ\text{C} - \text{rt}$, 3h; (g) NaOH, THF, rt, 12h, then 80°C , 3h, 82% for f, g 2 steps; (h) TBASAc, toluene, rt, 2h, 68%; (j) i: NaOMe, MeOH, 2h; ii: CHCl_3 , HCl, H_2O , rt, 87%.

Consequently, our preliminary efforts toward the synthesis of **2** were to try to obtain the key intermediate talose derivative **19** (pathway **a-b-c-d** in Scheme 2). Introduction of a triflate at C-2 in **19** followed by the S_N2 reaction with KSAc provided the desired **21**, which can be easily deprotected to afford **2** (pathway **c-h-j** in Scheme 2). Unfortunately, treatment of galactose derivative **14** with KNO₂ failed to afford the inversion talose derivative **19** due to steric hindrance from the 4,6-*O*-benzylidene, which was the key step for this synthetic route. In an attempt to overcome the problem of the steric hindrance from the 4,6-*O*-benzylidene in **14** to obtain a desired inversion at C-2, the strategy shown at pathway **e-c-f-g** in Scheme 2 was instead tested. The benzoylcarbamate *O*-cyclization has been investigated to illustrate that it was an efficient means to conquer the steric hindrance problem for the inversion reaction.⁶⁴ Treatment of **12** with benzoyl isocyanate gave **15**, where the selective carbamoylation was performed at C-3 in **12**. Treatment of **15** with triflic anhydride afforded the cyclization substrate **16**. Treatment of **16** with sodium hydride, and subsequent hydrolyzation under more vigorous basic conditions gave inversion product **18**. Finally, product **2** was successfully synthesized according to the synthetic route (pathway **a-e-c-f-g-b-c-h-j** in Scheme 2). Nevertheless, 6 steps were required to obtain key intermediate **19** starting from methyl β-D-galactoside. In an attempt to avoid the steric hindrance from the 4,6-*O*-benzylidene for the inversion reaction, an efficient means to obtain the key intermediate 2-OH taloside derivative **24** starting from methyl β-D-galactoside, where the hydroxyl group in the 2-position was free and the other positions were protected with benzoyl groups, was explored (Scheme 3).⁶⁵ Treatment of methyl β-D-galactoside with three equivalents of dibutyltin oxide and subsequent benzylation with three equivalents of benzoyl chloride at 90 °C in toluene afforded 2-OH methyl galactoside derivative **22** in a high yield. Attempted inversion of configuration at C-2 in **22**, via the triflate as described above, surprisingly yielded the desired C-2 inverted methyl taloside derivative **24**. Only 3 steps were thus required to obtain the key methyl 2-OH taloside derivative **24** starting from methyl β-D-galactoside.

SCHEME 3^a

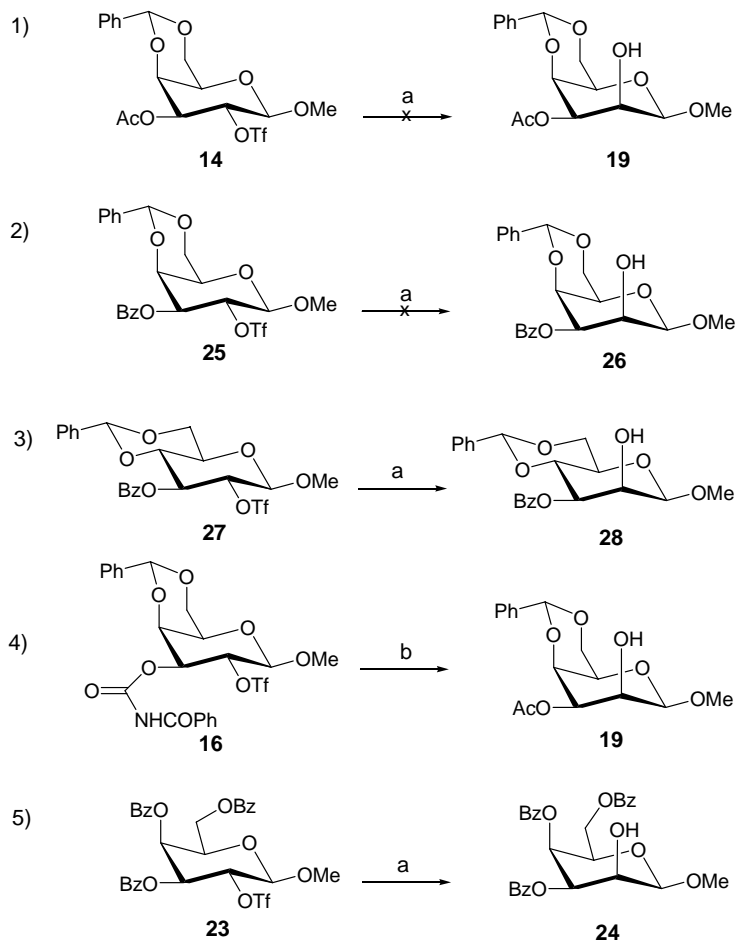


^a Reagents and conditions: (a) i: Bu₂SnO, MeOH, 70 °C, 2h; ii: BzCl, toluene, 90 °C, 2h, 90%; (b) Tf₂O, pyridine, CH₂Cl₂, -30 - 0 °C; 2h; (c) TBANO₂, CH₃CN, 50 °C, 30h, 70%.

To further study the effects of the protecting group pattern as well as the configuration for the inversion of the equatorial 2-OH in β -D-galactose derivatives, several different inversion routes were probed (Scheme 4). As can be seen, galactose derivative **14** failed to undergo the inversion reaction (entry **1** in Scheme 4) whereas the inversion reaction for the glucose derivative **27** was successful (entry **3** in Scheme 4), where its 2-OH was free and other hydroxyl groups protected using a 4,6-*O*-benzylidene and 3-OBz protecting strategy. As a comparison, the inversion reaction of an alternative galactose derivative **25**, using 3-OBz instead of 3-OAc, was tested (entry **2** in Scheme 4). It also failed to furnish the inversion product. The results indicated that the steric hindrance from the 4,6-*O*-benzylidene for the inversion reaction in galactose derivative was more than that in glucosederivative.

However, stronger nucleophilic reagents can overcome the hindrance from the 4,6-*O*-benzylidene to afford the inversion product (entry **4** in Scheme 4). Furthermore, the inversion reaction for galactose derivative **23**, was successful due to the less steric hindrance for the inversion from the benzoyl groups compared with the 4,6-*O*-benzylidene (entry **5** in Scheme 4).

SCHEME 4 ^a

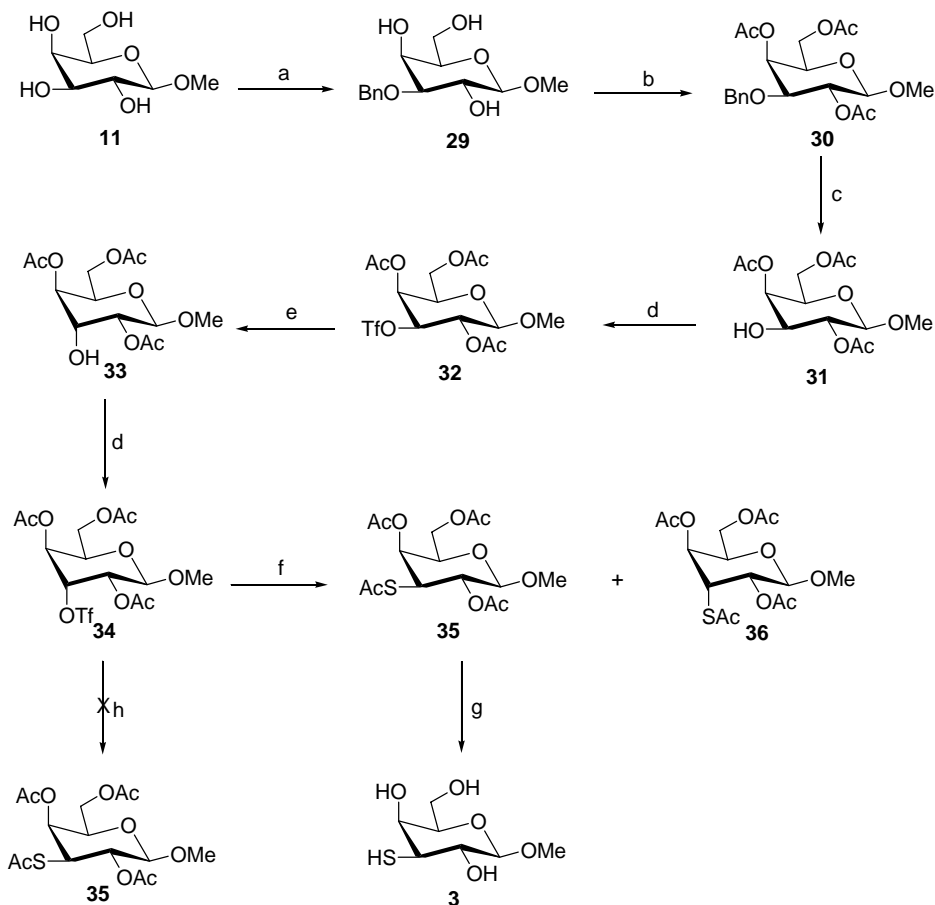


^a Reagents and conditions: (a) TBANO₂, CH₃CN, or KNO₂, DMF, 50 °C; (b) i: NaH, THF, 0 °C - rt, 3h; ii: NaOH, THF, rt - 80 °C; iii: Bu₂SnO, MeOH, reflux; iv: Ac₂O, DMF, rt.

2.1.1.3 Methyl 3-thiol-β-D-galactopyranoside (3)

The literature suggests that a 4,6-*O*-benzylidene plays a very important role for the synthesis of 3-thio-β-D-galactose derivative, with the key step involving the interconversion from 3-OTf gulose derivative to galactose derivative.^{66,67} Our initial strategy for the synthesis of 3-thio-β-D-galactose derivative is shown in Scheme 5.

SCHEME 5^a



^a Reagents and conditions: (a) i: Bu_2OSn , MeOH, reflux, 2h; ii: BnBr, TBAI, benzene, reflux, 2h, 70%; (b) Ac_2O , pyridine, DMAP, rt, 3h, 92%; (c) $\text{Pd}(\text{OH})_2$, H_2 , MeOH, rt, overnight, 95%; (d) TrfO , pyridine, CH_2Cl_2 , $-30 - 0^\circ\text{C}$, 2h; (e) TBANO_2 , CH_2Cl_2 , 50°C , 2h, 62%; (f) TBASAc , toluene, 4h, 78%; (g) NaOMe , MeOH, rt, 2h, 86%; (h) KSAC , DMF, rt.

A methyl guloside derivative compound **33**, where the hydroxyl group in the 3-position was free and the other positions were protected with acetyl groups, is crucial for the synthesis of 3-S galactose derivative. Normally, Compound **33** was easily obtained in 5 steps according to our synthetic strategy. However, treatment of **33** with triflic anhydride, and subsequent thiolation with KSAC in DMF instead afforded side product **31**, which was generated via the neighbouring ester group participation followed by hydrolysis. In order to suppress the

neighboring group participation where esters are used as protecting groups for thiolate of carbohydrates, the reaction was performed in non-polar solvent toluene using TBASAc as nucleophilic reagent. A mixture of **35** and **36** was then yielded. To understand these result, the dependence of nucleophile concentration for this reaction was studied. It was found that the reaction highly depended on the concentration of the thioacetate reagent, where the corresponding thioacetate of the gulose type (**36**) was afforded up to 40 % in strong competition with **35** (Table 3).

Table 3. Stereoselectivity in the reaction of **34** and different TBASAc concentrations.

Entry No.	TBASAc (equiv.)	relative yield (%)	
		35	36
1	5	60	40
2	10	75	25
3	20	88	12
4	40	96	4

¹H-NMR spectra clearly shows the results for the dependency of stereoselectivity on nucleophilic reagent concentration in the reaction (Figure 7).

The results indicate that the reaction highly depends on both the solvent and the concentration of the thioacetate reagent. In polar solvent, when **34** was reacted with KSAC (5 equiv.) in DMF mainly afforded the hydrolysis product **31** after workup, and neither product **35** nor **36** was formed (Scheme 6). In non-polar solvent, when TBASAc in toluene was employed to displace the OTf-group, a straightforward S_N2-reaction was anticipated to yield the 3-SAc-glycoside **35** of galactose type, whereas the corresponding thioacetate of the gulose type (**36**) was also formed in strong competition with **35**. The yield of **35** could be dramatically increased when the concentration of TBASAc was increased to close to the saturation limit (40 equiv.), resulting in almost quantitative formation of **35**. The main reason for this behavior is most likely due to the competing formation of an acetoxonium intermediate (**37**) in the reaction pathway. When an ester functionality in the axial 4-position is present, establishing an anti-diaxial relationship between the ester and the triflate, **37** may form slowly with time to compete with the attacking thioacetate in non-polar solvent (Scheme 6).

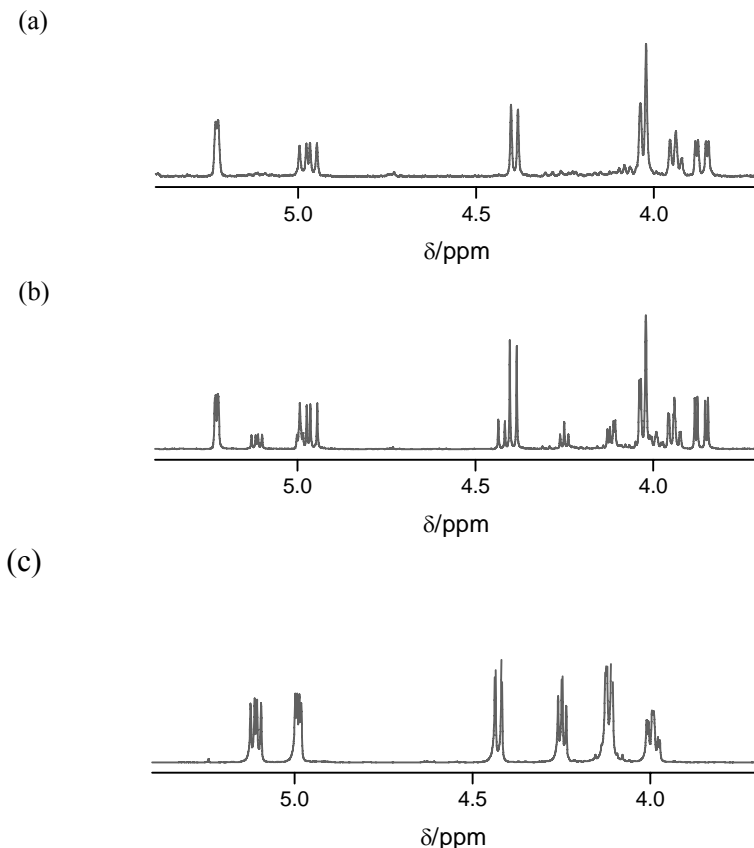
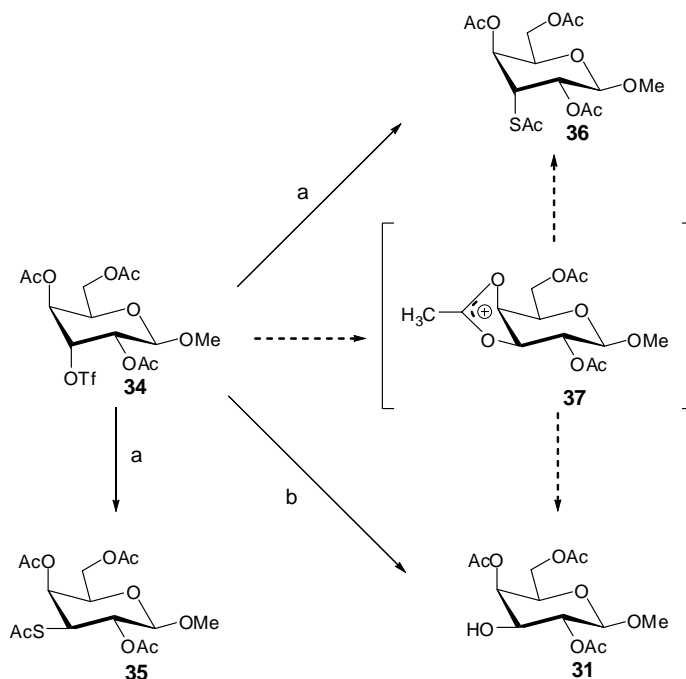


Figure 7. ^1H -NMR spectra: (a) product mixture resulting from **34** reacted with 40 equiv. TBASAc in toluene (96% **35**, 4% **36**), (b) product mixture resulting from **34** reacted with 10 equiv. TBASAc in toluene (75% **35**, 25% **36**), (c) gulose derivative **36**.

Preferred nucleophilic attack on the acetoxonium ion from the axial 3-position will then open the 5-ring and produce the gulose derivative. Attack at the equatorial 4-position proved less favored, and no 4-Sac-glucose analogs were identified in the reaction. The increasing yield of galactose-derivative **35** with increasing nucleophile concentration supports the notion of competing inter- and intramolecular reaction pathways. In a non-polar solvent (toluene), the formation of **36** is very slow, thus favoring an intermolecular $\text{S}_{\text{N}}2$ -reaction that is dependent on the nucleophile concentration (Scheme 6). Therefore, the formation of **35** is under kinetic control in toluene. When the reaction was carried out at 50 °C with 40 equivalents of TBASAc, a 66:34 ratio of **35** and **36** was obtained after workup, suggesting the thermodynamically controlled formation of **36** at these conditions.

SCHEME 6^a



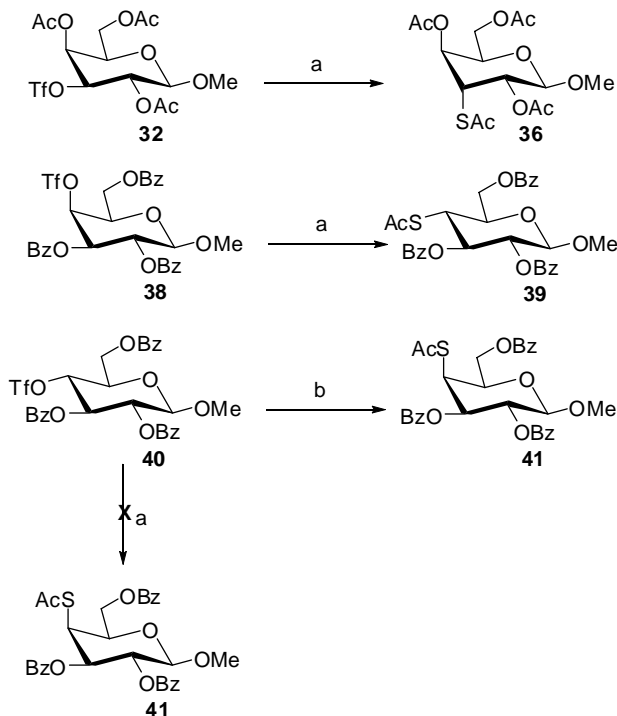
^a Reagents and conditions: (a) TBASAc, toluene, N₂, rt, 4 h; (b) DMF/KSAc or CH₂Cl₂/TBASAc, rt.

Finally, the total synthetic route for **3** is displayed in Scheme 5: the key intermediate 3-OH gulose derivative **33** was prepared from the corresponding 3-OTf galactose derivative **32**, which itself was obtained in 4 steps from methyl β-D-galactoside (route via **a**, **b**, **c**, **d**, **e** in Scheme 5). Introduction of a triflate at C-3 in **33** followed by the S_N2 reaction with 40 equivalents TBASAc in toluene at room temperature mainly provided the desired **35**. The byproduct 3-S gulose derivative **36** was competitively formed in only 4% (pathway **d**, **f** in Scheme 5). Deprotection of **35** afforded **3**.

To further explore the phenomenon of solvent-dependent kinetic control in thiolate reactions, other possible configurational isomers, compounds **32**, **38**, **40**, were subjected to the same reactions as compound **34** (Scheme 7). When the 3-OTf-galactose derivative **32** was employed, no competing reactions and no concentration dependence were found, and all reactions with SAc nucleophiles proceeded smoothly in DMF and toluene. Gulo-derivative **36** was thus formed in good yield without any complications. Likewise, reactions with 4-OTf-galactose derivative **38** in either solvent resulted in the glucose

derivative **39** without any complicating side-reactions. Both these compounds present a 3,4-*cis* configuration, for which the acetoxonium intermediate is unlikely to form. Since no other species were identified in the products, formation of the 2,3-acetoxonium from **32** or the potential 4,6-acetoxonium ion from **38**, can be largely ruled out. On the other hand, compound **40** displayed a similar behavior as **34**. In DMF the reaction led to a reaction mixture, whereas in toluene compound **41** was formed in good yield. In this case, however, no apparent concentration dependence was observed. Since the anti-diequatorial configurational relation between the triflate and the ester functionalities is less likely to produce an intermediate acetoxonium ring, the main reason for this solvent-dependence is likely the 6-membered acetoxonium ring arising from 6-OBz group. The formation of this species is however kinetically less favored than the corresponding 5-membered ring, and hence no concentration dependence is observed.

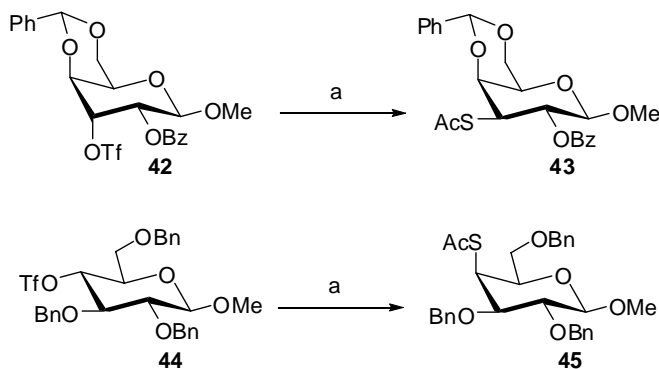
SCHEME 7^a



^a Reagents and conditions: (a) KSAc, DMF, N₂, rt, 8h; (b) TBASAc (< 20 equiv.), toluene, N₂, rt, 4h.

Our set of configurational isomers has led to the following conclusions concerning neighboring group participation in these reactions: (i) an anti-diaxial relationship between the ester and the triflate (**34**) likely leads to the formation of a reasonably stabilized acetoxonium intermediate in non-polar solvent, (ii) axial-equatorial (**32**) or equatorial-axial (**38**) relationships are unlikely to generate any acetoxonium intermediates, (iii) an anti-diequatorial relationship (**32**, **40**) is likely inefficient in forming this intermediate, (iv) the 4,6-anti-diequatorial relationship in compound **40** may potentially form a moderately stable intermediate in DMF, (v) a 4,6-axial-equatorial relation (**38**) is largely inefficient.

SCHEME 8^a



^a Reagents and conditions: (a) KSAc, DMF, N₂, rt.

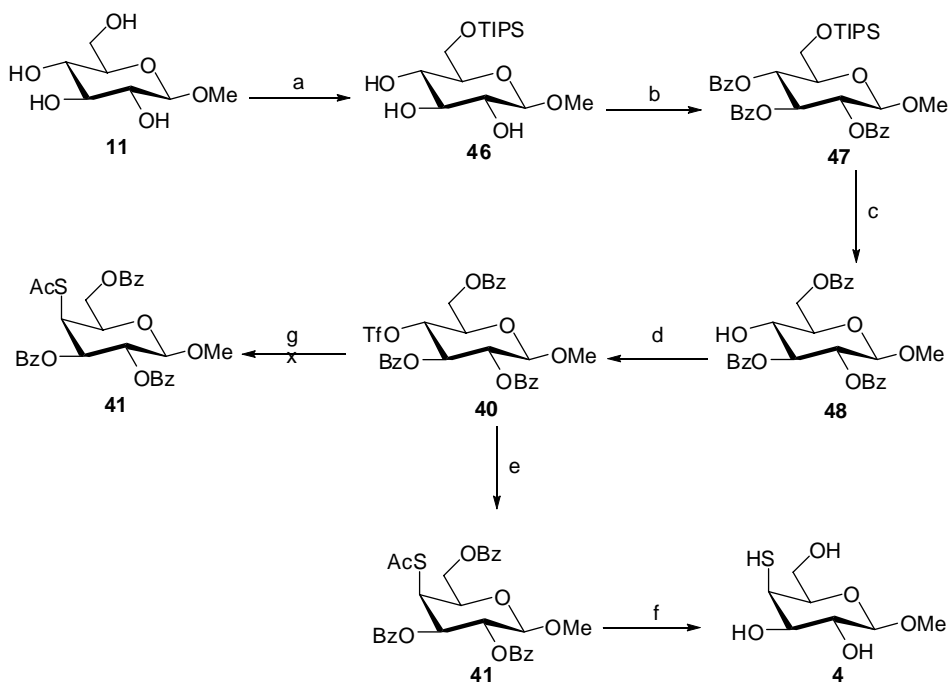
As a comparison, an alternative route to 3-SAc-galactosides, using the 4,6-*O*-benzylidene **42** instead of ester protecting groups,^{50,68} was carried out (Scheme 8). In this case, compound **43** was formed in good yield in DMF using KSAc as nucleophile. This supports the finding that an axial ester functionality in the 4-position is the major reason for competing reaction to occur, and also supports the lack of participation from the ester in the equatorial 2-position. In addition, compound **45** could be efficiently obtained from compound **44** in DMF, supporting the participation from the 6-OBz ester functionality in compound **40**. In the latter case, however, benzyl protecting groups are less favorable in these syntheses, owing to complications in deprotection by hydrogenation.

The results indicate that 3- and 4-SAc glycosides of the galacto-, gluco-, and gulo-series can be efficiently prepared using simple nucleophilic substitution of the parent triflates with thioacetate, where the potential influence from adjacent ester protecting groups has been mapped, and the desired products could be formed in good yields in all cases. Strong solvent-dependence was especially found for 3,4-*anti*-diaxial relationship between the ester and the leaving group, however, the galacto derivatives could nevertheless be generated under kinetic control.

2.1.1.4 Methyl 4-thiol- β -D-galactopyranoside (**4**)

Synthesis of **4** was reported by A. Maradufu and his coworkers. They used a rather complicated route without any analytical data.⁶⁹ In our preliminary study, the key intermediate methyl β -D-glucoside derivative **48**, where the hydroxyl group in the 4-position was free and the other positions were protected with benzoyl groups, was obtained in 3 steps from methyl β -D-glucoside (pathway **a**, **b**, **c** in Scheme 9).⁷⁰ Firstly, methyl β -D-glucoside was selectively converted into the corresponding 6-TIPS (triisopropylsilyl) derivative **46** by treatment of **11** with TIPSCl in DMF in the presence of imidazole, subsequent benzylation of all other positions gave **47**. Treatment of **47** with fluoride as reaction promoter led to the key intermediate 4-OH glucoside derivative **48**.

SCHEME 9 ^a



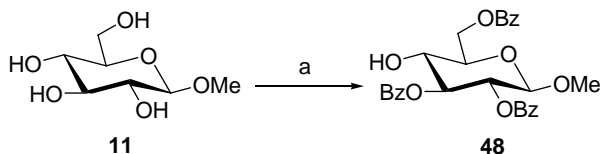
^a Reagents and conditions: (a) TIPSCl, DMF, imidazole, rt, 1h; (b) BzBr, DMF, rt, 2h, 80% for 2 steps; (c) TBAF, THF, 0 °C, 1h, 85%; (d) Tf₂O, pyridine, CH₂Cl₂, -30 - 0 °C, 2h; (e) TBASAc, toluene, rt, 4h, 76%; (f) NaOMe, MeOH, rt, 2h, 86%; (g) KSAc, DMF, rt.

Our initial strategy included the introduction of a triflate at C-4 in **48** to afford **40**, followed by inversion of **40** with potassium thioacetate in DMF to yield the desired C-4 inverted **41**. Unfortunately, attempted thiolation of **40** with potassium thioacetate in DMF

afforded a mixture of products (pathway **g** in Scheme 9). We assumed that the problem was caused from the six-membered acetoxonium ring arising from 6-OBz group in the polar solvents. To suppress this neighboring group participation in polar solvents, we attempted thiolation of **40** with potassium thioacetate in toluene to afford C-4 inverted **41** (pathway **e** in Scheme 9), and subsequent deprotection of **41** to obtain **4**.

In a recent study, a convenient route to obtain the key intermediate methyl 4-OH glucoside derivative **48** was developed based on a one-pot, organotin-mediated multiprotection procedure (Scheme 10).⁵⁵ Treatment of methyl β -D-glucoside with three equivalents of dibutyltin oxide and subsequent benzylation with three equivalents of benzoyl chloride at 90 °C in toluene afforded methyl 4-OH glucoside derivative **48** in a high yield.

SCHEME 10 ^a

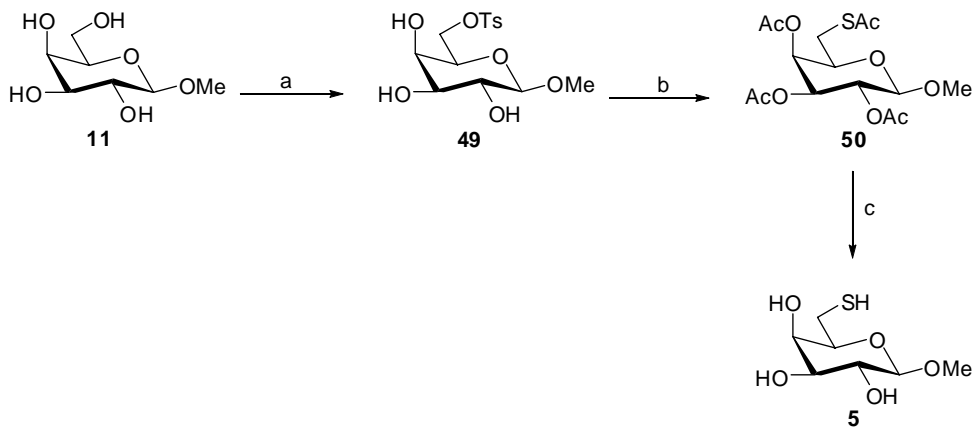


^a Reagents and conditions: (a) i: Bu₂OSn, MeOH, reflux, 2h; ii: BzCl, toluene, 0 °C - rt, 6h, 75%.

2.1.1.5 Methyl 6-thiol- β -D-galactopyranoside (**5**)

Compound **5** can also be easily synthesized due to the 6-OH being a primary hydroxyl group, which is more reactive than the other secondary hydroxyl groups. Synthesis of **5** was reported by B. P. Branchaud and his coworker, however without any analytical data.⁷¹ The synthetic route of Compound **5** is displayed in Scheme 11. Tosylation of **11** with tosyl chloride, subsequent acetylation, displacement with thioacetate, and final deprotection afforded **5**.

SCHEME 11 ^a



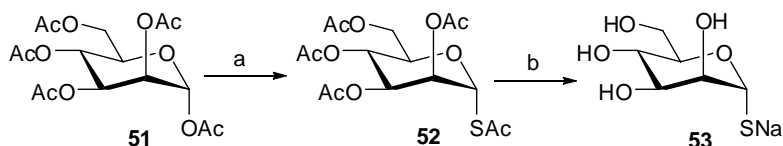
^a Reagents and conditions: (a) TsCl, pyridine, 0 °C - rt, 2h, 72%; (b) i: Ac_2O , pyridine, DMAP, rt, 3 h; ii: KSAC, DMF, 60 °C, 2h, 68%; (c) NaOMe, MeOH, rt, 2h, 93%.

2.1.2 Synthesis of other thiol-carbohydrates

2.1.2.1 1-Thiol- α -D-mannopyranoside sodium salt (paper I)

Compound **53** was easily prepared in two steps according to Scheme 12.⁷²

SCHEME 12 ^a

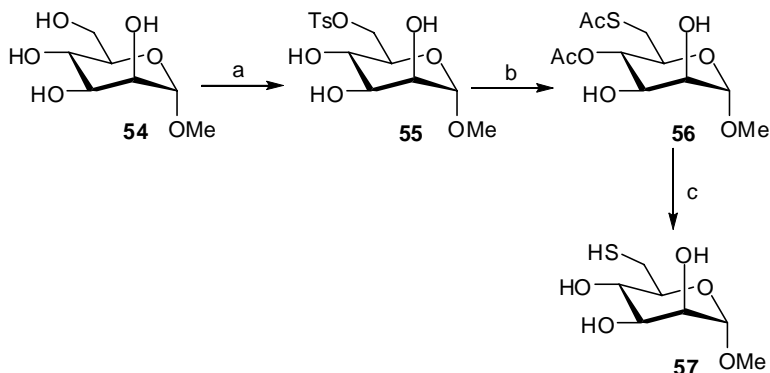


^a Reagents and conditions: (a) HSAc, $\text{BF}_3 \cdot \text{Et}_2\text{O}$, CH_2Cl_2 , 0°C - rt, 65%; (b) MeONa, MeOH, rt, 90%.

2.1.2.2 Methyl 6-thiol- α -D-mannopyranoside (paper I)

Tosylation of Methyl α -D-mannoside gave **55**,⁷³ subsequent nucleophilic displacement of the tosylate group of **55** by potassium thioacetate in DMF led to the thiol derivative **56** with an acetate protecting group in the 4 position (Scheme 13). It is suggested that the acetyl group migrates from the 6 position to the 4 position in polar solvent.

SCHEME 13 ^a

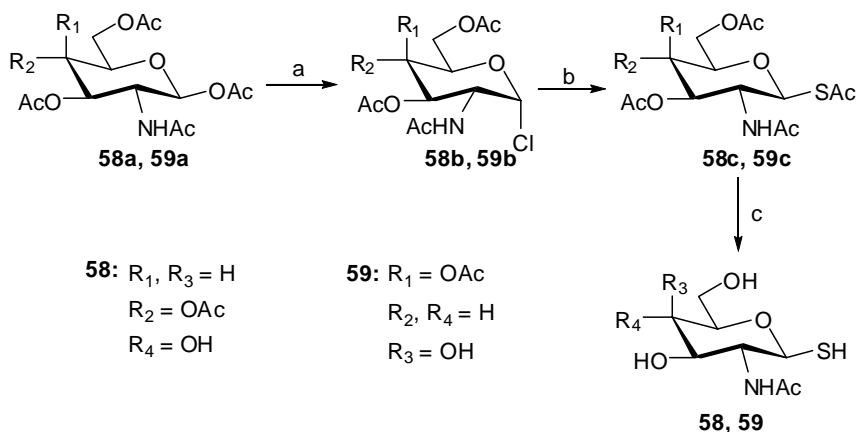


^a Reagents and conditions: (a) TsCl , pyridine, 0°C , rt, (70%); (b) KSAc, DMF, N_2 , 60°C , 60%; (c) i: LiOH, MeOH, H_2O , rt; ii: H^+ exchange resin, 90%.

2.1.2.3 2-(acetylamino)-2-deoxy-1-thio- β -D-glucopyranoside and 2-(acetylamino)-2-deoxy-1-thiol- β -D-galactopyranoside (paper II)

The two *N*-acetylated compounds **58** and **59** were prepared from their chloroacetyl derivatives, as outlined in Scheme 14. Thioacetic acid under biphasic conditions and a phase-transfer reagent were used to obtain the peracetylated 1-thioglycosides. Deprotection with lithium hydroxide solution produced the 1-thioglycosides (Scheme 14).⁷⁴

SCHEME 14^a

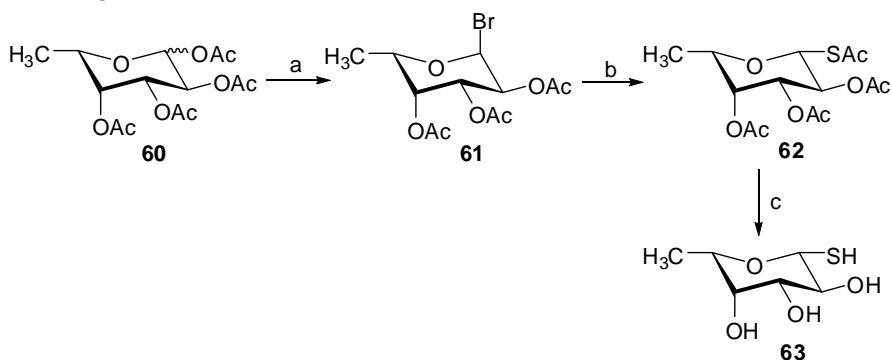


^a Reagents and conditions: (a) HCl, Ac₂O, rt, 60%; (b) HSAc, Na₂CO₃ (aq), TBAHS, CH₂Cl₂, rt, 50%; (c) i: LiOH, MeOH, H₂O, rt; ii: H⁺ exchange resin, 98%.

2.1.2.4 1-Thiol- β -L-fucoside and 1-thiol- β -D-lactoside (paper II)

The synthesis of the *S*-fucoside was generated via the bromoacetyl derivative **61** (Scheme 15). Treatment of **61** with thioacetic acid under biphasic conditions and a phase-transfer reagent afforded the peracetylated 1-thiol-fucoside **62**. Deprotection of **62** with lithium hydroxide solution produced the 1-thiofucoside **63**. 1-thiol- β -D-lactoside was synthesized using the same procedure as **63**.^{75,76}

SCHEME 15 ^a

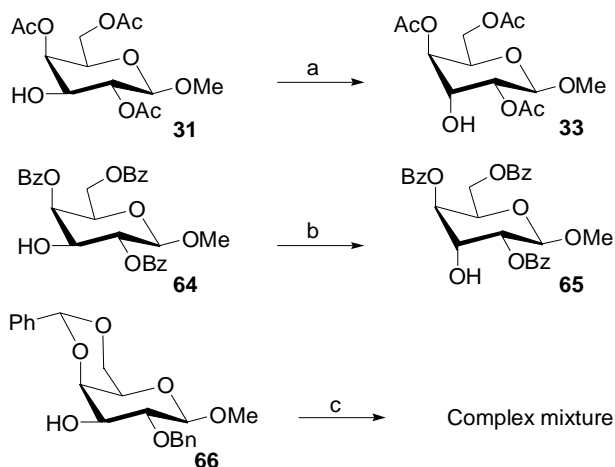


^a Reagents and conditions:: (a) HBr, HAc, CH_2Cl_2 , rt, 65%; (b) HSAc, Na_2CO_3 (aq), TBAHS, CH_2Cl_2 , rt, 50%; (c) i: LiOH, MeOH, H_2O , rt; ii: H^+ exchange resin, 98%.

2.2 Carbohydrate epimerization (paper III)

The Lattrell-Dax-method of nitrite-mediated substitution of triflates is an efficient method to generate structures of inverse configuration. Epimerization of carbohydrate structures to the corresponding epi-hydroxy stereoisomers, was first discovered by Lattrell and Lohaus,⁷⁷ and employed by Dax and co-workers, where it involved the triflation of the hydroxyl groups followed by substitution with nitrite. However, the structural implications influencing the outcome of the epimerization for specific carbohydrate structures have not been fully explored. In our study, epimerization of galacto- to gulo-, galacto- to gluco-, gluco- to galacto-, and gluco- to mannopyrannoside derivatives by triflation/nitrite treatment were therefore tested.

SCHEME 16^a



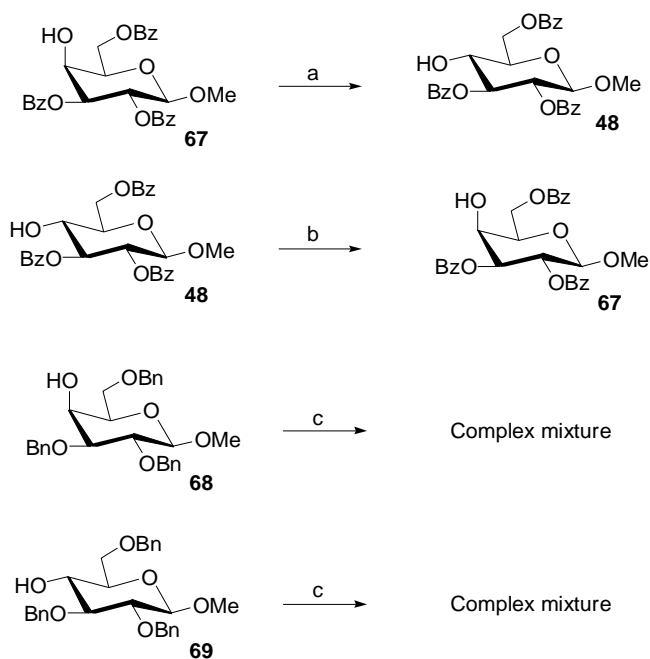
^a Reagents and conditions: (a) i: TiF_2O , pyridine, CH_2Cl_2 , $-20\text{ }^\circ\text{C} - 10\text{ }^\circ\text{C}$, 2h; ii: KNO_2 , DMF, $50\text{ }^\circ\text{C}$, 3h, 73%; (b) i: TiF_2O , pyridine, CH_2Cl_2 , $-20\text{ }^\circ\text{C} - 10\text{ }^\circ\text{C}$, 2h; ii: KNO_2 , DMF, $50\text{ }^\circ\text{C}$, 6h, 77%; (c) i: TiF_2O , pyridine, CH_2Cl_2 , $-20\text{ }^\circ\text{C} - 10\text{ }^\circ\text{C}$, 2h; ii: KNO_2 , DMF, $50\text{ }^\circ\text{C}$, 3h.

Firstly, an approach to study the effect of the protecting group pattern to the inversion reaction for the epimerization of galactoside derivatives, where the hydroxyl group in the 3-position was free and the other positions separately protected with acetyl (**31**), benzoyl (**64**), and benzyl/benzylidene groups (**66**), respectively, was investigated (Scheme 16). These compounds were subjected to conventional triflation by triflic anhydride followed by treatment with potassium nitrite in DMF at $50\text{ }^\circ\text{C}$. The result clearly showed that good yields were in these cases obtained only on condition that esters were chosen as protecting groups, benzoyl groups being slightly less activating than the acetyl counterparts. A

mixture of different products was obtained when the benzyl or benzylidene were used as protecting groups.

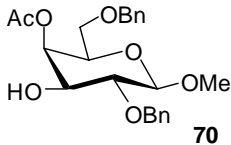
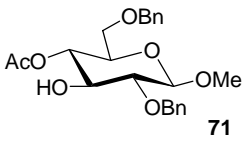
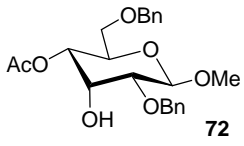
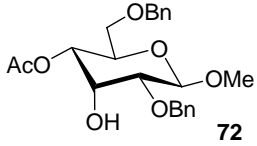
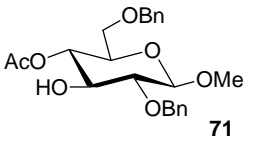
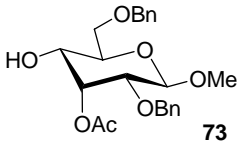
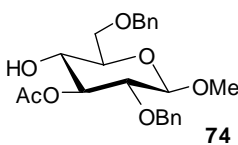
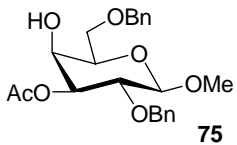
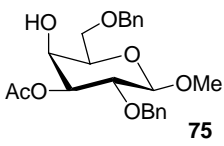
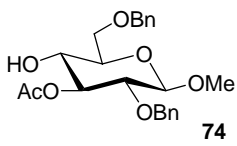
Secondly, the effect of the protecting group pattern to the inversion reaction for the epimerization of galactoside and glucoside derivatives, where the hydroxyl group in the 4-position was free and the other positions separately protected with benzoyl and benzyl groups, respectively, was probed (Scheme 17). It was found that the reaction was able to proceed smoothly only when an ester group was present at the carbon adjacent to the carbon atom carrying the leaving triflate group, the axially oriented triflate being less reactive than the equatorial leaving group. No efficient reaction occurred when benzyl groups were used, where side reactions instead rapidly occurred. These results propose that a neighbouring ester group is able to induce or activate the inversion reaction, whereas an ether derivative is unable to produce this effect. The results also show that the inversion reaction proceeded smoothly in disregard of the triflate configuration.

SCHEME 17^a



^a Reagents and conditions: (a) i: TiF_2O , pyridine, CH_2Cl_2 , $-20\text{ }^\circ\text{C}$ - $10\text{ }^\circ\text{C}$, 2h; ii: KNO_2 , DMF, $50\text{ }^\circ\text{C}$, 5h, 75%; (b) i: TiF_2O , pyridine, CH_2Cl_2 , $-20\text{ }^\circ\text{C}$ - $10\text{ }^\circ\text{C}$, 2h; ii: KNO_2 , DMF, $50\text{ }^\circ\text{C}$, 2h, 70%; (c) i: TiF_2O , pyridine, CH_2Cl_2 , $-20\text{ }^\circ\text{C}$ - $10\text{ }^\circ\text{C}$, 2h; ii: KNO_2 , DMF, $50\text{ }^\circ\text{C}$, 0.5h.

Table 4. Epimerization reactions studied

Reactant	Time/h	Product	Yield/%
 70	3	Complex mixture	-
 71	0.5	 72	69
 72	4	 71	73
 73	3	Complex mixture	-
 74	1.5	 75	72
 75	4	 74	75

Thirdly, in order to further explore the effect of neighbouring ester group configuration of triflate to the reactivity, other inversion schemes were designed (Table 4). To avoid the influences from the 2- and 6-positions and to isolate the effects caused from ester groups in the 3- and 4-positions, the 2- and 6-positions were protected with benzyl ether groups. Therefore, a range of compounds, where one of the hydroxyl groups in the 3- or 4-positions was protected with an acetyl group, were prepared, and subsequently tested in the nitrite-mediated inversion reactions. It was found that not only a neighboring ester group in

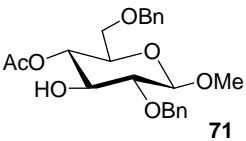
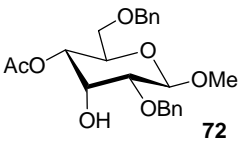
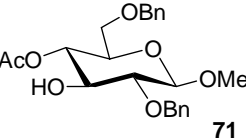
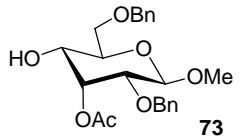
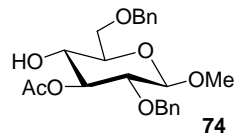
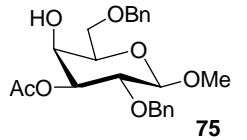
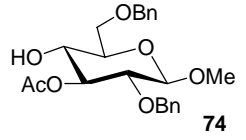
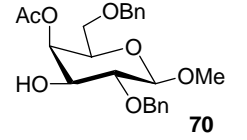
the equatorial position was necessary for the reactivity of the epimerization reaction, but also the relative configurations between the ester group and the leaving group was crucial for the efficiency of the reaction (Table 4). The result clearly showed that efficient inversion occurred when the structure contained a 3,4-*trans* configuration with diequatorial relationship.

The results obtained seem to point to the importance of a neighboring group (acyloxonium) effect. Compounds **71** and **74** (3,4-*trans*) expressed a higher reactivity due to activation from the neighbouring ester group in inducing the inversion reaction than compounds **72** and **75** (3,4-*cis*). This is reflected in the longer reaction times for the 3,4-*cis* compounds as displayed in Table 4. However, acyloxonium formation is still unlikely to be the sole explanation of the results, contradictory to the results for two reasons: i) starting compounds **67**, **72** and **75** all have *cis*-relationship between the ester and the leaving group, which largely disqualifies acyloxonium formation;^{78,79} ii) formation of a carbocation intermediate would result in nucleophilic displacement from the triflate face of the compound leading to retention (double inversion) of configuration rather than single inversion.

An acyloxonium formation is important in the *trans*-configuration cases. This was further supported by studies with added water. Thus, compounds **71** and **74**, both with 3,4-*trans*-diequatorial relationships, mainly yielded compounds **72** and **75** from reaction with potassium nitrite in dry DMF. If on the other hand wet DMF was used, compounds **70** and **73** were instead obtained as the main products (Table 5). This suggests acyloxonium formation to the five-membered ring intermediate, which rapidly collapses in the presence of water to produce the axial ester and the equatorial hydroxyl group. These results are indicative of (partial) acyloxonium formation in the *trans*-configuration cases, but that the nitrite ion is unable to open the five-membered ring from either the triflate face, or from attacking the carbonyl cation as has been suggested for the reaction with added water.⁸⁰ More importantly, the ester group is therefore likely to induce or stabilize the attacking nitrite ion regardless of the *trans*- or *cis*-configurational relationships.

The effects observed for the ether protected carbohydrates are likely due to their lower degree of positive charge destabilization than the corresponding ester groups, leading to side reactions such as ring contraction and elimination.^{81,82}

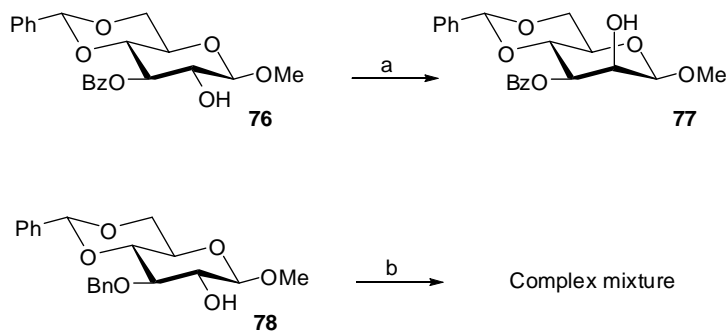
Table 5. Water effects in studied nitrite-mediated inversion reactions.

Reactant	Nucleophile ^a	Product	Yield/%
 71	KNO ₂	 72	69
 71	H ₂ O	 73	70
 74	KNO ₂	 75	72
 74	H ₂ O	 70	70

^a i: Tf₂O, pyridine, CH₂Cl₂, -20 °C - 10 °C, 2h; ii: KNO₂, 50 °C, DMF, 0.5-1.5h, or H₂O, rt, DMF, 6h.

To further prove the hypothesis of ester activation in the nitrite-mediated inversion reaction, the inversion reactions for glucopyranoside compounds **76** and **78** were tested (Scheme 18). In this case, the hydroxyl group in the 3-position was free and the other positions separately protected with acetyl (**31**), benzoyl (**64**), and benzyl/benzylidene groups (**66**), respectively. No inversion behavior in the 3- and 4-position of the hexopyranosides was observed, instead the 2- and 3-positions were retained (2,3-*trans*). The results clearly show that the hypothesis was valid also for these compounds, where the ester-protected glucopyranoside compound **76** afforded the inversion mannopyranoside product **77** in good yield, whereas the ether-protected compound **78** provided a mixture of products (Table 5). In this case, slightly longer reaction time was however necessary due to the lower reactivity of the 2-OTf derivative.

SCHEME 18^a



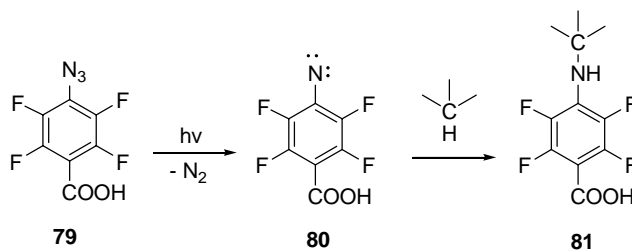
^a Reagents and conditions: (a) i: TiF_2O , pyridine, CH_2Cl_2 , $-20\text{ }^\circ\text{C} - 10\text{ }^\circ\text{C}$, 2h; ii: KNO_2 , DMF, $50\text{ }^\circ\text{C}$, 6h, 74%; (b) i: TiF_2O , pyridine, CH_2Cl_2 , $-20\text{ }^\circ\text{C} - 10\text{ }^\circ\text{C}$, 2h; ii: KNO_2 , DMF, $50\text{ }^\circ\text{C}$, 3h.

Our study clearly shows that ester protecting groups play highly important roles in the Lattrell-Dax reaction facilitating nitrite-mediated carbohydrate epimerizations. Ether protecting groups as well as benzylidene protecting groups proved to be inefficient. Furthermore, it was found that only neighboring ester groups in the equatorial configuration could induce the formation of inversion compounds in good yields in these reactions, whereas the axially oriented neighboring ester groups were inefficient.

2.3 Synthesis of PFPA derivatives (paper VII and paper VIII)

Aryl azides are photoactive compounds, which can produce aryl nitrenes that are capable of undergoing C-H and/or N-H insertion reactions with neighboring molecules upon photolysis (Scheme 19).⁸³ Keana and Cai in 1990 reported that fluoro- substituted aryl azides (perfluoro-phenylazides, PFPAs) give higher yield of C-H insertion than their nonfluorinated analogues, because of the higher reactivity of the nitrenes and of the lack of ring expansion.⁸⁴

SCHEME 19



The versatility of functionalized PFPAs makes them especially useful for surface modification.^{85,86} In the present study, a series of functionalized PFPAs was synthesized for the fabrication of the surfaces (Figure 8), where PEG-modified QCM system and carbohydrate microarrays based on the C-H and/or N-H insertion reaction between functionalized PFPAs and polymer, were developed.

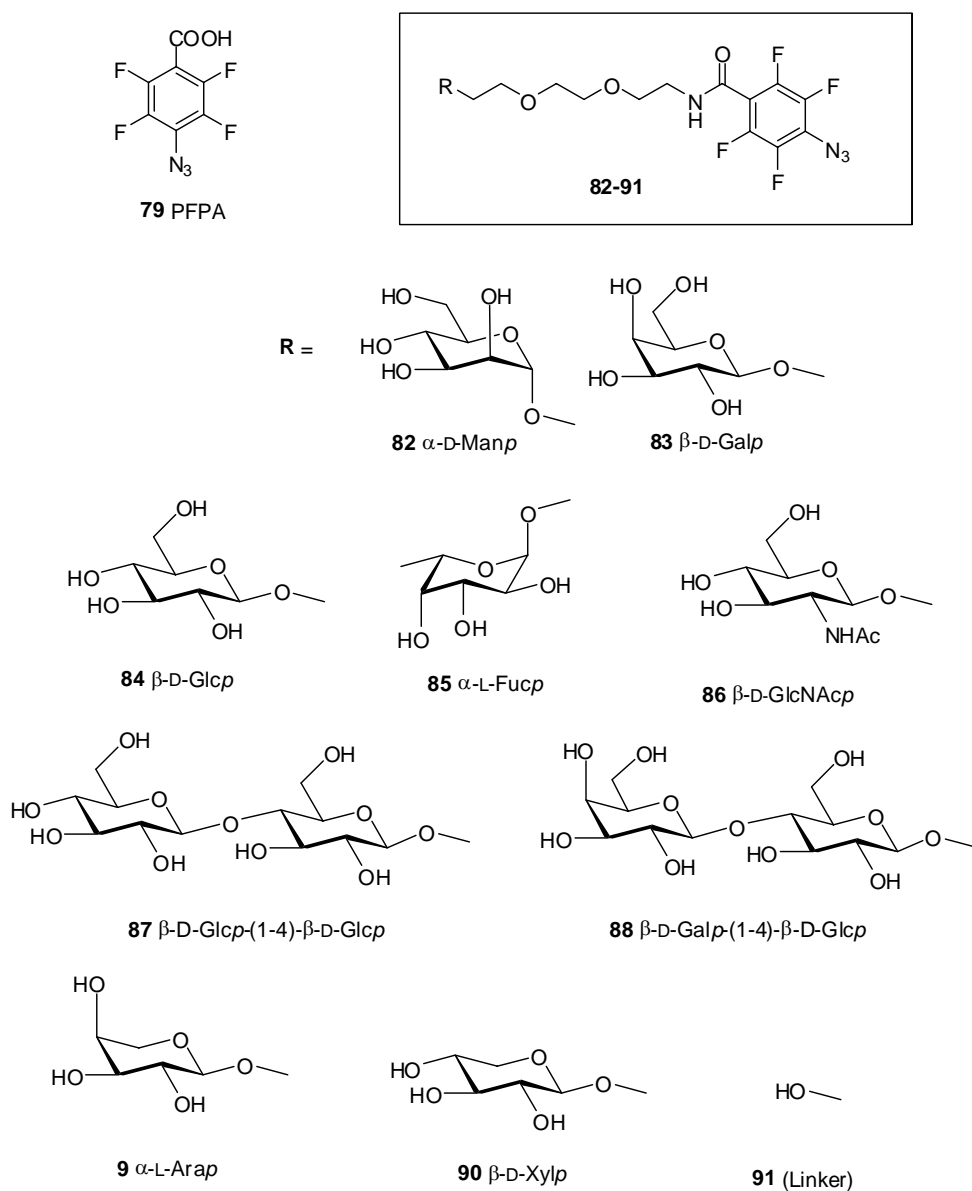
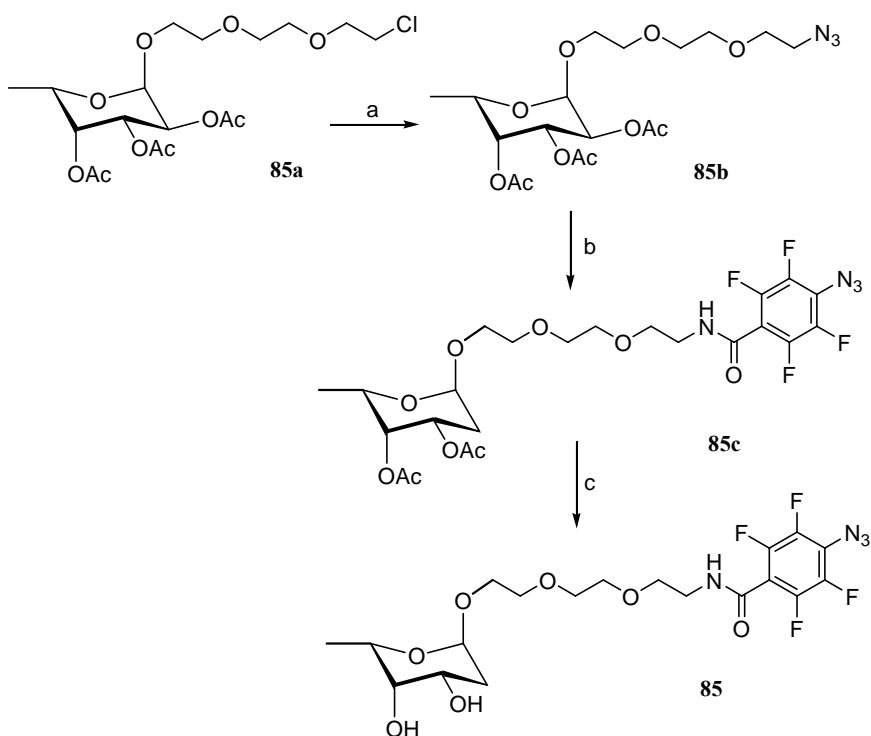


Figure 8. PFPA and Compounds used in array generation.

2.3.1 Synthetic routes for compounds 82, 83, 84, 85, 86

PFPA derivatives **82**, **83**, **84**, **85** and **86** were synthesized by using the same synthetic route (Scheme 20), as exemplified below for fucose derivative **85**. Firstly, fucose derivative **85a** was obtained by treatment of tetra-*O*-acetate- α -L-fucose with 2-[2-(2-chloro-ethoxy)-ethoxy]-ethanol using Lewis acid activation. The resulting **85a** can subsequently be converted to compound **85b** by nucleophilic substitution. Metal hydrogenation of **85b** with Pd/C under hydrogen atmosphere, followed by treatment with PFPA **79** using EDCI and triethylamine as catalyst gave **85c**. Compound **85** was then obtained after deprotection.

SCHEME 20^a

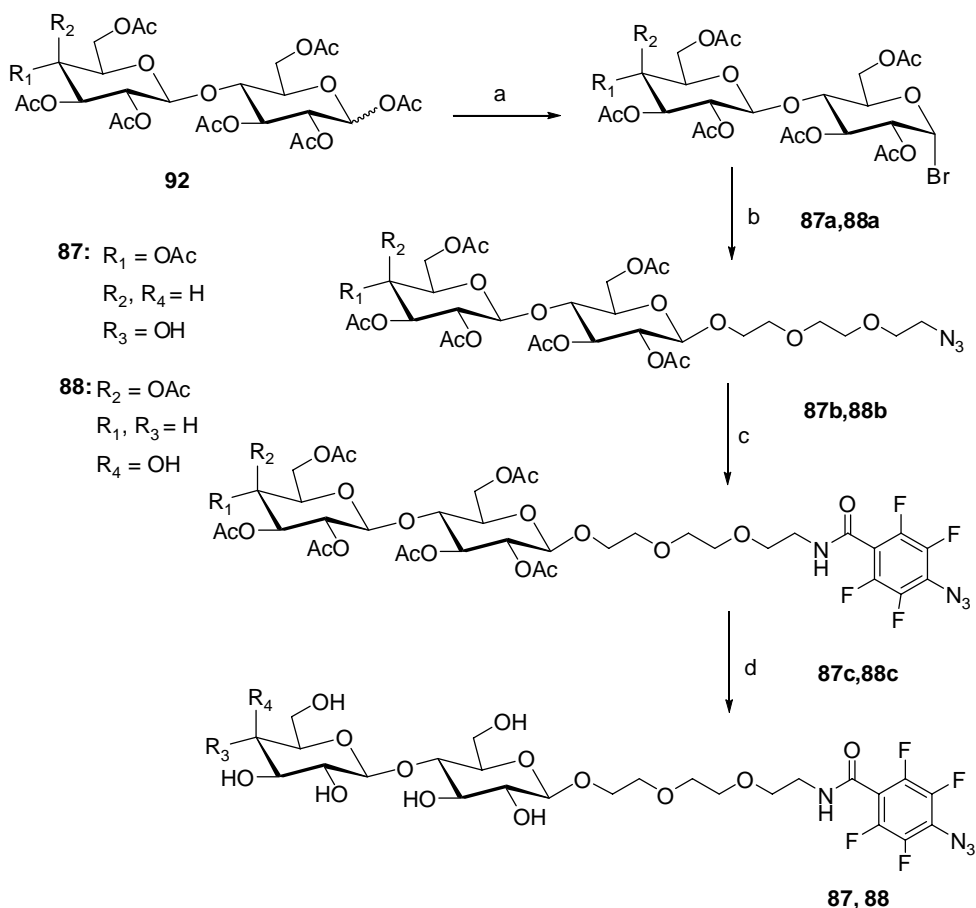


^a Reagents and conditions: (a) NaN₃, DMF, 90 °C, dark, 20h, 25% for 2 steps; (b) i: Pd/C, acetic acid, H₂, MeOH, rt, 4h, 95%; ii: PFPA, EDCI, Triethylamine, CH₂Cl₂, 0 °C - rt, overnight, 33%; (c) NaOMe, MeOH, rt, 2h, 64%.

2.3.2 Synthetic routes for compounds **87**, **88**, **89**, **90**

The syntheses of PFPA derivatives **87**, **88**, **89**, **90** were performed via the bromoacetyl derivatives (Scheme 21). For instance, treatment of bromoacetyl derivative **88a** with 2-[2-(2-azido-ethoxy)-ethoxy]-ethanol by the use of silver triflate as activator afforded **88b**. From **88b** to **88**, the same synthetic procedure as for compound **85** was used.

SCHEME 21^a

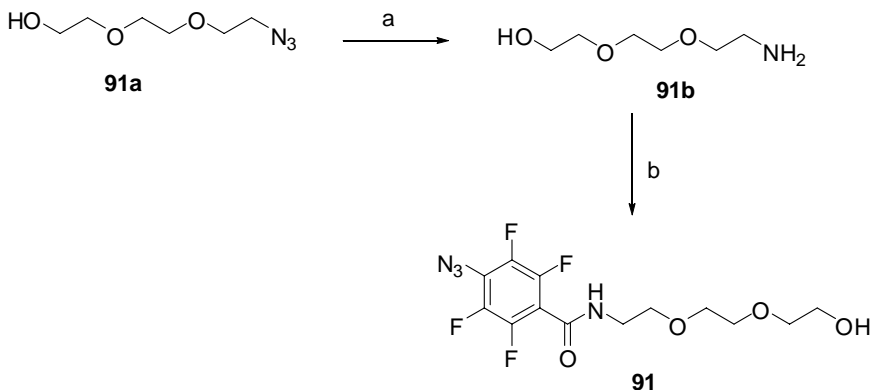


^a Reagents and conditions: (a) HBr, HAc, CH₂Cl₂, rt, 65%; (b) 2-[2-(2-azido-ethoxy)-ethoxy]-ethanol, AgOTf, CH₂Cl₂, -30 °C, dark, 2h, 60%; (c) i: Pd/C, acetic acid, H₂, MeOH, rt, 4h, 95%; ii: PFPA, EDCI, triethylamine, CH₂Cl₂, 0 °C - rt, overnight, 33%; (d) NaOMe, MeOH, rt, 2h, 60%.

2.3.3. Synthetic route for PFPA-linker (91)

PFPA-linker **91** was prepared in two steps from derivative **91a**, via reduction and coupling with PFPA acid (Scheme 22).

SCHEME 22^a

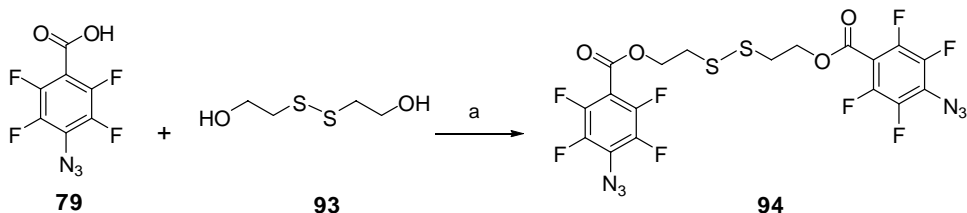


^a Reagents and conditions: (a) Ph₃P, THF, 0 °C - rt, H₂O, 5h; (b) PFPA, EDCI, Triethylamine, CH₂Cl₂, 0 °C - rt, overnight, 36% for 2 steps.

2.3.4 Synthetic route for PFPA-disulfide (94)

Synthesis of PFPA-disulfide **94** was performed according to the following strategy. Treatment of PFPA **79** with **93** gave product **94** in one step (Scheme 23).

SCHEME 23^a



^a Reagents and conditions: (a) DMAP, DCC, CH₂Cl₂, 0 °C - rt, dark, 12h, 40%.

3. Analysis and recognition

3.1 Target lectins (Lectin crystal structures from the website: <http://www.cermav.cnrs.fr/lectines>)

3.1.1 Concanavalin A (Con A)

Con A from jack bean is the first lectin whose structure became known, as well as one of the most widely used and well characterized lectins.^{7,9} Con A has broad applicability since it can recognize a commonly occurring sugar structure, α -linked mannose. A wide variety of serum and membrane glycoproteins have a "core oligosaccharide" structure which includes α -linked mannose residues, thus, many glycoproteins can be examined with Con A. Con A consists of 237 amino acids. Structural features of the amino acid chain are two antiparallel beta sheets. One of these is built from seven strands. The other sheet contains six strands. Above pH 7, Con A exists mainly as a tetramer: two six stranded sheets are joined together to form a twelve-stranded dimer, which in turn form a functional complex by interactions side by side with another dimer to result in four binding sites for the carbohydrates.⁸⁷ Con A has two metal binding sites: one Ca^{2+} binding site and one that binds to transition metal ion, usually Mn^{2+} . The metal atoms are bound by amino acids in a loop that points away from the seven-strand pleated sheet. Ligands for the transition metal are Glu₈, Asp₁₀, Asp₁₉ and His₂₄, the calcium ion is bound by Asp₁₀, Tyr₁₂, Asn₁₄ and Asp₁₉. The binding site for the sugar is adjacent to the metal atoms (in this example a trisaccharide formed from mannose is bound). Nitrogen atoms from Asn₁₄, Leu₉₉, Tyr₁₀₀, Asp₂₀₈ and Arg₂₂₈ are involved in the interactions with the saccharide. In addition, α -Man-1,2- α -Man-OMe-Con A complex (crystal structure) reveals a balance of forces involved in carbohydrate recognition (Figure 1 in Introduction).⁹

3.1.2 *Viscum album* agglutinin (VAA)

VAA, mistletoe lectins, are present in all mistletoe extracts in various concentrations. There are three similar lectins in mistletoe plants, called VAA-I, VAA-II and VAA-III, respectively.⁸⁸ The most important and often studied lectin in mistletoe is the galactose-specific VAA-I, which consists of two chains. The A-chain with a molecular weight of 29 kDa and with *N*-glycosidase activity is a potent ribosomal inactivator. The sugar-binding B-chain with a molecular weight of 34 kDa is responsible for the immunomodulatory effect of the molecule (Figure 2 in Introduction). The crystal structure at 3 Å of VAA-I, a dimeric type-II ribosome-inactivating protein, complexed with galactose, is displayed in Figure 9.⁸⁸



Figure 9. Crystal structure of VAA-I, a dimeric type-II ribosome-inactivating protein, complexed with galactose.⁸⁸

3.1.3 *Ulex europaeus* agglutinin I (UEA-I)

UEA-I, extracts from the seeds of *Ulex europaeus*, which is the agglutinating agent with a carbohydrate specificity for α -L-fucose. The crystal structure of UEA-I and α -L-fucose-OMe complex is displayed in Figure 10,⁸⁹ which consists of two UEA-I dimers within the asymmetric unit. The two dimers contain 240 amino acid residues in three of the four UEA-I monomers, and the fourth UEA-I monomer consists of 239 amino acid residues. Four calcium and four manganese ions are present in the structure, where one Ca^{2+} and one Mn^{2+} are in each subunit. There are also four bound α -L-fucose-OMe in the structure, where one α -L-fucose-OMe locates in each UEA-I monomer.



Figure 10. The crystal structure of UEA-I and α -L-fucose-OMe complex.⁸⁹

3.1.4 Soybean agglutinin (SBA)

The soybean agglutinin lectin (SBA), which is isolated from *Glycine max*, selectively binds terminal α - and β -N-acetyl-galactosamine and galactopyranosyl residues. SBA exists as a tetramer with a molecular weight of approximately 12 kDa with one sugar binding site per monomer, as well as one Ca^{2+} and one Mn^{2+} in each subunit.^{80,91} The structure of the SBA monomer consists of 234 of the total 253 residues and is similar to that of other legume lectins as expected from their sequence identity. The polypeptide fold contains two

separate sheets of antiparallel β -strands, there are six strands in the first β -sheet. The other β -sheet consists of seven antiparallel strands, and the outer two of which compose the support of the metal binding region. X-ray crystal structure of the soybean agglutinin complexed with β -Gal-(1-4)- β -GlcNAc is displayed in Figure 11.⁹²

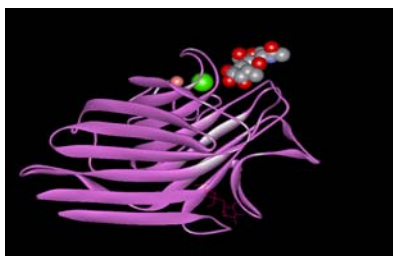


Figure 11. X-ray crystal structure of the soybean agglutinin complexed with β -Gal-(1-4)- β -GlcNAc.⁹²

3.1.5 Peanut agglutinin (PNA)

The peanut agglutinin PNA lectin, which is isolated from *Arachis hypogea*, is specific for terminal β -galactose. PNA exists as a tetramer composed of identical subunits, and has a molecular weight of approximately 110 kDa with one sugar binding site per monomer, as well as one Ca^{2+} and one Mn^{2+} in each subunit. The single chain in each subunit is 236 amino acid residues. The X-ray crystal structure of PNA complexed with β -Gal-(1-4)- β -GlcNAc is displayed in Figure 12.⁹³

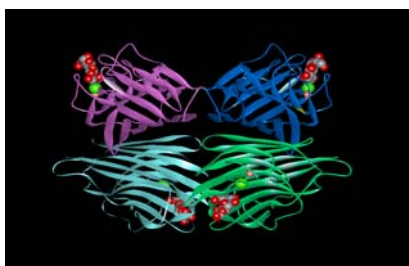


Figure 12. X-ray crystal structure of Peanut PNA complexed with β -Gal-(1-4)- β -Glc.⁹³

3.1.6 Griffonia simplicifolia lectin II (GS-II)

The lectin GS-II, isolated from the seeds of the tropical African legume *Griffonia simplicifolia* (formerly *Bandeiraea simplicifolia*),⁹⁴ is a 113 kDa tetramer composed of

identical subunits. Each subunit contains a single binding site specific for terminal, non-reducing α - and β -linked *N*-acetyl-glucosamine.⁹⁵

3.1.7 *Pisum sativum* agglutinin (PSA)

Pisum sativum agglutinin (PSA), isolated from the garden pea, which is very similar with Con A in the structural properties, but exhibits different binding affinities for the mano- and gluco- derivatives. PSA exists as dimer with a molecular weight of approximately 48000 daltons with one sugar binding site per monomer, as well as one Ca^{2+} and one Mn^{2+} in each subunit. The monomer consists of two different polypeptide chains, one 6 kDa (α -chain) and another 18000 (β -chain).⁹⁶ The X-ray crystal structure of PSA complexed with α -Man-(1,3)- α -Man-(1,6)- α -Man is displayed in Figure 13.⁹⁷

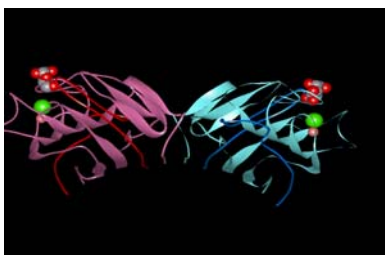


Figure 13. X-ray crystal structure of *Pisum Sativum* (PSA) complexed with α -Man-(1,3)- α -Man- α -(1,6)-Man.⁹⁷

3.1.8 Galectin-3

Galectin-3, a lectin of the galectin family, is defined by a conserved 14 kDa carbohydrate recognition domain with an approximate molecular weight of 30 kDa showing affinity for β -galactoside, which is extensively distributed in the animal kingdom.

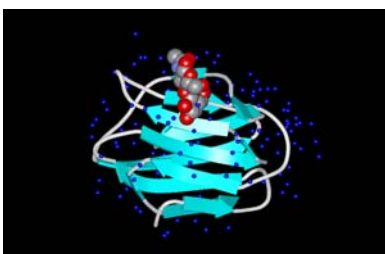


Figure 14. X-ray crystal structure of Galectin-3 complexed with β -Gal-(1,3)-GlcNAc.¹⁰⁰

It is composed of 5-stranded (F1-F5) and 6-stranded (S1-S6a/6b) β -sheets, where the carbohydrate binding site is formed by β -sheets S4-S6a/6b.⁹⁸ A variety of biological functions have been proposed for this protein, such as an involvement in the cell growth regulation, pre-mRNA splicing, cell adhesion to basement membranes and mast cells. Moreover, galectin-3 is generally associated with tissues in processes of differentiation and upregulated in neoplastic transformation.⁹⁹ The X-ray crystal structure of galectin-3 complexed with β -Gal-(1,3)-GlcNAc is displayed in Figure 14.¹⁰⁰

3.2 Quartz crystal microbalance (QCM)

Investigation of carbohydrate-protein interactions have previously been efficiently explored by various methods, such as SPR, NMR, ELISA, etc.¹⁰¹⁻¹⁰⁵ The advantage of QCM biosensors in studying carbohydrate-protein interactions is their ability to monitor the changes of small masses in real time, where such analyses can be carried out using the native or synthetic molecules without any labeling. Here, two different novel QCM biosensor systems have been developed.

3.2.1 Mannan coated QCM system

The yeast mannan has often been serving as immobilized ligand, and easily absorbed to polystyrene surfaces and well suited to various microtiter plate formats. In the present study, our efforts focused on the development of a QCM biosensor systems based on mannan surfaces, where polystyrene-coated crystals was used as substrate for mannan immobilisation. Furthermore, the carbohydrate-lectin interactions based on the mannan-coated QCM biosensors were explored.

3.2.1.1 Development of mannan-expressing surfaces for study of real-time lectin-carbohydrate interactions using QCM (paper IV)

3.2.1.1.1 Preparation of mannan surfaces

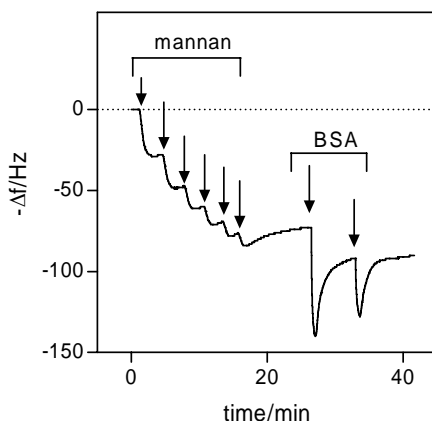


Figure 15. Immobilisation of yeast mannan and blocking with BSA on the polystyrene coated quartz crystal. Multiple injections were made to ensure sufficient binding time and optimal surface coverage. The negative frequency shifts indicate binding to the surface.

Gold-plated, 10 MHz quartz crystals were immersed into a polystyrene solution (0.5% in toluene), followed by evaporation of the solvent under a stream of nitrogen. The resulting crystals were subsequently mounted in the QCM system, equilibrated with buffer solution

(10 mM PBS, pH 7.4), and coated with yeast mannan (50 µg/mL in PBS) repeatedly until no further mass change was recorded (Figure 15). After blocking the surface with bovine serum albumin (10 mg/mL in PBS, repeated injections), the system was allowed to equilibrate until a stable condition was obtained.

The thickness of the polystyrene film (t) was tested by QCM measurements (standard crystals) and ellipsometry (polished crystals), before and after polystyrene coating. For the condensed layer of polystyrene, the Sauerbrey equation was applied (Equation 1), relating the frequency shift (Δf) to the mass difference (Δm), and the resulting layer thickness.¹⁰⁶

$$\Delta f = -2f_0^2 \Delta m / [nA(\mu_q \rho_q)^{0.5}] = -2f_0^2 \rho_f t / [n(\mu_q \rho_q)^{0.5}] = -C_f t \quad (\text{Equation 1})$$

Here, f_0 is the resonance frequency of the unloaded quartz, n is the harmonic resonance number, μ_q is the shear modulus of the quartz crystal, ρ_q is the density of the quartz crystal, A is the surface area, and ρ_f is the density of the polystyrene film. In the present case, with $f_0 = 10.0$ MHz, $n = 1$, $\mu_q = 2.95 \times 10^6$ N/cm², $\rho_q = 2.65$ g/cm³, $\rho_f = 1.05$ g/cm³, the proportionality constant C_f amounts to 2.4 Hz/Å. Frequency shifts of 650 ± 80 Hz (mean \pm SEM), as well as corresponding film thickness of 280 ± 30 Å were obtained due to polystyrene coating. Reference values given by ellipsometry measurements were found to be similar as the QCM data.

The coverage of the polystyrene film was further evaluated by XPS measurements. The results clearly showed that all the surfaces were covered with hydrocarbons significant for polystyrene and that no gold was visible to the XPS instrument.

3.2.1.1.2 QCM conditions and surface regeneration

All experiments were performed in at least duplicate at ambient temperature by the use of an Attana 80 QCM apparatus. A continuous flow of running buffer was employed throughout, and samples of lectins and/or used ligands were prepared in the identical buffer. The ligand-lectin interactions were monitored by frequency logging, and adsorption/desorption to the surface recorded as the resulting frequency shifts (Δf). Bound lectins were released from the surface between measurements by two successive injections of low pH buffer.

In order to regenerate the surfaces, two methods were tested, where the competition with carbohydrate ligands, and pH control were performed. Competition with concentrated solutions of different ligands (e.g., methyl- α -D-mannopyranoside) proved feasible, however, required multiple injections to restore the original level. Furthermore, this method needed a relatively long desorption time. More efficiently, injection with acidic buffer could remove the lectins completely from the surface, where pH value lower than around 2.5 proved favourable. However, surface degradation occurred at very low pH, and pH 1.5 was chosen as the best alternative, effectively removing all lectins in two successive injections with very low degradation of the surface. A typical

binding/regeneration cycle is displayed in Figure 16, where competition of Con A binding to mannan the surface could be efficiently regenerated with two successive injections of acidic buffer is recorded.

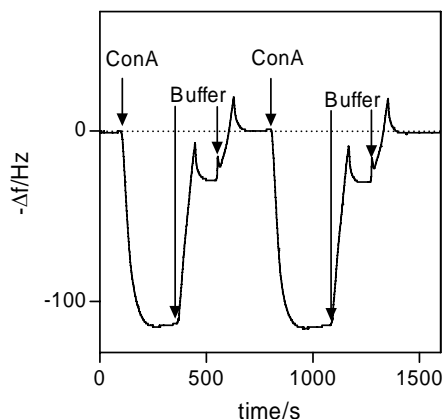
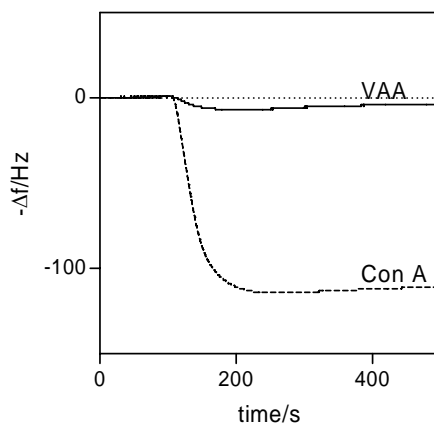


Figure 16. Binding and release of Con A to immobilised mannan. Frequency response plot of Con A binding, and subsequent release by injection of acidic buffer. The mannan surface was completely regenerated after two successive injections, with running buffer introduced into the cell between injections.

3.2.1.1.3 Evaluation of binding selectivity on the surface

The efficiency of the mannan-modified surfaces was initially evaluated by lectin binding, by the use of the α -D-mannopyranoside-specific Con A and the galactopyranoside-specific mistletoe lectin (VAA) as comparison. The resulting frequency-response graphs are displayed in Figure 17. The results clearly showed that the surfaces were selective for Con A, whereas only tiny effects could be recorded for VAA. Similarly, competition of the mannan-Con A interaction with methyl- α -D-mannopyranoside and methyl- β -D-galactopyranoside, respectively, indicated selective competitive effects for the mannoside without competition from the galactoside.

a)



b)

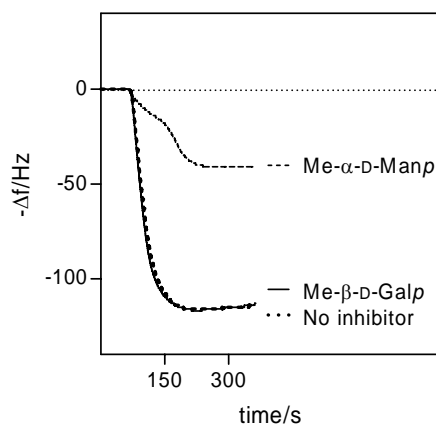


Figure 17. Evaluation of binding selectivity. a) Comparison of binding of Con A and mistletoe lectin (VAA) to mannan-coated surfaces. b) Comparison between methyl- α -D-mannopyranoside and methyl- β -D-galactopyranoside as competitors of the mannan-Con A interaction.

3.2.1.1.4 Saturation binding of Con A to immobilised mannan surface

The apparent K_D for mannan binding to Con A was estimated from saturation binding experiments. Increasing concentrations of Con A were injected over the QCM surface and the frequency decrease recorded. Non-linear regression analysis was for determining the apparent K_D using Equation 2, where Δf is the frequency difference, Δf_{max} the maximum frequency difference (maximum binding), and $[L]$ the lectin concentration.

$$\Delta f = \Delta f_{\max} [L] / (K_D + [L]) \quad (\text{Equation 2})$$

For visualisation purposes, linear transformation of the saturation data was performed using Equation 3.¹⁰⁷

$$[L] / \Delta f = [L] / \Delta f_{\max} + K_D / \Delta f_{\max} \quad (\text{Equation 3})$$

The K_D value for mannan binding to Con A was estimated from saturation binding experiments. Con A was injected over the QCM surface with a range of concentrations (ranging from 5 nM to 40 μ M), and the resulting frequency decrease was recorded. The graph for the resulting frequency is displayed in Figure 18, and indicating that the surface proved completely saturatable, and well following Langmuir-like isothermal behaviour. This is further demonstrated from the linear transformation of the data. Under the present conditions, no non-specific binding was discerned, showing complete coverage of the polystyrene surface by mannan/albumin. The apparent dissociation constant could be estimated to $K_D = 0.4 \mu$ M, a value well in accordance with reported literature values (0.1 - 1.1 μ M).^{108,109}

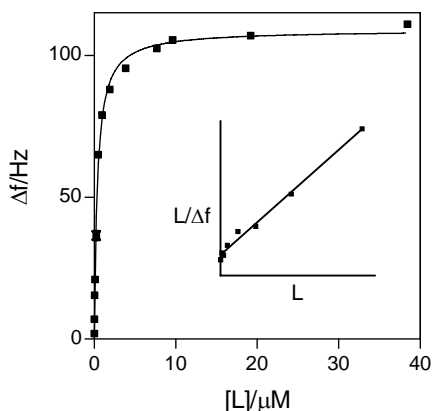


Figure 18. Saturation binding of Con A to immobilised mannan. The surface proved fully saturatable and followed normal Langmuir-like adsorption behaviour. Insert represents linear transformation of data, see text for further explanation. $[L]$: concentration of lectin.

3.2.1.1.5 Competition binding study

Competition experiments were carried out by mixing stock solutions of Con A with consecutively diluted concentrations of tested inhibitors. The reduced frequency difference was taken as a measure of the competitive effect of the analytes. EC_{50} values (50% competition of Con A binding), were estimated by non-linear regression using Equation 4,

where Δf_{min} is the minimum frequency difference, Δf_{max} is the maximum frequency difference, and C is the competitor concentration.

$$\Delta f = \Delta f_{min} + (\Delta f_{max} - \Delta f_{min}) / (1 + 10^{(C - LogEC_{50})}) \quad (\text{Equation 4})$$

Firstly, a typical example for the competition assay is displayed in Figure 19, where 4-nitrophenyl- α -D-mannopyranoside was employed as competitor for Con A/mannan binding. The results clearly show that increasing concentrations of competitor yielded gradually less binding of Con A to the surface, with reduced frequency difference as a consequence.

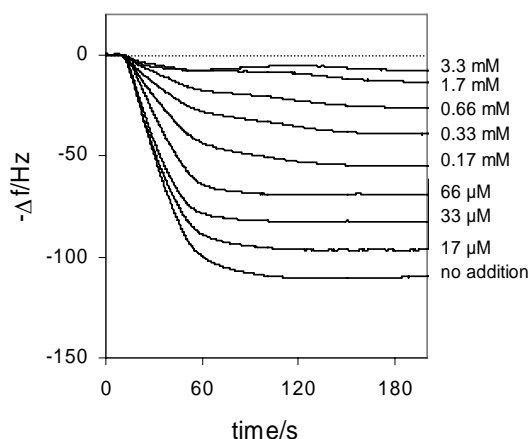
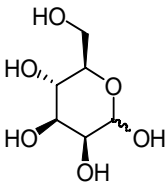
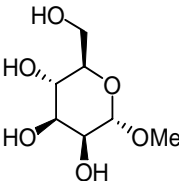
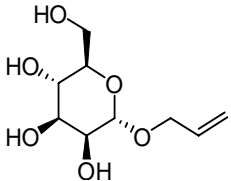
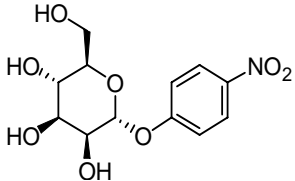


Figure 19. Frequency response plots of the inhibitory effect of 4-nitrophenyl- α -D-mannopyranoside on Con A/mannan binding. Increasing concentration of competitor resulted in reduced frequency response.

Moreover, the competition experiments were performed using a series of known Con A carbohydrate ligands, where D-mannose (mixture of α/β , 67% α -, and 33% β -D-mannose according to $^1\text{H-NMR}$ -analysis in $\text{D}_3\text{PO}_4\text{-NaOD}$ buffered saline, pD 7.4), methyl- α -D-mannopyranoside, allyl- α -D-mannopyranoside, and 4-nitrophenyl- α -D-mannopyranoside were all tested for their inhibitory effects of Con A/mannan binding. The resulting competitive binding curves of all four ligands are displayed in Figure 20. The competitive binding data were subjected to non-linear regression analysis, and the resulting EC_{50} -values are presented in Table 6.

Table 6. Comparison of EC₅₀-values for the QCM lectin biosensor and reported values from an enzyme-linked lectin assay (ELLA).¹⁰⁵

Ligand		EC ₅₀ /mM (QCM) [95% CI]	EC ₅₀ /mM (ELLA)
D-mannose (α/β)		5.3	>2.5
methyl-α-D-mannopyranoside		1.1	0.92
allyl-α-D-mannopyranoside		0.25	0.26
4-nitrophenyl-α-D-mannopyranoside		0.18	0.11

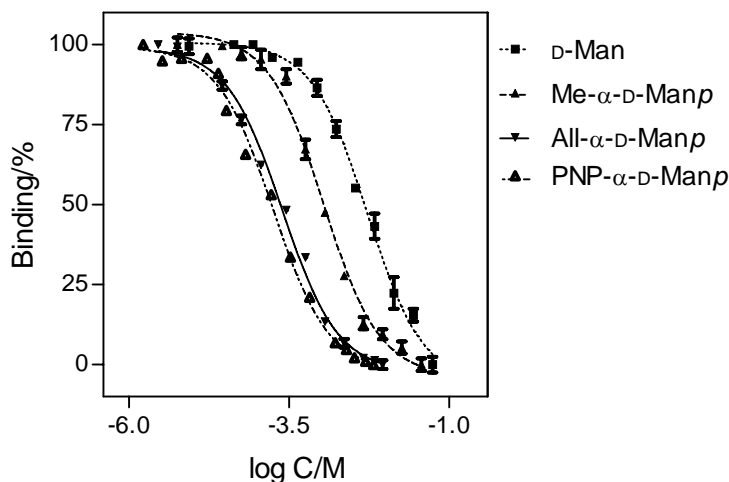


Figure 20. Competition plots of four different carbohydrates for Con A binding (mean \pm SEM). D-Man: D-mannose; Me- α -D-Manp: methyl- α -D-mannopyranoside; All- α -D-Manp: allyl- α -D-mannopyranoside; PNP- α -D-Manp: 4-nitrophenyl- α -D-mannopyranoside.

To compare the resulting EC_{50} -values of the tested ligands with reported data from the enzyme-linked lectin assay (ELLA) binding assay,¹¹⁰ indicates that the QCM biosensor system we developed is an efficient mean to study the ligand-lectin interaction in real time without any labeling.

3.2.1.2 Study of calcium-dependent binding effects in glycosyldisulfide interactions with Con A (paper VI)

Thiol-containing carbohydrates can be easily oxidized to form disulfide-bridged dimers, and the resulting glycosyldisulfides have been suggested as efficient glycosyl donors and potentially useful glycomimetics.⁴⁵⁻⁴⁷ Glycosyldisulfides can occupy a larger conformational space, as compared to natural glycosides, due to the increased flexibility and extended length of the disulfide bond, as well as their differences in electronic properties. Thus, to further investigate the glycosyldisulfide-lectin interactions, a range of 1-thio- or 6-thio-saccharides were measured for their inhibitory effects against lectin Con A using the modified QCM systems discussed above,⁵⁶ where six thiosaccharide monomers, together with their corresponding disulfide-bridged dimers, were evaluated (Figure 21). These six sugars include the 1-thio-derivatives of five common carbohydrates D-mannose (**53**), D-glucose (**93**), D-galactose (**1**), *N*-acetyl-D-glucosamine (**58**) and *N*-acetyl-D-galactosamine (**59**). Since Con A is selective for mannose-containing carbohydrate structures, methyl-6-thio- α -D-mannopyranoside (**57**) was also tested. The corresponding dimers, **53-53** to **57-57**, were easily obtained from the monomers by mild oxidation with hydrogen peroxide.

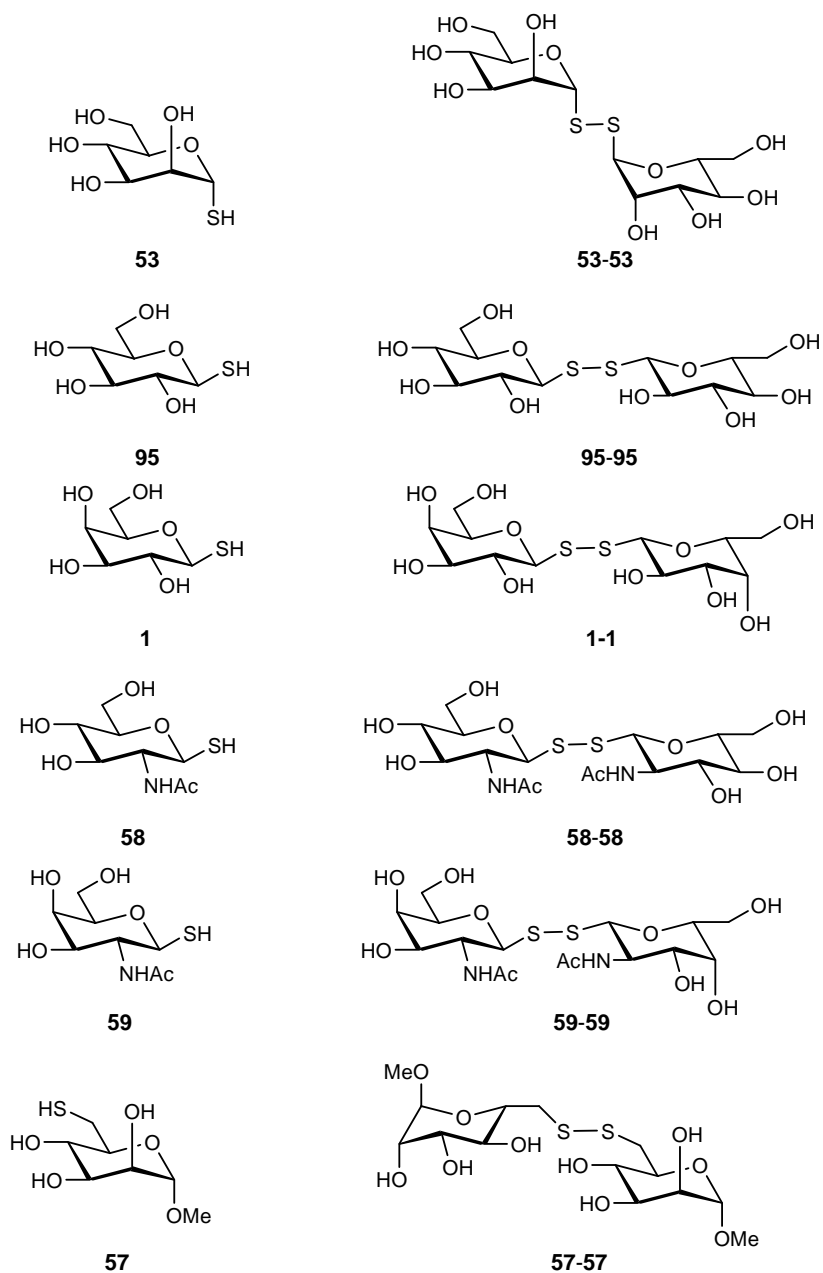


Figure 21. Thiosaccharides and glycosyldisulfides tested.

The inhibitory effects of the thiosaccharides were monitored by the mannan-modified QCM-system,⁵⁶ where competition assays were performed over a concentration range, and the inhibitory effects were quantified as IC₅₀-values and Hill coefficients, respectively. During the measurement, to maintain reducing conditions while analyzing the thiol monomers, a minimal amount of dithiothreitol (DTT), showing no influence on the binding in itself, was added to the samples. The results indicated that inhibitory effects from the thiol monomers were very weak even at concentration up to 10 mM, with the exception for 1-thio- α -D-mannopyranose (**53**). For comparison, the inhibitory effects of α -D-mannose and methyl- α -D-mannopyranoside (IC₅₀: 5.3 and 1.1 mM, respectively),⁵⁶ well show the importance of a hydroxyl group in the 1- and 6-position for these structures, as compared to a thiol moiety. In contrast to the thiol monomers, several of the dimers proved to be efficient inhibitors (Table 7). The 1-thio- α -D-mannose dimer (**53-53**) showed an IC₅₀-value of 1.2 mM, considerably lower than the 6-thio-derivative (**57-57**), which proved inefficient as expected from the monomer effect. On the other hand, 1-thio- β -D-glucose-, 1-thio- β -D-galactose-, and *N*-acetyl-1-thio- β -D-glucosamine-based dimers displayed relatively high inhibitory effects, despite the total lack of response of the corresponding monomers. 1-thio- β -D-glucose- (**93-93**), and 1-thio- β -D-galactose- (**1-1**) dimers displayed very similar effects with IC₅₀-values approximately of the same order as the 1-thio- α -D-mannose dimer (**53-53**), whereas the *N*-acetyl-1-thio- β -D-glucosamine dimer (**58-58**) proved slightly less efficient (IC₅₀: 2.0 mM). Interestingly, the corresponding *N*-acetyl-1-thio- β -D-galactosamine derivative (**59-59**) indicated no inhibition under these conditions.

Table 7. Estimation of IC₅₀ values for carbohydrate structure based on consecutively diluted concentrations of tested inhibitors in the QCM-assay with Con A. None of the thiosaccharide monomers **53** to **57** showed any significant inhibitory effect in the concentration range tested.

Glycosyldisulfide	Inhibition IC ₅₀ /mM	Hill coefficient
53-53	1.2	1.0
95-95	1.4	6.1
1-1	1.4	6.2
58-58	2.0	5.2
59-59	na	na
57-57	na	na

^a na = not active. ^b The program GraphPad Prism (GraphPad Software) was adopted for non-linear regression analysis determining IC₅₀ values and Hill coefficients.

Most interestingly, the ligands **95-95**, **1-1** and **58-58** displayed strong positive apparent cooperativity effects in the binding to Concanavalin A with Hill coefficients up to 6.2 (Figure 22, Table 7), whereas the ligand 1-thio- α -D-mannose dimer (**53-53**) displayed a binding pattern with no apparent cooperativity effects (Table 7). These unexpected effects suggest that the 4-subunit lectin undergoes a dramatic change upon interacting with these

dimer ligands in the present system.

Since Concanavalin A is a metal ion-dependent lectin, with metal ion-binding sites for, preferentially, calcium and a transition metal ion (e.g., manganese) situated in close proximity to the carbohydrate-binding pocket,^{111,112} the calcium-dependence of the binding was further explored. Carbohydrates may form complexes with calcium,^{113,114} and the effects observed could potentially arise from interactions with the calcium binding site, or with the calcium ions *per se*. Demetallisation of Con A strongly influences the carbohydrate binding, and may also induce structural changes.^{115,116} Therefore, all dimer ligands were also measured in presence of excess calcium ions. The resulting effects clearly showed a strong calcium-dependence, where none of the cooperativity-inducing ligands showed any binding effect in the presence of calcium (Figure 23). These results suggest that these three thiosaccharide dimers interfere primarily with the calcium binding, and not with the carbohydrate-binding site.

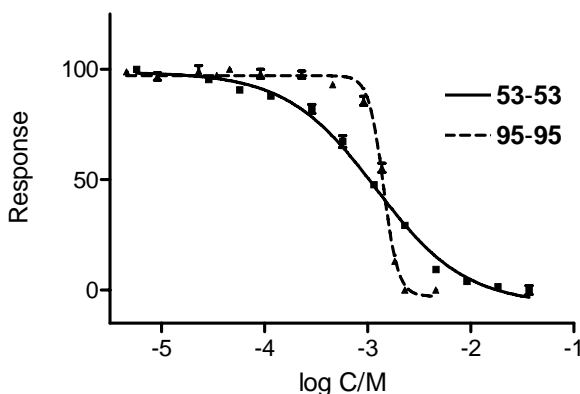


Figure 22. Inhibitory responses of Con A/mannan binding in presence of substances **53-53** and **95-95**.

To further study the cooperativity effects, the compound **95-95** at a concentration showing complete inhibition after treated with DTT, was subsequently evaluated with Con A. The results indicated that the inhibitory effect to the mannan-surface against Con A fully eliminated (Figure 23). This redox controlled phenomenon could potentially be used to specifically turn on or turn off the ligand binding ability of Con A, creating a carbohydrate binding switch.

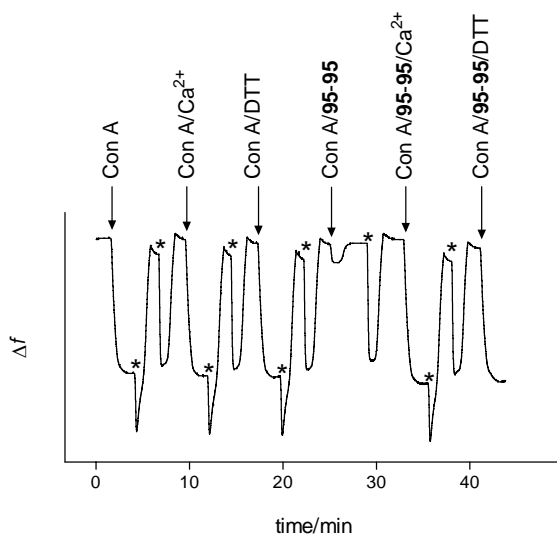


Figure 23. QCM frequency shifts upon addition of Con A in combination with ligand **95-95** (2.3 mM). Negative frequency shifts indicate binding. Arrows indicate different injections: Con A alone (Con A), and in combination with Ca²⁺ (Con A/Ca²⁺), or DTT (Con A/DTT), show identical response indicating no calcium- or DTT dependence. Con A in presence of **95-95** results in complete inhibition (Con A/**95-95**). Con A in presence of **95-95** and Ca²⁺ eliminates inhibition and restores full QCM response (Con A/**95-95**/Ca²⁺). The inhibition could also be reversibly eliminated by addition of DTT (Con A/**95-95**/DTT). * indicates washing steps.

The results indicated that thiosaccharide dimers display inhibitory effects against Con A, where the 1-thio- α -D-mannose dimer showed an IC₅₀-value in the low mM range but with no apparent cooperativity, but 1-thio- β -D-glucose-, 1-thio- β -D-galactose-, and *N*-acetyl-1-thio- β -D-glucosamine-based dimers displayed very high positive apparent cooperativity effects. However, the corresponding *N*-acetyl-1-thio- β -D-galactosamine-based dimer was inefficient at the concentration levels tested. These effects were mainly dependent on the calcium-levels of the system. Thus, glycosyldisulfides may indeed be useful glycomimetics in exploring carbohydrate-binding entities. In addition, thiol-disulfide interchange, shown to be a highly useful method to generate and screen DCLs *in situ* against biological macromolecules,¹¹⁷ was used to prepare all libraries.

3.2.1.3 Rapid identification of glycosyldisulfide lectin inhibitors from a dynamic combinatorial library (paper I)

As mentioned in the previous chapter, thiosaccharides are also potentially subjective to reversible systems, where thiol-disulfide exchange can be used to generate dynamic libraries under very mild conditions, at neutral to alkaline pH, and the resulting libraries can be screened by the biological targets.^{117,118}

In the present study, in order to generate a library composed of structures that mimic the natural carbohydrate ligands for the target lectin, as well as composed of relatively "compact" ligands with short spacers between the carbohydrate units, a range of thiosaccharides and other thiol-components were chosen as DCL building blocks (Figure 24). These included six different thiosaccharides: (**1**, **53**, **57**, **58**, **59**, **95**), α -D-mannose, β -D-glucose, β -D-galactose, *N*-acetyl- β -D-glucosamine, and *N*-acetyl- β -D-galactosamine, and eight non-carbohydrate building blocks (**96-103**) (Figure 24). The chosen non-carbohydrate building blocks contained different functionalities, where carboxylic (**96**, **99**), hydroxyl (**97**, **98**), amine (**100**, **101**), amide (**102**) and ester (**103**) groups were probed for their potential interactions with the lectin binding site.

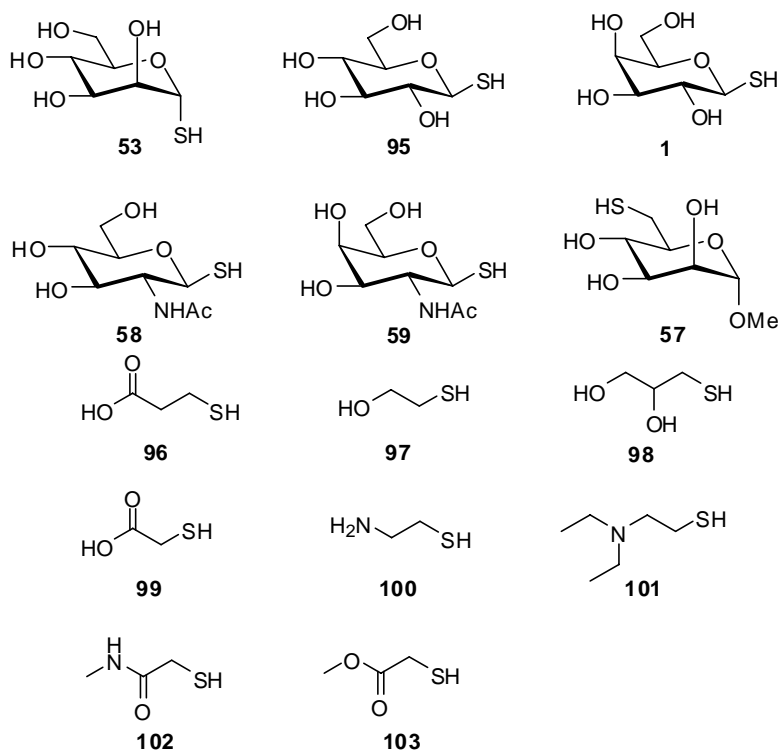


Figure 24. Thiol components used in DCL generation.

The dynamic combinatorial libraries were prepared by mixing the chosen thiol components in neutral phosphate buffer, subsequently oxidized with a minimal amount of hydrogen peroxide within a few hours. Once the libraries were fully oxidized to disulfides, the interconversion was essentially blocked and no further scrambling could be recorded.

All 14 thiol-components were employed as components for the first dynamic combinatorial library (**DCL-A**), resulting in up to 105 different disulfide dimers by oxidation. In order to screen the library for individual component activity, a deconvolution strategy was used.¹¹⁹ Therefore, fourteen sub-libraries were prepared in the same way, where one of the components was substituted for buffer solution. These fourteen sub-libraries were composed of 91 different constituents, respectively.

The libraries were screened against Con A using mannan-modified QCM system in presence of excess calcium ions, since dimers **1-1**, **95-95**, and **58-58** interfere with the Ca^{2+} binding in Con A.⁵⁷ Screening was performed using competitive binding between the mannan and the tested ligands in the DCLs. Samples were thus prepared with Con A and the different DCLs (full DCL and sublibraries, respectively) and injected consecutively. The frequency shift was recorded after each injection, corresponding to Con A binding to the surface, and the bound Con A was subsequently released from the mannan-surface by injection of lower pH buffer. The graph for the resulting screening of the fifteen libraries is displayed in Figure 25, compared to the binding of Con A with no competing ligand (maximum frequency shift). The results clearly indicated that components **53** and **57** are important constituents competing with mannan for binding to the lectin due to the sublibraries A1 and A6, both of which showed reduced activity. Since none of the other sublibraries showed any diminished action, it was concluded that constituents based on combinations of **53** and/or **57** were more active.

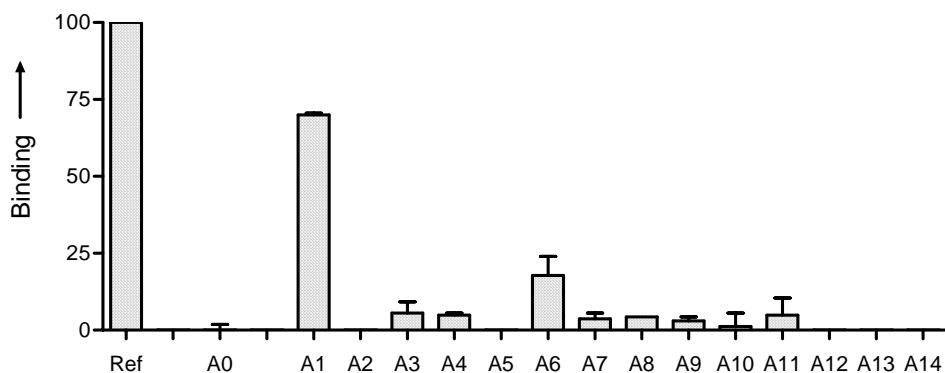


Figure 25. Dynamic deconvolution of glycosyldisulfide **DCL-A**. Con A binding to mannan in absence of DCLs (Ref), in presence of complete library A0, and sublibraries

A1-A14. Sublibraries A1 and A6 indicate strong dependence from compounds **53** and **57**, respectively.

Because the non-carbohydrate components did not show any apparent activity, a focused dynamic combinatorial library (**DCL-B**) was subsequently prepared, composed of only the thiosaccharide components **1**, **53**, **57**, **58**, **59** and **96**. These six components resulted in the generation of 21 different dimers using the identical mean as **DCL-A**. At the same time, six sublibraries were generated from using five of the components to form 15-dimer sublibraries. The screening results are displayed in Figure 26, clearly indicating that components **53** and **57** are important in generating constituents able to compete with mannan for binding to Con A, where the other thiosaccharides proved inefficient.

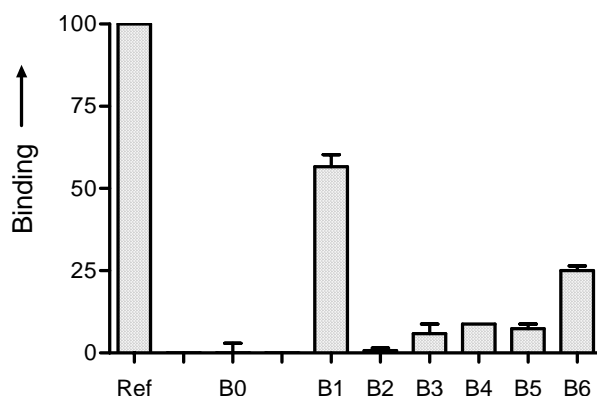


Figure 26. Dynamic deconvolution of glycosyldisulfide **DCL-B**. Con A-binding to mannan in absence of DCLs (Ref), in presence of complete library B0, and sublibraries B1 to B6. Sublibraries B1 and B6 indicate strong dependence from compounds **53** and **57**, respectively.

To further evaluate the active constituents of the libraries, the apparently efficient components **53** and **57**, as well as their dimers: **53-53**, **57-57**, and **53-57** were measured to compete with mannan for binding to Con A, respectively (Figure 27). The mannoside dimers were synthesized from their parent monomers using the same method as for the library generation. The homodimers **53-53** and **57-57** could be directly used in individual testing after oxidation without further purification, whereas the heterodimer **53-57** was purified by flash chromatography after oxidation.

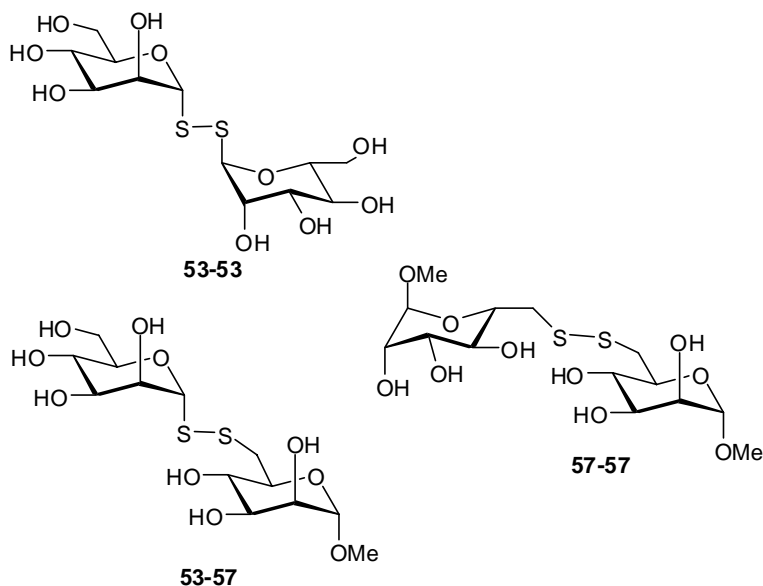


Figure 27. Structures of glycosyldisulfides **53-53**, **57-57**, and **53-57**.

The resulting competition curves are displayed in Figure 28, and the calculated EC_{50} -values are showed in Table 8. The results indicated that compounds **53-53** and **53-57** are the most active of the library constituents with EC_{50} -values of 1.2 mM, whereas compound **57-57** proved essentially inefficient with an EC_{50} -value exceeding 20 mM.

Table 8. Estimation of EC_{50} values (50% inhibition of Concanavalin A binding) for tested carbohydrate structures.

Compound	EC_{50}/mM
53	>5.0
57	>>20
53-53	1.2
57-57	>20
53-57	1.2

Interestingly, monomer **53** shows lower activity compared to methyl α -D-mannopyranoside (EC_{50} : 1.1 mM), indicating that the exchange of a methoxy group for a thiol group at the anomeric position distinctly reduces the Con A binding activity. It suggests that the sulfhydryl group is largely unstabilised by the Con A aglycon binding pocket. However, component **57** proved much less active than its analogue methyl α -D-mannopyranoside, with an EC_{50} -value more than 20 times higher, indicating that the exchange of a methoxy group for a thiol group at the 6-position, dramatically reduces the Con A binding activity. Since the only difference between these two compounds lies in the exchange of an oxygen for a sulfur, and because SH is both larger and considerably poorer hydrogen-bond donor than OH, this result suggests that this hydroxyl group is involved in pronounced interactions with the Con A lectin in accordance with known binding patterns.¹¹²

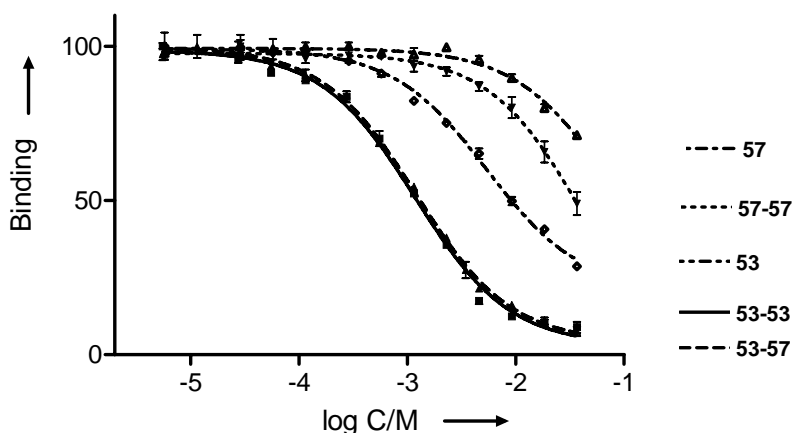


Figure 28. Inhibitory response of Con A binding in presence of DCL constituents **53**, **57**, **53-53**, **57-57**, and **53-57**. The curves were based on consecutively diluted concentrations of tested inhibitors included in the QCM-assay with Concanavalin A.

The results also indicated that the monomers **53** and **57** proved less active than their corresponding dimers **53-53** and **57-57**, respectively, where the divalent effects arise from two equal units tied together. Therefore, it suggests that both monomer units of the homoditopic constituent **53-53** bind to the same site. Most interestingly, in spite of the inefficiency of monomer **57**, its combination with **53** produced an efficient inhibitor **53-57**, which shows the same activity as homodimer **53-53**. It suggests that both units interact with different parts of the Con A binding sites. Not only proved compound **57-57** to be inefficient, leading to the conclusion that the **57**-unit is unable to bind to the **53**-binding site, but compound **53-57** also mimics the natural trimannoside ligand, inasmuch as it resembles the α -D-Man-(1,6)- α -D-Man-part of the trimannoside.

3.2.2 PEG coated QCM system (paper VIII)

In this study, investigations of carbohydrate-protein interactions were explored by use of a novel QCM system, where a range of carbohydrates were immobilized on the surfaces of QCM-crystals.⁵⁸ Gold-plated, 10 MHz quartz crystals were first immersed into a solution of compound **94** to form a self-assembled layer, followed by removing the solvent under a stream of nitrogen. Subsequently, a thin film of PEG (Mr 20000) was covalently attached to the layer by thermally induced nitrene immobilization.^{120,121} Finally, the carbohydrates were fixed on the PEG surface by UV irradiation.

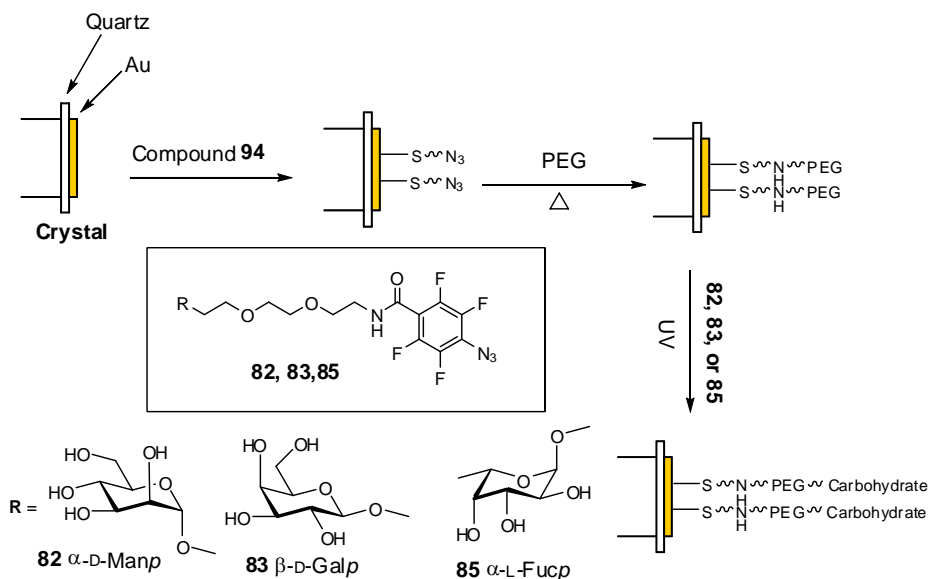


Figure 29. Procedure of the preparation of PEG coated surface.

3.2.2.1 Development of a range of carbohydrate surfaces

Gold-plated, 10 Hz quartz crystals were immersed into the mixture of H_2O_2 (33%), NH_3 (33%) and distilled water with a ratio of 1:1:3 at 80 °C for 5 minutes to clean the surfaces. The resulting crystals were rinsed with distilled water several times, and dried under a stream of nitrogen. The cleaned crystals were dipped into a solution of compound **94** in CH_2Cl_2 at room temperature in the dark overnight, then rinsed with CH_2Cl_2 to remove the excess of compound and dried in a nitrogen atmosphere as schematically illustrated in Figure 29. The resulting crystals were dipped into a melt of PEG (Mr. 20,000) at 70 °C, then the temperature was increased to 140 °C and heated for 20 minutes. The resulting PEG-coated crystals were withdrawn from the melt and cooled down to room temperature,

then sonicated in distilled water to remove unbound PEG, and dried in a nitrogen atmosphere. Finally, the PEG-coated crystals were immersed in a solution of carbohydrates (in ethanol) for 5 minutes. After drying under nitrogen, the crystals were irradiated with a medium pressure Hg lamp for 5 minutes. After UV irradiation, the crystals were rinsed with ethanol and then dried in a nitrogen atmosphere. A range of carbohydrates were in this way covalently attached to the surfaces of crystals (Figure 29).

3.2.2.2 Recognition by a range of lectins

The carbohydrate-lectin interactions were probed by a flow-through QCM-system. The carbohydrate-modified crystals were mounted in the QCM system, then equilibrated with buffer solution until no mass change could be recorded. BSA in buffer was injected to block the surface, and the system was allowed to equilibrate to get a stable baseline. The affinities of different lectins to the carbohydrate-modified surfaces could subsequently be analyzed using the developed QCM system by injecting lectin solutions in the same buffer. The bound lectins were removed by two successive injections of low pH buffer. A flow rate, together with an injection volume, was used throughout the analyses.

The binding affinities of the carbohydrate-coated surfaces were initially evaluated for four different lectins: Con A, VAA, UEA I, and PSA. The α -D-mannopyranoside-specific Con A showed binding to three of carbohydrate-coated surfaces: the mannose-type, galactose-type, and fucose-type surfaces, respectively, and the resulting frequency-response graphs are displayed in Figure 30. The results show that Con A binds strongly to the mannose surface, whereas only low binding effects could be recorded for the galactose and fucose surfaces.

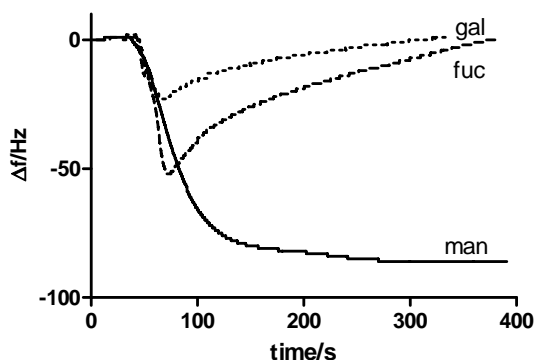


Figure 30. Comparison of binding of Con A to different carbohydrates immobilized on the PEG 20,000 coated surface.

3.2.2.3 Evaluation of VAA binding affinity to a range of carbohydrate-coated surfaces

As a comparison, when the galactopyranoside-specific mistletoe lectin (VAA) was evaluated for the three different carbohydrate-surfaces, the resulting frequency-response graphs clearly show that VAA was selective for the galactose surface only (Figure 31).

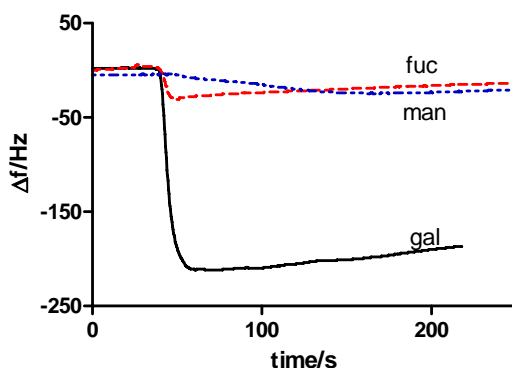


Figure 31. Comparison of binding of VAA to different carbohydrates immobilized on the PEG 20,000 coated surface.

To further investigate the interaction of lectins with different carbohydrate surfaces, two other lectins were also tested, UEA-I and PSA. The results for the binding effects with three different carbohydrate surfaces, together with the results for Con A and VAA, are displayed in Figure 32, indicating that PSA was selective for the methyl- α -D-mannopyranoside, whereas UEA-I was selective for the fucose-type surface.

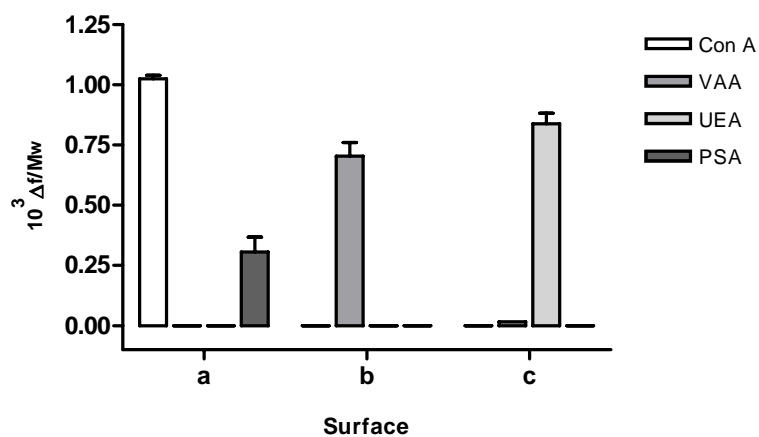


Figure 32. Evaluation of binding selectivity on the surface: Surfaces (a) Man, (b) Gal, and (c) Fuc. Recognising a range of lectins: Con A, VAA, UEA, PSA.

3.3 Carbohydrate arrays (paper VII)

In this study, a novel efficient strategy to carbohydrate microarrays technologies has been developed, where a controllable and robust method to array preparation, both on the carbohydrate chemistry level as well as the surface chemistry level were employed.¹²² The resulting carbohydrate arrays can be efficiently used to screen a range of lectins in parallel in a single operation.

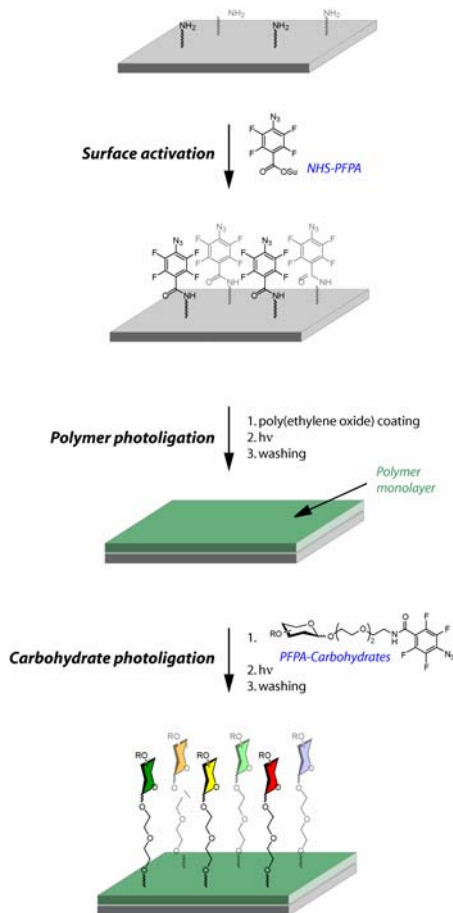


Figure 33. Array generation by double photoligation. A layer of poly(ethylene glycol) was photoligated to a perfluorophenylazide (PFPA)-activated surface. Photoprobe-conjugated carbohydrates were subsequently arrayed and photoligated to the resulting polymer surface.

3.3.1 Microarray preparation

The microarrays were prepared in three steps: (1) amino-derivatized glass slides were initially functionalized by the reaction of *N*-hydroxylsuccinimide-derivatized PFPA (NHS-PFPA)¹²²⁻¹²⁶ to the amino groups on the glass slides, creating a monolayer of PFPA on the surface; (2) the resulting glass slides were coated with a solution of PEG and subsequent UV irradiation to produce a thin layer of PEG that was efficiently attached to the surface; (3) PFPA-derivatized carbohydrates were subsequently immobilized in an array format on the PEG surface by way of photoinitiated insertion chemistry, where a range of carbohydrates were employed, including monosaccharides (α -D-mannose, β -D-glucose, β -D-galactose, *N*-acetyl- β -D-glucosamine, α -L-fucose, α -L-arabinose, β -D-xylose), and disaccharides (lactose, cellobiose) (Figure 8). In this step, PFPA-derivatized carbohydrates were spotted on the modified glass slides using a high-density DNA-array machine, and subsequent photochemical UV-activation was employed to immobilize the carbohydrates to the substrate surface via insertion reactions of PFPA to the polymer film. The general design of the arrays produced is displayed in Figure 34. A three-by-four array, with every structure printed in quadruplicate, was employed.

3.3.2 Screening by a range of lectins

The fabricated microarrays were screened against a range of lectins, where fluorescence-tagged lectins and fluorescence imaging were employed in developing the array binding patterns. Four different lectins were thus targeted for the arrays, including the lectin from *Griffonia simplicifolia* II (GSII), the peanut agglutinin (PNA), the jack bean lectin (ConA), and the soybean agglutinin (SBA). The scanning results for the arrays are displayed in Figure 34, indicating that arrays were efficient in demonstrating the specific binding patterns of the chosen lectins, where both the primary binding partners as well as the secondary ligands could be identified. (1) GS-II, thus showed a clear binding preference to its major binding partner, β -D-GlcNAc (**84**); (2) PNA was revealed to mainly bound by lactose (**86**), followed by lower binding of β -D-galactose (**81**) and cellobiose (**85**); (3) the ConA interaction with α -D-mannoside structures is clearly demonstrated, showing efficient binding to the carbohydrate part of compound **80**, the α -D-mannoside PFPA. Furthermore, this lectin also showed low binding to the β -D-glucoside (**82**) and very low binding to the *N*-acetyl- β -D-glucosamine (**84**) structure; (4) SBA is specific for terminal β -D-galactoside units and thus showed binding to both β -D-galactose (**81**) and lactose (**86**). These results indicate that the resulting carbohydrate arrays can be efficiently used to screen a range of lectins in parallel in a single analysis.

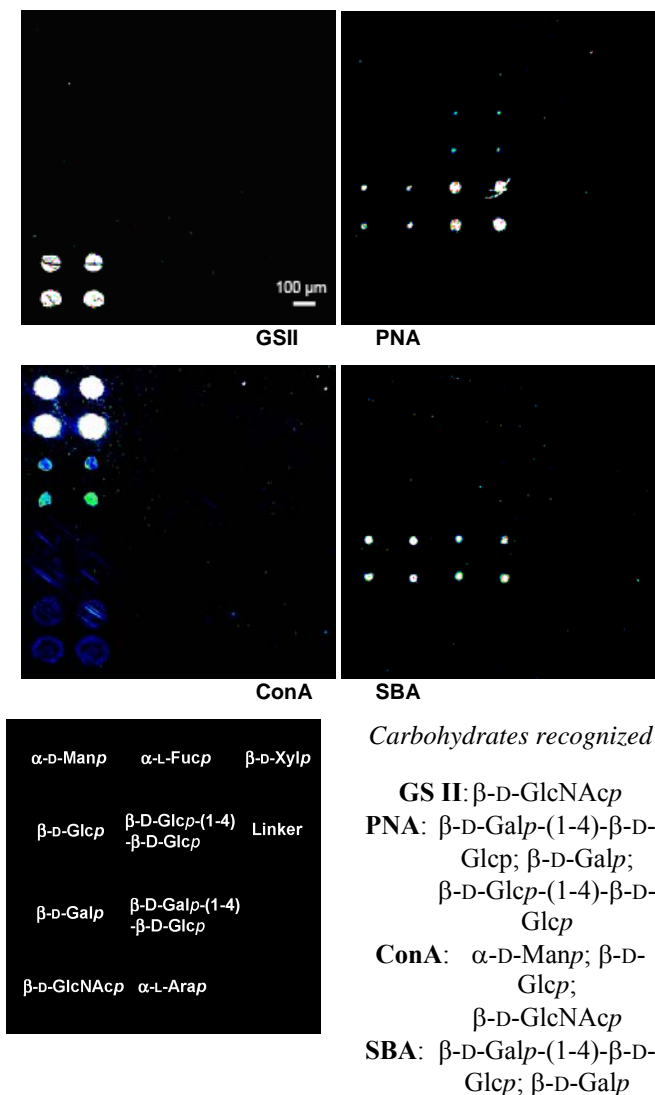


Figure 34. Carbohydrate microarray results with four different lectins: *Griffonia simplicifolia* lectin II (GSII), peanut agglutinin (PNA), Concanavalin A (ConA), and soybean agglutinin (SBA). Active carbohydrates for each lectin are easily identified from the arrays, and carbohydrates recognized are listed. The design of the library is indicated at the lower left, all carbohydrates were repeated in quadruplicate [2 x 2].

This study has demonstrated that the versatility of photochemical immobilization chemistry can be combined with microarray techniques to create high-density and spatially addressable carbohydrate microarrays, where the photochemical properties of PFPAs can be fully employed to produce polymer thin films, and to locate the carbohydrate ligands to specific areas on the surface. The PEG- polymer film on the substrate can furthermore be selected to reduce the non-specific adsorption of ligands to the surface. The fabricating arrays could be screened a range of lectins in parallel in a single analysis. Given expanded carbohydrate repertoires, these microarrays have the potential to facilitate and accelerate various aspects of glycomics and proteomics.

3.4 Analysis of the carbohydrate-lectin interactions by other methods (paper II)

Glycosyldisulfides constitute a new class of carbohydrate derivatives with interesting chemical and physical properties. Their generation from thioglycosides via thiol-disulfide exchange, also operative in formation of disulfide-linked glycopeptides, has recently been reported,^{45,46} revealing them to be suitable building blocks for dynamic combinatorial chemistry.⁵⁷ In order to reveal lectin-binding properties of this type of non-hydrolyzable sugar derivative, libraries originating from a mixture of common building blocks of natural glycans and thiocompounds were tested against three plant agglutinins lectins and one endogenous lectin with specificity to galactose, fucose or *N*-acetylgalactosamine, respectively, in a solid-phase assay or in a cell binding assay. Extent of lectin binding to matrix-immobilized neoglycoprotein presenting the cognate carbohydrate structure could be reduced, and evidence for dependence on type of carbohydrate was provided by dynamic deconvolution.^{54,119} In this study, four thiosaccharides and two thiol-components were chosen as DCL building blocks (Figure 35), and the libraries were screened against a range of lectins: *Viscum album* agglutinin VAA, (*Ulex europaeus*) agglutinin UEA-I, soybean agglutinin SBA, and an endogenous lectin (galectin-3), respectively.

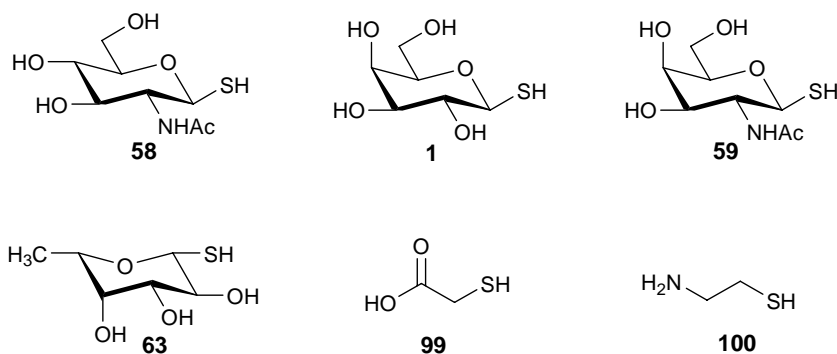


Figure 35. Thiol-containing components for generating dynamic combinatorial libraries.

All 6 thiol-components were used as components for the first library (L01), generating 21 different disulfide dimers in the resulting dynamic combinatorial library. In order to screen the library for individual component activity, a deconvolution strategy was employed.¹¹⁹ Therefore, aside from the full L01, based on all six components and composed of 21 constituents, six sublibraries were prepared in the same way where one of the components was substituted for buffer solution. These sublibraries (L02-L07) were composed of 15 different constituents, respectively. In addition, to further evaluate the active constituents of the libraries, 6 two-component libraries (L08-L13) were prepared, where digalactoside and the constituents resulting from galactoside with the other thiol-components were produced (Table 9).

Table 9. Composition of the tested dynamic combinatorial libraries and glycosyldisulfides

Library	Components
L-01	complete library
L-02	without 63
L-03	without 58
L-04	without 1
L-05	without 59
L-06	without 99
L-07	without 100
L-08	1-1
L-09	1, 63
L-10	1, 58
L-11	1, 59
L-12	1, 99
L-13	1, 100

3.4.1 Solid-phase assays

Two plant lectins which primarily target a monosaccharide in glycans, i. e. the galactoside-specific *Viscum album* agglutinin (VAA) and the fucoside-specific *Ulex europaeus* agglutinin (UEA-I), were first tested for binding. By adsorption of neoglyoproteins bearing lactose or fucose moieties to the surface of microtiter plate wells, ligand-presenting matrices with characteristics cell surfaces were established. The lectins bound to the matrix in a carbohydrate-dependent and saturable manner.

The resulting screening of the 7 libraries is displayed in Figure 36 compared to the binding of the lectins with Gal/Fuc ligands. As can be seen from the graph, the sublibraries L-02 (without Fuc) and L-04 (without Gal) were nearly completely devoid of inhibitory capacity for UEA-I and VAA, respectively (Figure 36). In contrast, reduction of constituent complexity by omission of any other compound resulted in rather small effects. There was a tendency that the absence of the two non-carbohydrate compounds led to a decrease of binding slightly lower than that for the pyranoses (Figure 36).

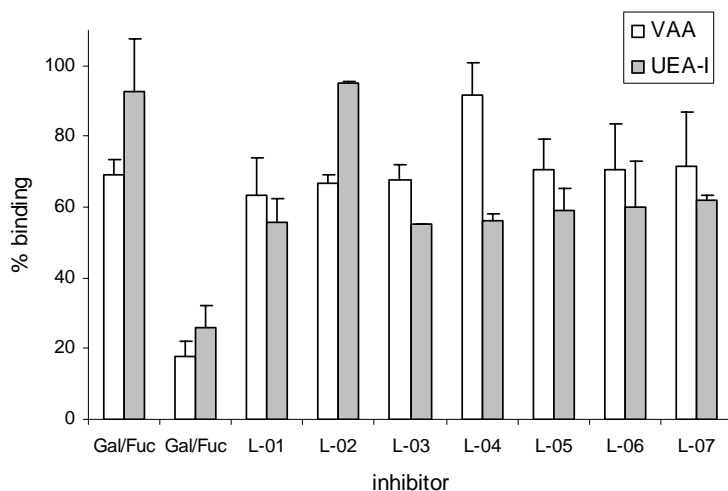


Figure 36. Illustration of inhibitory potency on extent of lectin binding [(galactose-binding mistletoe (*Viscum album*) agglutinin VAA and α -L-fucoside-binding gorse (*Ulex europaeus*) agglutinin UEA-I)] to surface-immobilized neoglycoproteins with lactose (VAA) or L-fucose (UEA-I) as bioactive ligands.

3.4.2 Cell-binding assays

The principle of the cell-binding assay is illustrated in Figure 37. The binding properties of VAA and UEA-I were initially analyzed.

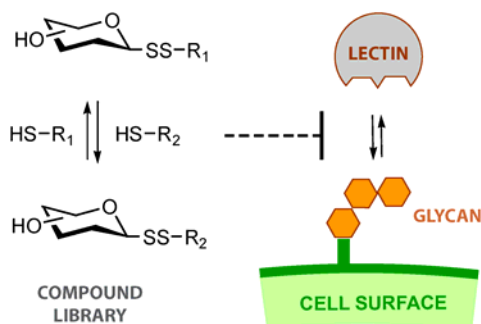


Figure 37. Schematic representation of the principle of the cell-binding assay (right part), in which components of a glycosyldisulfide-based dynamic combinatorial library (left part) are tested for interference of lectin binding to cell surface glycans.

The libraries (L01-L07) were screened against two lectins VAA and UEA-I, directly on surfaces of a range of cells. The libraries were screened against VAA using cells of a B-lymphoblastoid line (Croco II). The screening results of the 7 libraries are displayed in the first row of Figure 38, clearly showing that sublibrary L-04 was of low inhibitory activity. This indicates that component **1** is crucial for competing with the glycan on the cell surface (Figure 38). The libraries were also screened against VAA using a solid tumor line (colon adenocarcinoma line, SW 480), and the screening results are shown in the second row of Figure 38. These results also show that component **1** is the most efficient for competing with the glycan on the cell surfaces. Additional screening results are displayed in the third row and fourth row of Figure 38, where the libraries were screened against UEA-I on cells of SW 480 and cells of human pancreatic carcinoma line Capan-1, respectively. As can be seen from the graphs, library L-02 is devoid of inhibitory capacity competing with the glycan on both cell surfaces because of lack of fucose.

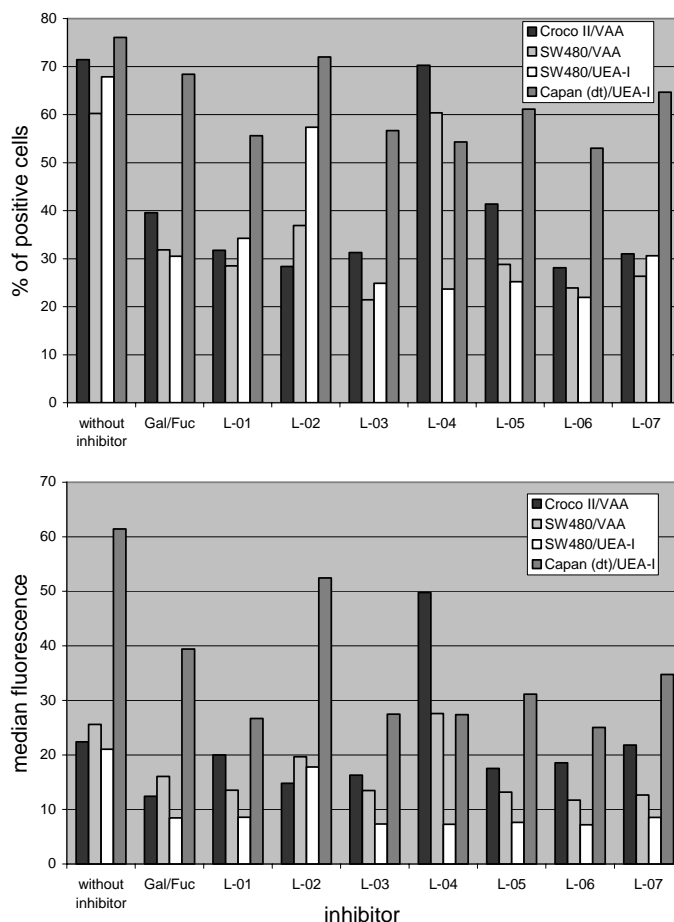


Figure 38. Comparison of the effects of the two monosaccharides (Gal or Fuc) and the libraries on staining parameters (upper panel: percentage of positive cells; bottom panel: median fluorescence) in flow cytometric analysis.

To further investigate the carbohydrate-lectin interactions, a human lectin, galectin-3, which is involved in tumor spread and cardiac dysfunction,¹²⁷⁻¹³⁰ was introduced to this assay system for screening of the libraries on surfaces of T-lymphoblastoid cells. The fluorescent staining graph for the results is displayed in Figure 39, indicating that absence of Gal was rather tolerable (L-04), whereas absence of GalNAc, precluding formation of GalNAc-GlcNAc disulfides, impaired the activity more strongly (L-05) (Figure 39). The omission of the two aliphatic thiocompounds led to mixtures which were as effective as library L-01, pointing to a lack of effect of their presence. In addition, the libraries were also screened against galectin-3 on the surface of ovarian adenocarcinoma cells NIH-OVCAR3. Binding of galectin-3 at 10 $\mu\text{g/ml}$ reached levels of 61% positive cells and a

median fluorescence of 104.2, which was lowered by Gal to 52%/62.6 and by L-01 to 43.8%/48.6. Libraries L-04 (40.2%/46.4) and L-05 (50.0%/56.8) showed effects comparable to those of the lymphoma cell system but L-06 failed to reach the activity of library L-01 on the ovarian cancer cells (52.0%/63.1). Thus, as measured for the plant lectins, the libraries could also exert a negative impact on cell binding of an endogenous lectin.

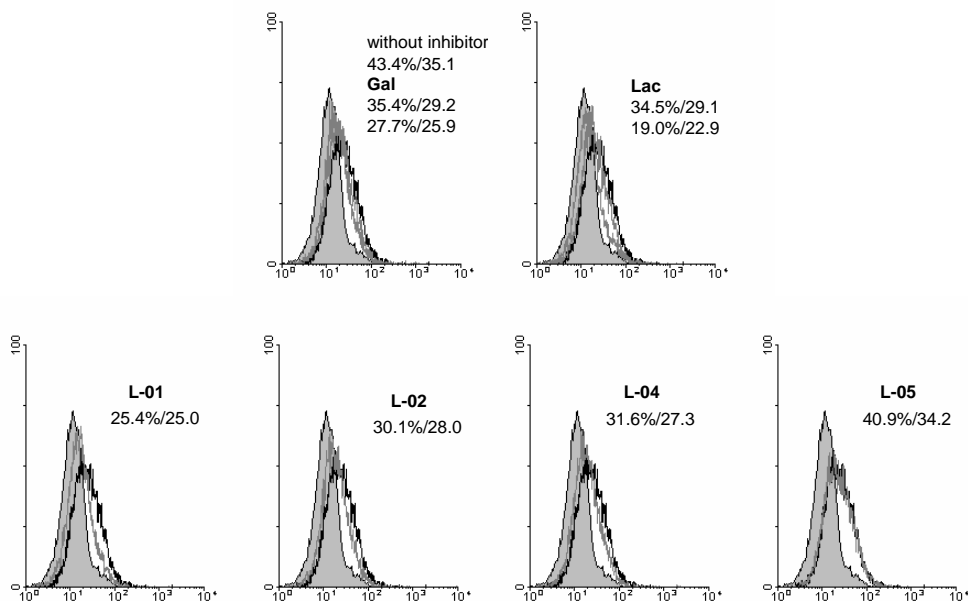


Figure 39. Semilogarithmic representation of fluorescent surface staining of cells of the human T-lymphoblastoid cell line CCRF-CEM in the absence of labeled lectin (negative control, shaded) and in the presence of human galectin (solid line), Gal or lactose (grey lines) as haptenic inhibitors with increasing efficiency (top panel) as well as four libraries. Quantitative data on control value (top panel, left side), effects of haptenic inhibitors and libraries (center and bottom panels) are given.

To further evaluate the active constituents of the libraries against VAA, 6 two-component libraries (L08-L13) were prepared, in which the constituents resulting from galactoside with the other thiol-components were produced. The screening results are displayed in Figure 40, indicating that the galactose disulfide even surpassed lactose in inhibitory capacity, whereas presence of Fuc, GalNAc or GlcNAc in the disaccharide had comparatively small effects. The galactose disulfides can thus act as binding partners for this lectin. Among them, the digalactose disulfide was clearly superior to the other disulfides.

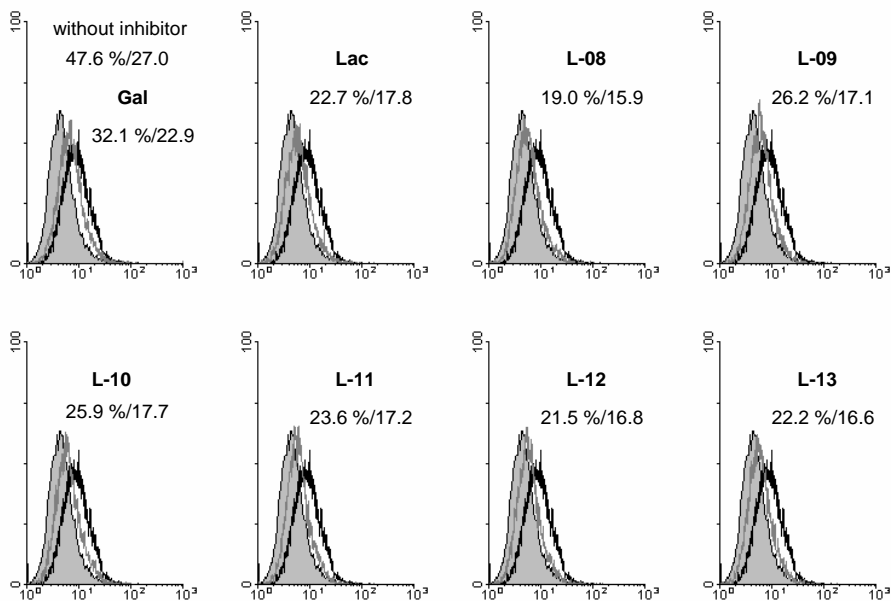


Figure 40. Semilogarithmic representation of fluorescent surface staining of cells of the human colon adenocarcinoma line SW480 in the absence of labeled lectin (negative control, shaded) and in presence of VAA (solid line), next using Gal or lactose as haptenic inhibitors, and defined 1-thiogalactoside-containing disulfides at the same concentration (grey line). Quantitative data on control value and effects of inhibitors are given.

4. Concluding remarks

A range of thio- β -D-galactose- as well as other glycoside derivatives have been successfully synthesized. Different protecting group strategies have been applied. Choices of solvent and nucleophilic reagent concentration have been shown to be essential. The results also indicate that ester protecting groups play a highly important role for the synthesis of thio-containing carbohydrates, when the inversion of triflated hydroxyl groups is performed with nitrite anion. Non-polar solvents are efficient to suppress the neighboring group participation when esters are used as protecting groups. Furthermore, facile approaches to acquire the key intermediates for the synthesis of methyl 2-thio- β -D-galactoside and methyl 4-thio- β -D-galactoside were developed based on multiple regioselective acylation via the respective stannylene intermediates. The stereoselectivity depending on solvent and nucleophilic reagent concentration for the synthesis of 3-thio- β -D-galactoside have been studied.

The stereospecific ester activation in nitrite-mediate carbohydrate epimerization was investigated. The results clearly show that esters play highly important roles in the Lattrell-Dax reaction facilitating nitrite-mediated carbohydrate epimerizations. In spite of the higher reactivity of carbohydrate triflates protected with ether functionalities, these compounds proved inefficient in these reactions where mixtures of compounds were rapidly obtained. Neighboring ester groups, on the other hand, could induce the formation of inversion compounds in good yields. The reactions further demonstrated stereospecificity, since axially oriented neighboring ester groups were unproductive and only equatorial ester groups induced the nucleophilic displacement reaction. These findings expand the utility of this highly useful reaction in carbohydrate synthesis as well as for other compound classes.

QCM biosensors have been demonstrated to be an efficient technique to investigate carbohydrate-lectin interactions in real time. Two different QCM systems have been presented, where mannan-coated surfaces and PEG-coated surfaces of a range of carbohydrates were developed.

i) For mannan coated surfaces, the interactions of Con A and a range of thiosaccharide dimers were tested. It was found that the 1-thio- α -D-mannose dimer showed an IC_{50} -value in the low mM range but with no apparent cooperativity. On the other hand, 1-thio- β -D-glucose-, 1-thio- β -D-galactose-, and *N*-acetyl-1-thio- β -D-glucosamine-based dimers displayed very high positive apparent cooperativity effects. These unprecedented effects were shown to depend mainly on the calcium-levels of the system, with no effects observed in the presence of calcium ions. The results also indicate that glycosyldisulfides may indeed be useful glycomimetics in exploring carbohydrate-binding entities. Secondly, glycosyl-disulfide libraries, generated from the corresponding thiols by mild oxidation, were screened against Con A using mannan-coated QCM system, where the dynamic deconvolution procedure was used. It was found that heterodimer **53-57** displays the same activity as **53-53**, whereas **57** shows much less active than **53**. The results indicate that the

hydroxyl group in the 6-position of methyl α -D-mannoside is the key to efficient binding to Con A, compared with the corresponding 6-thio derivative, whereas the hydroxyl group in the anomeric centre in D-mannose is less important in this side. The heterodimer **53-57** is more active due to its resemblance to the natural trimannoside ligand for Con A.

ii) PEG-coated surfaces, where a range of carbohydrates were immobilized on the PEG surfaces of the electrodes, have been developed for investigating the interactions between carbohydrates and lectins. The results indicate that Con A selectively bound to the mannose surface, VAA was selective for the galactose surface, PSA was selective for the methyl- α -D-mannopyranoside, whereas UEA-I was selective to fucose-type surface. These QCM biosensor systems have proved to be efficient means for studying carbohydrate-lectin interactions.

A novel strategy to carbohydrate microarrays has been developed. It constitutes a controllable and robust method to array fabrication, both on the carbohydrate chemistry level, as well as the surface chemistry level, and the fabricating arrays could be used to a range of lectins in parallel in a single analysis. Our results demonstrate that the versatility of photochemical immobilization chemistry can be combined with microarray techniques to create high-density and spatially addressable carbohydrate microarrays, where the photochemical properties of PFPA can be fully used to produce polymer thin films, and to locate the carbohydrate ligands to specific areas on the surface. In addition, the screening results clearly indicate that the produced arrays efficiently pinpoint not only the binding patterns of selected lectins for their optimal binding partners, but also the relative binding efficiency for individual array compounds.

Dynamic combinatorial libraries generated from thiocomponents were screened against a range of lectins using solid-phase assays and cell-binding assays technologies. The results clearly show that *N*-Acetylgalactosamine was the most important building block of libraries for the human lectin, and the digalactoside as most potent compound acting on the toxic mistletoe agglutinin.

Acknowledgements

I wish to express my heartfelt thanks to:

Dr. Olof Ramström for offering me the opportunity to study as a PhD student, being an excellent supervisor and for your support and guidance during these years. It is a great pleasure working with you!

Prof. Mingdi Yan, Prof. Hans-Joachim Gabius, Prof. Jean-Marie Lehn, Dr. Teodor Aastrup, and Prof. Peter Nilsson for our fruitful collaborations.

Rikard Larsson, Hai Dong, Dr. Hui Yu, Dr. Yuxin Pei, Matthias Theurer, Dr. Sabine André, Dr. Hans-Christian Siebert, Annelie Waldén and Henrik Anderson and all collaborators in different projects for our marvellous collaborations.

Marcus Angelin, Pornrapee Vongvilai, Rémi Caraballo, Gunnar Dunér, Oscar Norberg, Alexandra Martinsson, and all present and former members in Ramström's group for being good friends and spending wonderful time together.

Prof. Christina Moberg, Prof. Peter Somfai, Prof. Torbjörn Norin, Prof. Licheng Sun, Prof. Anna-Karin Borg Karlson, Dr. Zoltán Szabó, Prof. Paul Helquist, Prof. Göran Widmalm, Prof. Stefan Oscarson for interesting graduate courses.

Dr. Ulla Jacobsson for support with the NMR instruments.

Lena Skowron, Henry Challis for all your help with whatever was needed.

A special thanks to Prof. Torbjörn Norin for taking time and efforts of proof-reading this thesis, and to Prof. Licheng Sun for being an opponent of my half-time presentation during my PhD study.

Everybody in the Chemistry/Organic Chemistry Department for a friendly working atmosphere and for enjoying life together.

The Aulin-Erdtman foundation, Attana AB, Svenska Kemistsamfundet, Knut och Alice Wallenbergs Stiftelse, and Ragnar och Astrid Signeuls Stiftelse for conferences and travelling support.

The Swedish Research Council, the Swedish Foundation for International Cooperation in Research and Higher Education, and the Carl Trygger Foundation for financial support.

My parents for their endless care and encouragement.

My wife Yuxin and my son Yihan for their endless support and love!

References

1. Boyd, W. C.; Shapleigh, E. Separation of individuals of any blood group into secretors and non-secretors by use of a plant agglutinin (lectin). *Blood* **1954**, *9*, 1194-1198.
2. Gabius, H. -J. Non-carbohydrate binding partners/domains of animal lectins. *Int. J. Biochem.* **1994**, *26*, 469-477.
3. Drickamer, K.; Taylor, M. E. Biology of animal lectins. *Annu. Rev. Cell Biol.* **1993**, *9*, 237-264.
4. Sharon, N.; Lis, H. Lectins as cell recognition molecules. *Science* **1989**, *246*, 227-234.
5. Gabius, H. J.; Springer, W. R.; Barondes, S. H. Receptor for the cell binding site of discoidin I. *Cell* **1985**, *42*, 449-56.
6. Barondes, S. H. Bifunctional properties of lectins: lectins redefined. *Trends Biochem. Sci.* **1988**, *13*, 480-482.
7. Sumner, J. B. The globulins of the jack bean, *canavalia ensiformis*. *J. Biol. Chem.* **1919**, *37*, 137-142.
8. Watkins, W. M.; Morgan, W. T. J. Neutralization of the anti-H agglutinin in Eel serum by simple sugars. *Nature* **1952**, *169*, 825-826.
9. Moothoo, D. N.; Canan, B.; Field, R. A.; Naismith, J. H. Man alpha1-2-man-alpha-OMe-concanavalin A complex reveals a balance of forces involved in carbohydrate recognition. *Glycobiology* **1999**, *6*, 539-545.
10. Lis, H.; Sharon, N. Lectins: Carbohydrate-specific proteins that mediate cellular recognition. *Chem. Rev.* **1998**, *98*, 637-674.
11. Poretz, R. D. Protein-carbohydrate interaction: On the mode of binding of aromatic moieties to concanavalin A, the phytohemagglutinin of the jack bean. *Biochem. Pharmacol.* **1971**, *20*, 2727-2739.
12. Perillo, N. L.; Marcus, M. E.; Baum, L. G. Galectins: versatile modulators of cell adhesion, cell proliferation, and cell death. *J. Mol. Med.* **1998**, *76*, 402-412.
13. Leffler, H. Introduction to galectins. *Trends Glycosci Glycotechnol.* **1997**, *9*, 9-19.
14. Barondes, S. H.; Cooper, D. N. W.; Gitt, M. A.; Leffler, H. Galectins. Structure and function of a large family of animal lectins. *J. Biol. Chem.* **1994**, *269*, 20807-20810.
15. Weis, W. I.; Drickamar, K. Structural basis of lectin-carbohydrate recognition. *Annu. Rev. Biochem.* **1996**, *65*, 441.
16. Rini, J. M. Lectin structure. *Annu. Rev. Biophys. Biomol. Struct.* **1995**, *24*, 551-577.
17. Sharon, N.; Lis, H. Carbohydrate-protein interactions. *Chem. Brit.* **1990**, *26*, 679-682.
18. Young, N. M.; Oomen, R. P. Analysis of sequence variation among legume lectins: A ring of hypervariable residues forms the perimeter of the carbohydrate-binding site. *J. Mol. Biol.* **1992**, *228*, 924-934.
19. Sharma, V.; Surolia, A. Analyses of carbohydrate recognition by legume lectins: size of the combining site loops and their primary specificity. *J. Mol. Biol.* **1997**, *267*, 433-445.

20. Ravishankar, R.; Ravindran, N.; Suguna, A.; Surolia, A.; Vijayan, M. Crystal structure of the peanut lectin-T-antigen complex. Carbohydrate specificity generated by water bridges. *Curr. Science* **1997**, *72*, 855-861.
21. O'Sullivan, C. K.; Guilbault, G. C. Commercial quartz crystal microbalances – theory and applications. *Biosens. Bioelectron.* **1999**, *14*, 663-670.
22. Marx, K. A. Quartz crystal microbalance: a useful tool for studying thin polymer films and complex biomolecular systems at the solution-surface interface. *Biomacromolecules.* **2003**, *4*, 1099-1120.
23. Curie, J.; Curie, P. Développement, par pression, de l' électricité polaire dans les cristaux hémiedres á faces inclinées. *Comput. Rend. Acad. Sci. Paris.* **1880**, *91*, 294.
24. Rayleigh, L. On the free vibrations of an infinite plate of homogeneous, isotropic elastic matter. *Proc. London. Math. Soc.* **1889**, *20*, 225.
25. Janshoff, A.; Galla, H. J.; Steinem, C. Piezoelectric mass-sensing devices as biosensors - an alternative to optical biosensors? *Angew. Chem. Int. Ed.* **2000**, *39*, 4004-4032.
26. Pavey, K. D.; Olliff, C. J.; Paul, F. Quartz crystal resonant sensor (QCRS) model for label-free, small molecules-receptor studies. *Analyst* **2001**, *126*, 1711-1715
27. Perou, C. M. Molecular portraits of human breast tumours. *Nature* **2000**, *406*, 747-752.
28. Ramsey, G. DNA chips: State-of-the art. *Nat. Biotechnol.* **1998**, *16*, 40-44.
29. Zhu, H. Global analysis of protein activities using proteome chips. *Science* **2001**, *293*, 2101-2105.
30. MacBeath, G.; Schreiber, S. L. Printing proteins as microarrays for high-throughput function determination. *Science* **2000**, *289*, 1760-1763.
31. Lee, Y. C.; Lee, R. T. Carbohydrate-protein interactions: basis of glycobiology. *Acc. Chem. Res.* **1995**, *28*, 321-327.
32. Mannen, M.; Choi, S.-K.; Whitesides, G. M. Polyvalente wechselwirkungen in biologischen systemen: auswirkungen auf das design und die verwendung multivalenter liganden und inhibitoren. *Angew. Chem.* **1998**, *110*, 2908-2953.
33. Shin, I.; Park, S.; Lee, M.-R. Carbohydrate microarrays: an advanced technology for functional studies of glycans. *Chem. Eur. J.* **2005**, 2894-2901.
34. Wang, D.; Liu, S.; Trummer, B. J.; Deng, C.; Wang, A. Carbohydrate microarrays for the recognition of cross-reactive molecular markers of microbes and host cells. *Nat. Biotechnol.* **2002**, *20*, 275-281.
35. Park, S.; Shin, I. Fabrication of Carbohydrate chips for studying protein-carbohydrate interactions. *Angew. Chem.* **2002**, *114*, 3312-3314.
36. Ratner, D. M.; Adams, E. W.; Su, J.; O'Keefe, B. R.; Mrksich, M.; Seeberger, P. H. Probing protein-carbohydrate interactions with microarrays of synthetic oligosaccharides. *ChemBioChem.* **2004**, *5*, 379-383.
37. Houseman, B. T.; Mrksich, M. Carbohydrate arrays for the evaluation of protein binding and enzymatic modification. *Chem. Biol.* **2002**, *9*, 443-454.
38. Fazio, F.; Bryan, M. C.; Blixt, O.; Paulson, J. C.; Wong, C. -H. Synthesis of sugar arrays in microtiter plate. *J. Am. Chem. Soc.* **2002**, *124*, 14397-14402.

39. Park, S.; Lee, M. -R.; Pyo, S. -J.; Shin, I. Carbohydrate chips for studying high-throughput carbohydrate-Protein interactions. *J. Am. Chem. Soc.* **2004**, *126*, 4812-4819.
40. Lee, M.-r.; Shin, I. Solution-Phase Synthesis of aminooxy peptoids in the C to N and N to C directions. *Org. Lett.* **2002**, *4*, 869-872.
41. Varki, A. Biological roles of oligosaccharides: all of the theories are correct. *Glycobiology*. **1993**, *3*, 97-130.
42. Crocker, P. R.; Feizi, T. Carbohydrate recognition systems: functional triads in cell—cell interactions. *Curr. Opin. Struct. Biol.* **1996**, *6*, 679-691.
43. Gabius, H.-J.; Andre, S.; Kaltnar, H.; Siebert, H. C. The sugar code: functional lectinomics. *Biochim. Biophys. Acta.* **2002**, *1572*, 165-167.
44. Perez, S.; Vergelati, C. Structure and conformational analysis of methyl α -thiomaltoside, C₁₃H₂₄O₁₀S. *Acta Crystallogr. Sect. B.* **1984**, *40*, 294-299.
45. Davis, B. G.; Ward, S. J.; Rendle, P. M. Glycosyldisulfides: a new class of solution and solid phase glycosyl donors. *Chem. Commun.* **2001**, 189-190.
46. Szilagyi, L.; Illyes, T. -Z.; Herczegh, P. Elaboration of a novel type of interglycosidic linkage: syntheses of disulfide disaccharides. *Tetrahedron. Lett.* **2001**, 3901-3903.
47. Hummel, G.; Hindsgaul, O. Solid-phase synthesis of thio-oligosaccharides. *Angew. Chem. Int. Ed.* **1999**, *38*, 1782-1784.
48. Driguez, H. Thiooligosaccharides in glycobiology. *Top. Curr. Chem.* **1997**, *187*, 85-116.
49. Kiefel, M. J.; Beisner, B.; Benneet, S.; Holmes, I. D.; Itzstein, M. von. Synthesis and biological evaluation of N-acetylneuraminic acid-based rotavirus inhibitors. *J. Med. Chem.* **1996**, *39*, 1314-1320.
50. Pei, Z.; Dong, H.; Ramström, O. Solvent-Dependent, Kinetically controlled stereoselective synthesis of 3- and 4-thioglycosides. *J. Org. Chem.* **2005**, *70*, 6952-6955.
51. Dong, H.; Pei, Z.; Ramström, O. Stereospecific ester activation in nitrite-mediated carbohydrate epimerization. *J. Org. Chem.* **2006**, *71*, 3306-3309.
52. Pei, Z.; Dong, H.; Ramström, O. Synthesis of thiogalactose derivatives for S-linked oligosaccharides. Submitted for publication.
53. Andre, S.; Pei, Z.; Siebert, H. -C.; Ramström, O.; Gabius, H. -J. Glycosyldisulfides from dynamic combinatorial libraries as O-glycoside mimetics for plant and endogenous lectins: Their reactivities in solid-phase and cell assays and conformational analysis by molecular dynamics simulations. *Bioorg. Med. Chem.* **2006**, *18*, 6314-6326.
54. Pei, Z.; Rikard, L.; Aastrup, T.; Anderson, H.; Lehn, J. -M.; Ramström, O. Quartz crystal microbalance bioaffinity sensor for rapid identification of glycosyldisulfide lectin inhibitors from a dynamic combinatorial library. *Biosens. Bioelectron.* **2006**, *22*, 42-48.
55. Dong, H.; Pei, Z.; Byström, S.; Ramström, O. Reagent-dependent regioselective control in multiple carbohydrate esterification. Submitted for publication.
56. Pei, Z.; Anderson, H.; Aastrup, T.; Ramström, O. Study of real-time lectin-carbohydrate interactions on the surface of a quartz crystal microbalance. *Biosens. Bioelectron.* **2005**, *21*, 60-66.

57. Pei, Z.; Aastrup, T.; Anderson, H.; Ramström, O. Redox-responsive and calcium-dependent switching of glycosyldisulfide interactions with Concanavalin A. *Bioorg. Med. Chem. Lett.* **2005**, *15*, 2707-2710.
58. Pei, Y.; Yu, H.; Pei, Z.; Theurer, M.; Yan, M.; Ramström, O. Photoderivatized QCM surfaces for the study of real-time lectin-carbohydrate interactions. Submitted for publication.
59. Zhu, X.; Stolz, F.; Schmidt, R. R. Synthesis of thioglycoside-based UDP-sugar analogues. *J. Org. Chem.* **2004**, *69*, 7367-7370.
60. Wallenfels, K.; Malhotra, O. P. Galactosidases. *Adv. Carbohydr. Chem.* **1961**, *16*, 239-298.
61. Zanini, D.; Park, W. K. C.; Roy, R. Synthesis of novel dendritic glycosides. *Tetrahedron Lett.* **1995**, *36*, 7383-7386.
62. Gamblin, D.P.; Garnier, P.; Kasteren, S.; Oldham, N. J.; Fairbanks, A. J.; Davis, B. G. Glyco-SeS: selenenylsulfide-mediated protein glycoconjugation - a new strategy in post-translational modification. *Angew. Chem. Int. Ed.* **2004**, *43*, 828-833.
63. Albert, L.; Dax, K.; Link, R. W.; Stutz, A. E. Carbohydrate triflates: reaction with nitrite, leading directly to epi-hydroxy compounds. *Carbohydr. Res.* **1983**, *118*, C5-C6.
64. Knapp, S.; Kukkola, P. J.; Sharma, S.; Murali Dhar, T. G.; Naughton, A. B. J. Amino alcohol and amino sugar synthesis by benzoylcarbamate cyclization. *J. Org. Chem.* **1990**, *55*, 5700-5710.
65. Dong, H.; Pei, Z.; Angelin, M.; Byström, S.; Ramström, O. Efficient synthesis of β -D-mannosides and β -D-talosides by double parallel or double serial inversion. Submitted for publication.
66. Eisele, T.; Toepfer, A.; Kretzschmar, G.; Schmidt, R. R. Synthesis of a thio-linked analogue of sialyl Lewis X. *Tetrahedron Lett.* **1996**, *37*, 1389-1392.
67. Liakatos, A.; Kiefel, M. J.; von Itzstein, M. Synthesis of lactose-based S-linked sialylmimetics of α -(2,3)-sialosides. *Org. Lett.* **2003**, *5*, 4365-4368.
68. Nicotra, F. Synthesis of C-glycosides of biological interest. *Top. Curr. Chem.* **1997**, *187*, 55-83.
69. Maradufu, A.; Dax, K.; Perlin, A. S. Synthesis of analogs of methyl β -D-galactopyranoside modified at C-4. *Carbohydr. Res.* **1974**, *32*, 261-277.
70. Graziani, A.; Passacantilli, P.; Piancatelli, G.; Tani, S. A mild and efficient approach for the regioselective silyl-mediated protection-deprotection of C-4 hydroxyl group on carbohydrates. *Tetrahedron Lett.* **2001**, *42*, 3857-3860.
71. Wachter, R. M.; Branchaud, B. P. Thiols as mechanistic probes for catalysis by the free radical enzyme galactose oxidase. *Biochemistry*, **1996**, *35*, 14425-14435.
72. Defaye, J.; Driguez, H.; Ohleyer, E.; Orgeret, C.; Viet, C. Stereoselective syntheses of 1,2-*trans*-related 1-thioglycoses. *Carbohydr. Res.* **1984**, *130*, 317-321.
73. Kondo, Y. Partial tosylation of methyl α -D-mannopyranoside. *Carbohydr. Res.* **1986**, *154*, 305-309.
74. Cohen, S. B.; Halcomb, R. L. Synthesis of S-linked glycosyl amino acids in aqueous solution with unprotected carbohydrates. *Org. Lett.* **2001**; *3*; 405-407.

75. Baisch G.; Öhrhein R. Convenient chemoenzymatic synthesis of β -purine-diphosphate sugars (GDP-fucose-analogues). *Bioorg. Med. Chem.* **1997**, *5*, 383-388.
76. Tsai J. -H.; Behrman, E. J. Synthesis of β -L-fucopyranosyl phosphate from L-fucose orthoacetates. *Carbohydr. Res.* **1978**, *64*, 297-301.
77. Lattrell, R.; Lohaus, G. Attempted total synthesis of cephalosporin derivatives. II. Substitution reactions with trans-3-(sulfonyloxy)-2-azetidinones. Synthesis of cis-3-(acylamino)-4-(alkylthio)-2-azetidinones. *Justus Liebigs Ann. Chem.* **1974**, *6*, 901-920.
78. Anslyn, E. V.; Dougherty, D. A. *Modern Physical Organic Chemistry*; University Science Books: Sausalito, **2006**, p 659.
79. Winstein, S.; Grunwald, E.; Ingraham, L. L. The role of neighboring groups in replacement reactions. XII. Rates of acetolysis of 2-substituted cyclohexyl benzenesulfonates. *J. Am. Chem. Soc.* **1948**, *70*, 821-828.
80. Binkley, R. W. Inversion of configuration in 2,6-dideoxy sugars. Triflate displacement by benzoate and nitrite anions. *J. Org. Chem.* **1991**, *56*, 3892-3896.
81. Kassou, M.; Castillon, S. Ring Contraction vs fragmentation in the intramolecular reactions of 3-O-(trifluoromethanesulfonyl)pyranosides. Efficient synthesis of branched-chain furanosides. *J. Org. Chem.* **1995**, *60*, 4353-4358.
82. El Nemr, A.; Tsuchiya, T. α - and β -hydrogen eliminations in the reactions of some 3-O-triflylglycosides with BuOk and pyridine. *Carbohydr. Res.* **1997**, *303*, 267-281.
83. Banks, R. E.; Sparkes, G. R. J. Azide chemistry. V. Synthesis of 4-azido-2,3,5,6-tetrafluoro-4-azido-3-chloro-2,5,6-trifluoro-, and 4-azido-3,5-dichloro-2,6-difluoro-pyridine, and thermal reactions of the tetrafluoro compound. *Chem. Soc., Perkin Trans. I*, **1972**, *23*, 2964-2970.
84. Keana, J. F. W.; Cai, S. X. New reagents for photoaffinity labeling: synthesis and photolysis of functionalized perfluorophenyl azides. *J. Org. Chem.* **1990**, *55*, 3640-3647.
85. Bartlett, M.; Yan, M. Fabrication of polymer thin films and arrays with spatial and topographical controls. *Adv. Mater.* **2001**, *13*, 1449-1451.
86. Yan, M.; Harnish, B. A Simple method for the attachment of polymer films on solid substrates. *Adv. Mater.* **2003**, *15*, 244-248.
87. Wang, J. L.; Cunningham, B. A. The covalent and three-dimensional structural of concanavalin A. I. Amino acid sequence of cyanogen bromide fragments F1 and F2. *J. Biol. Chem.* **1975**, *250*, 1490-1502.
88. Niwa, H.; Tonevitsky, A.G.; Agapov, I. I.; Saward, S.; Pfuller, U.; Palmer, R. A. Crystal structure at 3 Å of mistletoe lectin I, a dimeric type-II ribosome-inactivating protein, complexed with galactose. *Eur. J. Biochem.* **2003**, *270*, 2739-2749.
89. Audette, G. F.; Olson, D. J. H.; Ross, A. R. S.; Quail, J. W.; Delbaere, L. T. J. Examination of the structural basis for O(H) blood group specificity by Ulex europaeus Lectin I. *Can. J. Chem.* **2002**, *80*, 1010-1021.
90. Olsen, L. R.; Dessen, A.; Gupta, D.; Sabesan, S.; Sacchettini, J. C.; Brewer, C. F. X-ray crystallographic studies of unique cross-linked lattices between four

- isomeric biantennary oligosaccharides and soybean agglutinin. *Biochemistry* **1997**, *36*, 15073-15088.
91. Buts, L.; Hamelryck, T. W.; Dao-Thi, M.; Loris, R.; Wyns, L.; Etzler, M. E. Weak protein-protein interactions in lectins: the crystal structure of a vegetative lectin from the legume *Dolichos biflorus*. *J. Mol. Biol.* **2001**, *309*, 193-201.
 92. Dessen, A.; Gupta, D.; Sabesan, S.; Brewer, C. F.; Sacchettini, J. C. X-ray crystal structure of the soybean agglutinin cross-linked with a biantennary analog of the blood group I carbohydrate antigen. *Biochemistry* **1995**, *34*, 4933-4942.
 93. Banerjee, R.; Das, K.; Ravishankar, R.; Suguna, K.; Surolia, A.; Vijayan, M. Conformation, Protein-carbohydrate interactions and a novel subunit association in the refined structure of peanut lectin-lactose complex. *J. Mol. Biol.* **1996**, *259*, 281-296.
 94. Shankar Iyer, P. N.; Wilkinson, K. D.; Goldstein, I. J. An *N*-acetyl-D-glucosamine binding lectin from *Bandeiraea Simplicifolia* seeds. *Arch. Biochem. Biophys.* **1976**, *177*, 330-333.
 95. Prasthofer, T.; Phillips, S. R.; Suddath, F.L.; Engler, J.A. Design, expression, and crystallization of recombinant lectin from the garden pea (*Pisum sativum*). *J. Biol. Chem.* **1989**, *264*, 6793-6796.
 96. Ruzeinikov, S. N.; Mikhailova Yu, I.; Tsygannik, I. N.; Pangborn, W.; Duax, W.; Pletnev, V. Z. The structure of the pea lectin-D-mannopyranose complex at 2.1 Å resolution. *Russ. J. Bioorg. Chem.* **1998**, *24*, 277-282.
 97. Rini, J. M.; Hardman, K. D.; Einspahr, H.; Suddath, F. L.; Carver, J. P. X-ray crystal structure of a pea lectin-trimannoside complex at 2.6 Å resolution. *J. Biol. Chem.* **1993**, *268*, 10126-10132.
 98. Iglesias, M. M.; Rabinovich, G. A.; Ambrosio, A. L.; Castagna, L. F.; Sotomayor, C. E.; Wolfenstein-Todel, C. Purification of galectin-3 from ovine placenta: developmentally regulated expression and immunological relevance. *Glycobiology* **1998**, *8*, 59-65.
 99. Sorme, P.; Arnoux, P.; Kahl-Knutsson, B.; Leffler, H.; Rini, J. M.; Nilsson, U. J. Structural and thermodynamic studies on cation- Π interactions in lectin-ligand complexes: high-affinity galectin-3 inhibitors through fine-tuning of an arginine-arene interaction. *J. Am. Chem. Soc.* **2005**, *127*, 1737-1743.
 100. Seetharaman, J.; Kanigsberg, A.; Slaaby, R.; Leffler, H.; Barondes, S.H.; Rini, J.M. X-ray crystal structure of the human galectin-3 carbohydrate recognition domain at 2.1-Å resolution. *J. Biol. Chem.* **1998**, *273*, 13047-13052.
 101. Duverger, E.; Frison, N.; Roche, A.-C.; Monsigny, M. Carbohydrate-lectin interactions assessed by surface plasmon resonance. *Biochimie* **2003**, *85*, 167-179.
 102. Holmskov, U.; Fischer, P.B.; Rothmann, A.; Hojrup, P. Affinity and kinetic analysis of the bovine plasma C-type lectin collectin-43 (CL-43) interacting with mannan. *FEBS Lett.* **1996**, *393*, 314-316.
 103. Pagé, D.; Zanini, D.; Roy, R. Macromolecular recognition: Effect of multivalency in the inhibition of binding of yeast mannan to concanavalin A and pea lectins by mannosylated dendrimers. *Bioorg. Med. Chem.* **1996**, *4*, 1949-1961.

104. Ebara, Y.; Okahata, Y. A Kinetic Study of concanavalin A binding to glycolipid monolayers by using a quartz-crystal microbalance. *J. Am. Chem. Soc.* **1994**, *116*, 11209-11212.
105. Meyer, B.; Peters, T. NMR spectroscopy techniques for screening and identifying ligand binding to protein receptors. *Angew. Chem. Int. Ed.* **2003**, *42*, 864-890.
106. Vogt, B. D.; Soles, C. L.; Lee, H.-J.; Lin, E. K.; Wu, W.-I. Moisture absorption and absorption kinetics in polyelectrolyte films: influence of film thickness. *Langmuir* **2004**, *20*, 1453-1458.
107. Niikura, K.; Matsuno, H.; Okahata, Y. Binding behavior of lysine-containing helical peptides to DNA duplexes immobilized on a 27 MHz quartz-crystal microbalance. *Chem. Eur. J.* **1999**, *5*, 1609-1616.
108. Mislavicova, D.; Masarova, J.; Svitel, J.; Mendichi, R.; Soltes, L.; Gemeiner, P.; Danielsson, B. Neoglycoconjugates of mannan with bovine serum albumin and their interaction with lectin concanavalin A. *Bioconj. Chem.* **2002**, *13*, 136-142.
109. Horisberger, M. An application of ellipsometry: Assessment of polysaccharide and glycoprotein interaction with lectin at a liquid/solid interface. *Biochim. Biophys. Acta.* **1980**, *632*, 298-309.
110. Pagé, D.; Roy, R. Optimizing lectin-carbohydrate interactions: improved binding of divalent α -mannosylated ligands towards concanavalin A. *Glycoconj. J.* **1997**, *14*, 345-356.
111. Rudiger, H. and Gabius, H.J. Plant lectins: Occurrence, biochemistry, functions and applications. *Glycoconj. J.* **2001**, *18*, 589-613.
112. Naismith, J.H. and Field, R.A. Structural basis of trimannoside recognition by concanavalin A. *J. Biol. Chem.* **1996**, *271*, 972.
113. Yang, L., Su, Y., Xu, Y., Wang, Z., Guo, Z., Weng, S., Yan, C., Zhang, S. and Wu, J. Interactions between metal ions and carbohydrates. Coordination behavior of neutral erythritol to Ca (II) and lanthanide ions. *Inorg. Chem.* **2003**, *42*, 5844-5856.
114. Bugg, C. E. Calcium binding to carbohydrates. Crystal structure of a hydrated calcium bromide complex of lactose. *J. Am. Chem. Soc.* **1973**, *95*, 908-913.
115. Bouckaert, J., Poortmans, F., Wyns, L. and Loris, R. Sequential structural changes upon zinc and calcium binding to Metal-free concanavalin A. *J. Biol. Chem.* **1996**, *271*, 16144-16150.
116. Brown, R.D., Koenig, S.H.; Brewer, C. F. Conformational equilibrium of demetalized concanavalin A. *Biochemistry* **1982**, *21*, 465-469.
117. Ramström, O.; Lehn, J.-M. In situ generation and screening of a dynamic combinatorial carbohydrate library against concanavalin A. *ChemBioChem.* **2000**, *1*, 41-48.
118. Ramström, O.; Lehn, J.-M. Drug discovery by dynamic combinatorial libraries. *Nat. Rev. Drug Discov.* **2002**, *1*, 26-36.
119. Bunyapaiboonsri, T.; Ramström, O.; Lohmann, S.; Lehn, J.-M.; Peng, L.; Goeldner, M. Dynamic deconvolution of a pre-equilibrated dynamic combinatorial library of acetylcholinesterase inhibitors. *ChemBioChem.* **2001**, *2*, 438-444.

120. Maegel, I.; Jaehne, E.; Henke, A.; Adler, H. J.; Bram, C.; Jung, C.; Stratmann, M. Self-assembling adhesion promoters for corrosion resistant metal polymer interfaces. *Prog. Org. Coat.* **1997**, *34*, 1-12.
121. Takano, H.; Porter, M. D. Monitoring Chemical Transformations at Buried Organic Interfaces by Electric Force Microscopy. *J. Am. Chem. Soc.* **2001**, *123*, 8412-8413.
122. Yan, M.; Cai, S. X.; Wybourne, M. N.; Keana J. F. W. N-Hydroxysuccinimide ester functionalized perfluorophenyl azides as novel photoactive heterobifunctional crosslinking reagents. The covalent immobilization of biomolecules to polymer surfaces. *Bioconjugate Chem.* **1994**, *5*, 151-157.
123. Scriven (Ed.), E. F. U. *Azides and Nitrenes: Reactivity and Utility*, Academic Press, New York, **1984**.
124. Joester, D.; Klein, E.; Geiger, B.; Addadi, L. Temperature-sensitive micrometer-thick layers of hyaluronan grafted on microspheres. *J. Am. Chem. Soc.* **2006**, *128*, 1119-1124.
125. Yan, M.; Ren, J. Covalent immobilization of ultrathin polymer films by thermal activation of perfluorophenyl azide. *Chem. Mater.* **2004**, *16*, 1627-1632.
126. Yan, M.; Bartlett, M. Micro/Nanowell arrays fabricated from covalently immobilized polymer thin films on a flat substrate. *Nano Lett.* **2002**, *2*, 275-278.
127. Kayser, K.; Hoeft, D.; Hufnagi, P.; Caselitz, J.; Zick, Y.; Andre, S.; Kaltner, H.; Gabius, H. J. Combined analysis of tumor growth pattern and expression of endogenous lectins as a prognostic tool in primary testicular cancer and its lung metastases. *Histol. Histopathol.* **2003**, *18*, 771-779.
128. Lahm, H.; André, S.; Hoefflich, A.; Kaltner, H.; Siebert, H.-C.; Sordat, B.; von der Lieth, C.-W.; Wolf, E.; Gabius, H.-J., Tumor galectinology: Insights into the complex network of a family of endogenous lectins. *Glycoconj. J.* **2003**, *20*, 227-238.
129. Sharma, U. C.; Pokharel, S.; Van Brakel, T. J.; Van Berlo, J. H.; Cleutjens, J. P. M.; Schroen, B.; André, S.; Crijns, H. J. G. M.; Gabius, H.-J.; Maessen, J.; Pinto, Y. M. Galectin-3 marks activated macrophages in failure-prone hypertrophied hearts and contributes to cardiac dysfunction. *Circulation* **2004**, *110*, 3121-3128.
130. Takenaka, Y.; Fukumori, T.; Raz, A. Galectin-3 and metastasis. *Glycoconj. J.* **2004**, *19*, 543-549.